รายงานวิจัยฉบับสมบูรณ์

โครงการ การสังเคราะห์เซนเซอร์ฟลูออเรสเซนต์จากเฮซาโฮโมไตรเอซาคาลิกซ์[3]เอรีน

โดย รองศาสตราจารย์ ดร.บัญชา พูลโภคา

วันที่แล้วเสร็จโครงการ 30 พฤษภาคม พ.ศ. 2551

สัญญาเลขที่ RMU4880041

รายงานวิจัยฉบับสมบูรณ์

โครงการ การสังเคราะห์เซนเซอร์ฟลูออเรสเซนต์จากเฮซาโฮโมไตรเอซาคาลิกซ์[3]เอรีน

รศ. ดร.บัญชา พูลโภคา
ภาควิชาเคมี คณะวิทยาศาสตร์ จุฬาลงกรณ์มหาวิทยาลัย

สนับสนุนโดยสำนักงานกองทุนสนับสนุนการวิจัย
และ สำนักงานคณะกรรมการการอุดมศึกษา

(ความเห็นในรายงานนี้เป็นของผู้วิจัย สกว. และ สกอ. ไม่จำเป็นต้องเห็นด้วยเสมอไป)

กิตติกรรมประกาศ

งานวิจัยนี้ได้รับเงินสนับสนุนการวิจัยจากสำนักงานกองทุนสนับสนุนการวิจัย (สกว.) และ สำนักงานคณะกรรมการการอุดมศึกษา (สกอ.) รหัสโครงการ: RMU4880041 ซึ่งผู้วิจัยขอขอบพระคุณมา ณ ที่นี้ ขอขอบคุณโครงการปริญญาเอกกาญจนาภิเษก (คปก.) ที่ได้สนับสนุนทุนการศึกษาให้แก่ ดร. ชาติไทย แก้วทอง ผู้ที่เป็นกำลังสำคัญในการทำวิจัยนี้ นอกจากนี้ผู้วิจัยขอขอบคุณจุฬาลงกรณ์มหาวิทยาลัย คณะวิทยาศาสตร์ ภาควิชาเคมีและหน่วยวิจัยเคมีซุปราโมเลคิวลาร์และหน่วยวิจัยเคมีอินทรีย์สังเคราะห์ที่ได้อำนวยความสะดวกในด้านเครื่องมือ สถานที่ทำวิจัยและอุปกรณ์ต่างๆ รวมทั้งความช่วยเหลือ ผู้วิจัยขอกราบขอบพระคุณ ศาสตราจารย์ ดร. ประมวล ตั้งบริบูรณ์รัตน์ ภาควิชาเคมี คณะวิทยาศาสตร์ มหาวิทยาลัยมหิดล ที่ปรึกษานักวิจัย ที่ได้ให้กำลังใจและคำปรึกษาตลอดมา สุดท้ายขอขอบคุณสมาชิกในหน่วยวิจัยทั้งสองและเจ้าหน้าที่ฝ่ายวิชาการ สำนักงานกองทุนสนับสนุนการวิจัย สำหรับความช่วยเหลือที่ดีตลอดการทำวิจัยนี้

บทคัดย่อ

รหัสโครงการ: RMU4880041

ชื่อโครงการ: การสังเคราะห์เซนเซอร์ฟลูออเรสเซนต์จากเฮซาโฮโมไตรเอซาคาลิกซ์[3]เอรีน

ชื่อนักวิจัย: นายบัญชา พูลโภคา

ภาควิชาเคมี คณะวิทยาศาสตร์ จุฬาลงกรณ์มหาวิทยาลัย

E-mail Address: buncha.p@chula.ac.th

ระยะเวลาดำเนินโครงการ: 29 กรกฎาคม 2548 - 28 กรกฎาคม 2551

ในงานวิจัยนี้ได้ทำการสังเคราะห์และฟังก์ชันนัลไลซ์เฮกซาโฮโมไตรเอซา-*พารา*-คลอโรคาลิกซ์[3]-เอรีนได้เฮเทอโรไดทรอปิกเซนเซอร์ใหม่ 2 ชนิดและเครื่องมือในรูปอัลตร้าธินฟิล์มสำหรับการตรวจวัดไอออน 1 ชนิด จากการศึกษาการเกิดสารประกอบเชิงซ้อนพบว่าเฮกซาโฮโมไตรเอซา-*พารา*-คลอโรคาลิกซ์[3]เอรีนเองสามารถใช้ในการตรวจหาแอนไอออนได้ โดยพบว่าเฮกซาโฮโมไตรเอซา-*พารา*-คลอโรคาลิกซ์[3]เอรีนจะเปลี่ยนจากสารละลายใสไม่มีสีเป็นสารละลายสีเหลืองได้เมื่อจับกับ F^- และ $H_2PO_4^-$ เมื่อนำเอาเฮกซาโฮโมไตรเอซา-*พารา*-คลอโรคาลิกซ์[3]เอรีนมาทำปฏิกิริยา O-alkylation โดยเอทิลโบรโมแอซิเตรทจะได้เฮกซาโฮโมไตรเอซา-*พารา*-คลอโรคาลิกซ์[3]-ไตร(เอทิล แอซิเตรท) ทั้งในรูป cone และ partial cone เมื่อนำสารทั้งสองมาควบแน่นกับ 1-อะมิโนเมทิลแนฟธีลีนจะได้เฮกซาโฮโมไตรเอซา-*พารา*-คลอโรคาลิกซ์[3]-ไตรแนฟทิลลาไมด์เฉพาะรูปแบบ partial cone เท่านั้น จากการศึกษาความสามารถในการเป็นฟลูออเรสเซ้นต์เซนเซอร์พบว่าโฮโมไตรเอซา-*พารา*-คลอโรคาลิกซ์[3]-ไตรแนฟทิลลาไมด์สามารถเลือกจับกับ Cd^{2+}, Pb^{2+} และ F^- ได้ เมื่อเอาเฮกซาโฮโมไตรเอซา-*พารา*-คลอโรคาลิกซ์[3]-ไตร(เอทิล แอซิเตรท)มาควบแน่นกับเอมีนได้เป็นเฮกซาโฮโมไตรเอซา-*พารา*-คลอโรคาลิกซ์[3]-คริปแตนด์ ซึ่งมีขนาดโพรงที่แน่นอน พบว่าสามารถเลือกจับกับ Cl^- ได้ดีกว่าเฮไลด์อื่นๆ แต่เมื่อนำเอาไอออนของสังกะสีมาสร้างสารประกอบเชิงซ้อนกับเฮกซาโฮโมไตรเอซา-*พารา*-คลอโรคาลิกซ์[3]-คริปแตนด์ พบว่าสารประกอบเชิงซ้อนของโฮโมไตรเอซา-*พารา*-คลอโรคาลิกซ์[3]-คริปแตนด์จับกับ Br^- ได้ดีกว่า นอกจากนี้ยังได้นำเอาโฮโมไตรเอซา-*พารา*-คลอโรคาลิกซ์[3]เอรีนมาใช้เป็นเคโมเซ็นเซอร์โดยสร้างเป็นอุปกรณ์อัลตร้าธินฟิล์มของพอลิคาร์บาโซลพบว่าฟิล์มนี้สามารถใช้ในการตรวจวัด Zn^{2+} ได้อย่างเฉพาะเจาะจง

คำสำคัญ: เอซาคาลิกซ์[3]เอรีน, ตัวรับ, เซนเซอร์, สารประกอบเชิงซ้อน, แอนไอออน, แคทไอออน

Abstract

Project Code: RSA/06/2545

Project Title: Synthesis of Fluorescent Sensors based on Azacalix[4]arene.

Investigator: Mr. Buncha Pulpoka

Department of Chemistry, Faculty of Science, Chulalongkorn University

Phayathai Road, Pathumwan, Bangkok 10330

E-mail Address: buncha.p@chula.ac.th

Project Period: July 29, 2005-July 28, 2008

The hexahomotriaza-*p*-chlorocalix[3]arene was successfully synthesized and functionalized to provide two novel heteroditopic sensors. From complexation studies, the hexahomotriaza-*p*-chlorocalix[3]arene, itself, can be use for a selective chromogenic sensor for F^- and $H_2PO_4^-$. The tri-O-alkylation by ethyl bromoacetate of hexahomotriaza-*p*-chlorocalix[3]arene afforded hexahomotriaza-*p*-chlorocalix[3]-tri(ethyl acetate) in both cone and partial cone conformations. They were further condensed with 1-aminomethylnaphthalene providing selectively partial-cone hexahomotriaza-*p*-chlorocalix[3]-trinaphthylamide. The complexation studies by UV-vis and fluorescence spectroscopies showed that hexahomotriaza-*p*-chlorocalix[3]-trinaphthylamide exhibits a selective fluorescent sensor for Cd^{2+}, Pb^{2+} and F^-. The hexahomotriaza-*p*-chlorocalix[3]-cryptand which is fixed in cone conformation and processes a close well-defined cavity showed a high selectivity for Cl^- ion. By tuning of this ligand by complexing with zinc ion on hexahomotriaza-*p*-chlorocalix[3]arene framework, its anion binding selectivity changed to Br^- ion. Moreover, a new class of chemosensor recognition element based on conjugated polymer network ultra-thin films from electrochemical cross-linking of hexahomotriaza-*p*-chlorocalix[3]arene-carbazole was successfully realized in which it demonstrated high selectivity and sensitivity towards Zn^{2+}.

Keywords: azacalix[3]arene, complexation, receptor, cation, anion, sensor, ultra-thin film

Supporting Information

Azacalixarene-Carbazole Conjugated Polymer Network (CPN) Ultrathin Films for Specific Cation Sensing

Chatthai Kaewtong[1,2], Guoqian Jiang[1], Yushin Park[1], Tim Fulghum[1], Akira Baba[1]
Buncha Pulpoka[2]* and Rigoberto Advincula[1]*

[1]Department of Chemistry and Department of Chemical Engineering, University of Houston, 136 Fleming Building, Houston, TX 77204-5003
[2]Supramolecular Chemistry Research Unit and Organic Synthesis Research Unit, Department of Chemistry, Faculty of Science, Chulalongkorn University, Bangkok 10330, Thailand.

Content:

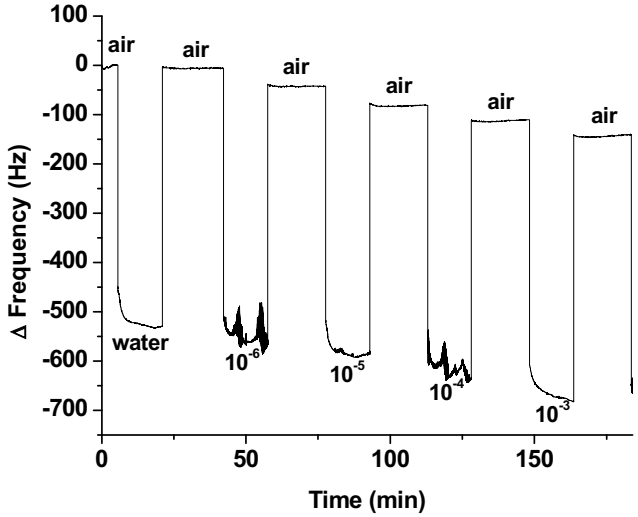

Figure S1. Sensor diagram studies by using QCM

Sensitivity and selectivity studies of PCC-CBz by using EC-SPR and SPR.

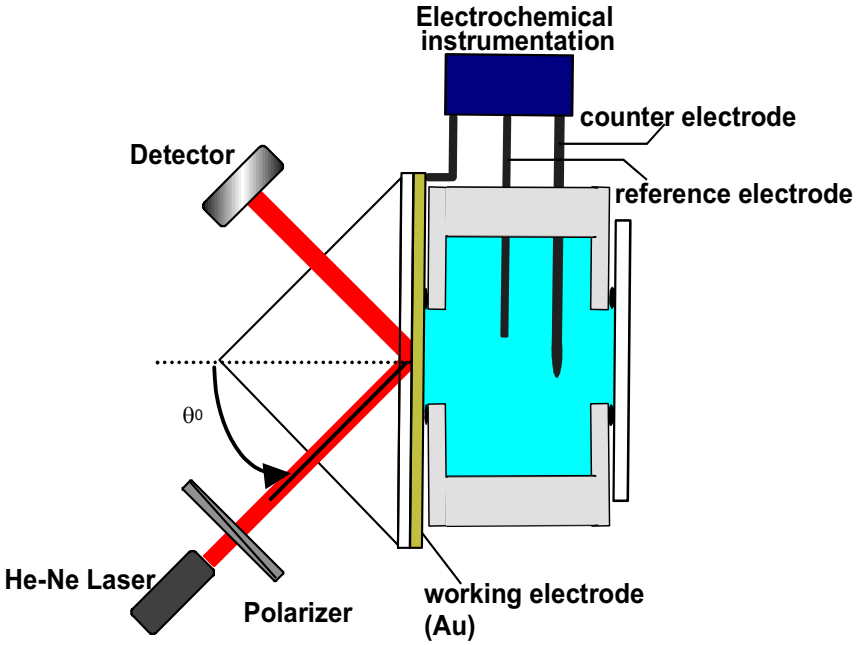

Figure S2. Sensor setup for in *situ* EC-SPR/SPR measurement.

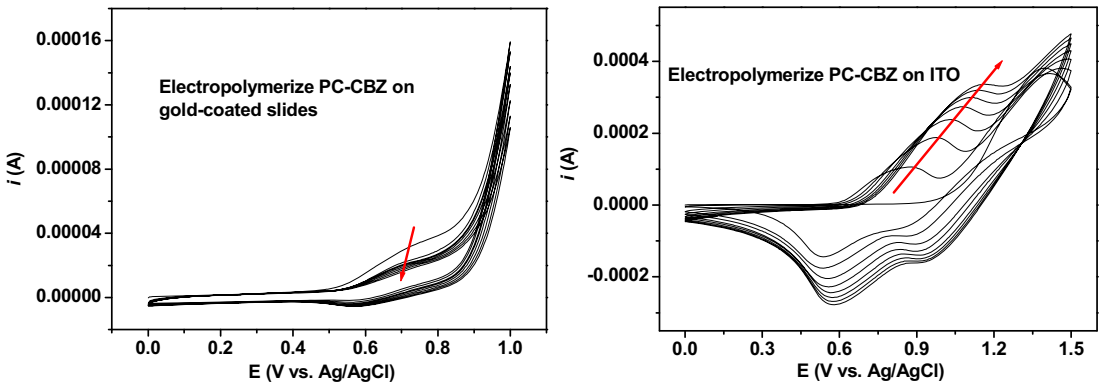

Figure S3. Cyclic voltammograms of electrochemical cross-linking/deposition of PC-CBz polymerization at a scan rate of 50 mv/s, 8 cycles: (a) deposited material on gold-coated slides, (b) deposited material on ITO substrates.

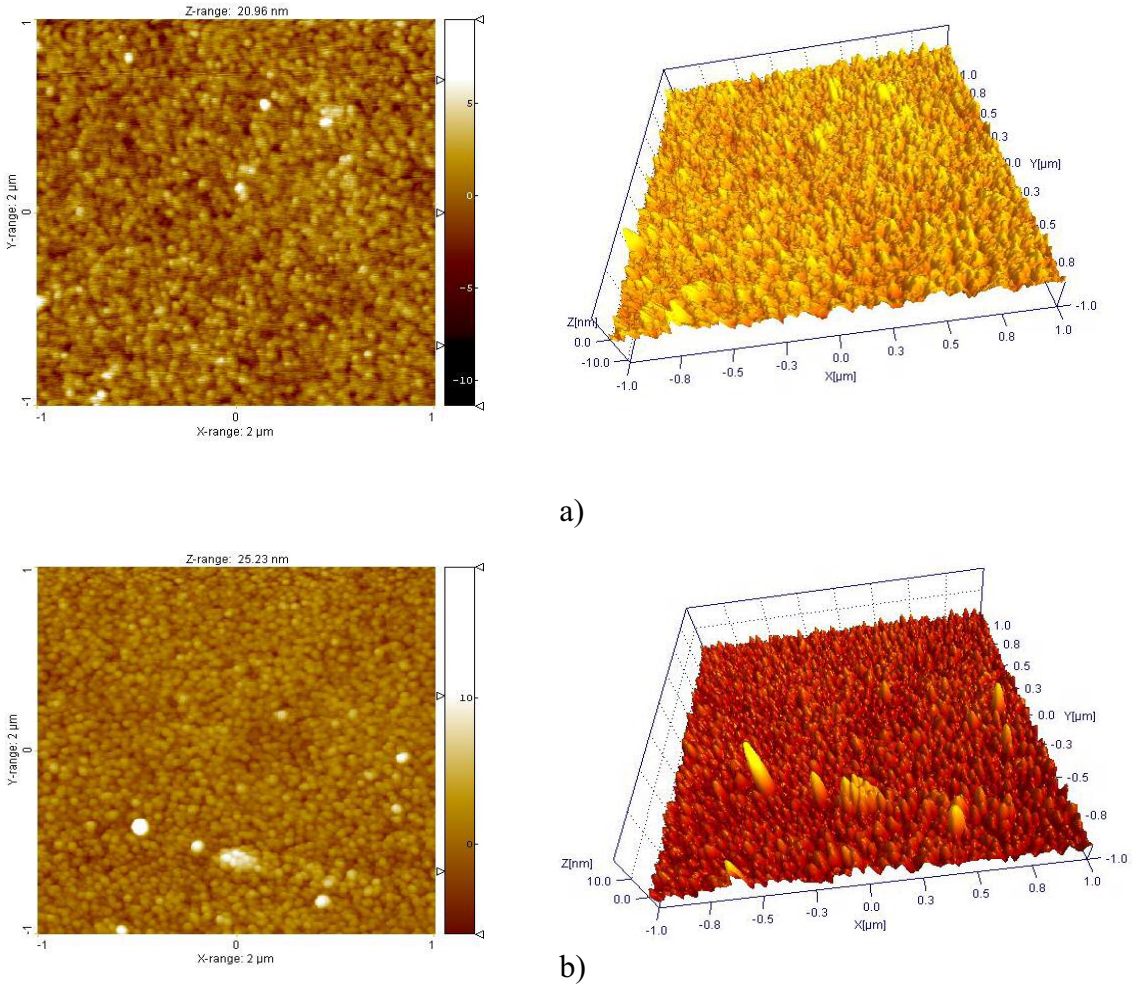

Figure S4. AFM images, the topological or height images (left) and three-dimentional topographic images (right): (a) bare gold, (b) after electropolymerized PPC-CBz electropolymerized at 50 mV/s (0 to 1.0), 8 cycles in $TBAPF_6/CH_2Cl_2$ electrolyte (WE, gold-coated slides; CE, Pt wire; RE, Ag/AgCl wire).

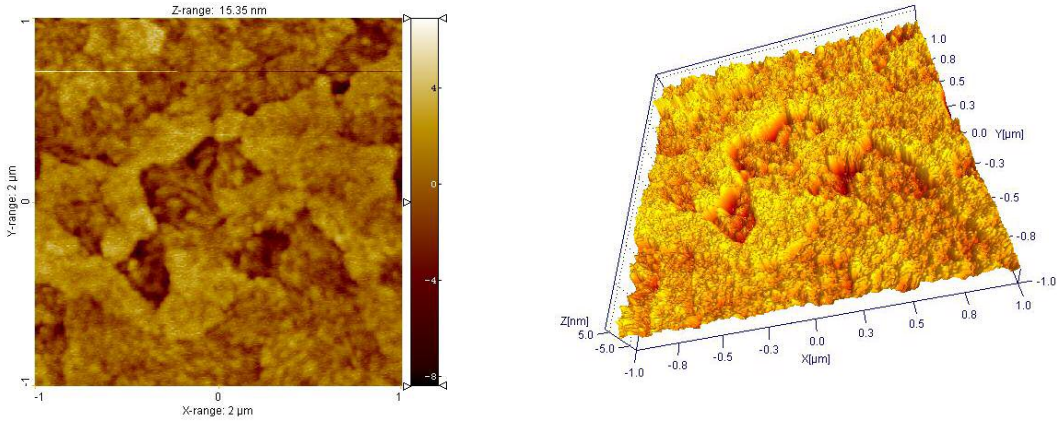

(a)

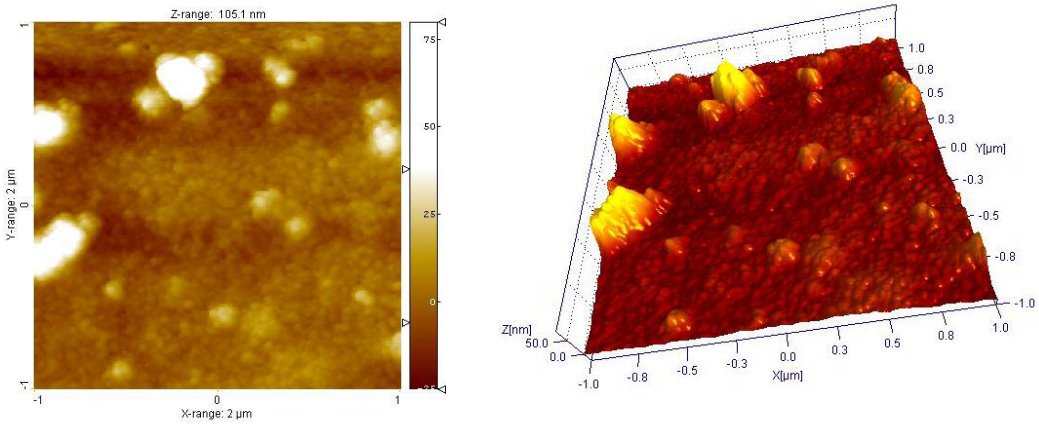

(b)

Figure S5. AFM images, the 2D topoıogical or height images (left) and 3D topographic imagse (right): (a) bare ITO, (b) after electropolymerization of PC-CBz at 50 mV/s (0 to 1.5), 8 cycles in $TBAPF_6/CH_2Cl_2$ electrolyte (WE, ITO; CE, Pt wire; RE, Ag/AgCl wire)

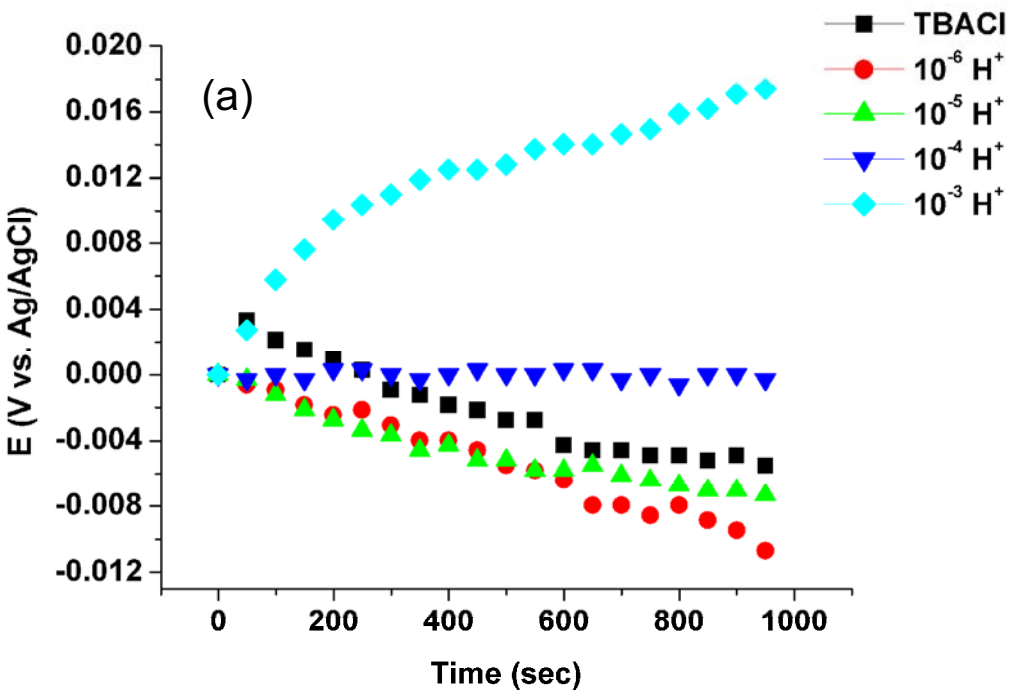
(a)
TBACl
10-6 H+
10-5 H+
10-4 H+
10-3 H+
E (V vs. Ag/AgCl)
0.020
0.016
0.012
0.008
0.004
0.000
-0.004
-0.008
-0.012
0
200
400
600
800
1000
Time (sec)

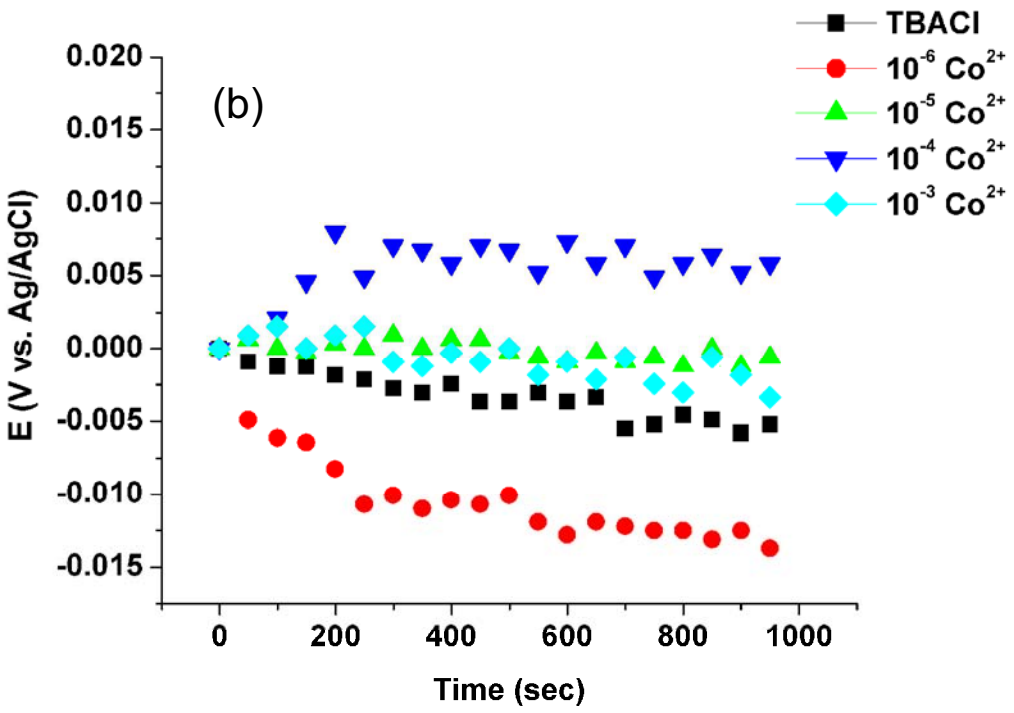
(b)
TBACl
10-6 Co2+
10-5 Co2+
10-4 Co2+
10-3 Co2+
E (V vs. Ag/AgCl)
0.020
0.015
0.010
0.005
0.000
-0.005
-0.010
-0.015
0
200
400
600
800
1000
Time (sec)

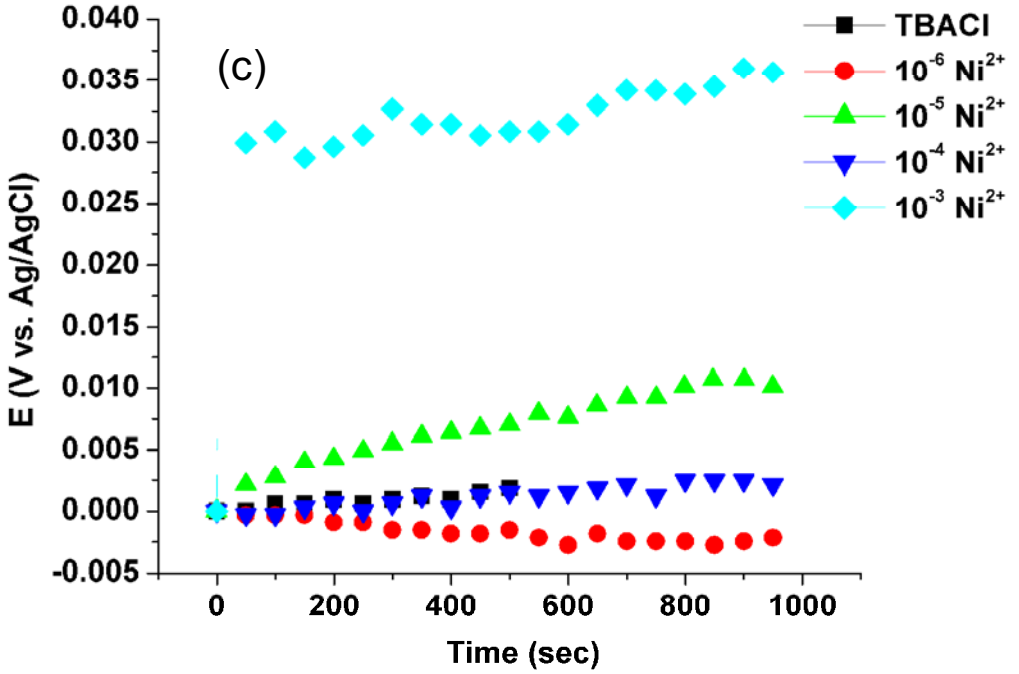
(c)
TBACl
10-6 Ni2+
10-5 Ni2+
10-4 Ni2+
10-3 Ni2+
E (V vs. Ag/AgCl)
Time (sec)
0.040
0.035
0.030
0.025
0.020
0.015
0.010
0.005
0.000
-0.005
0
200
400
600
800
1000

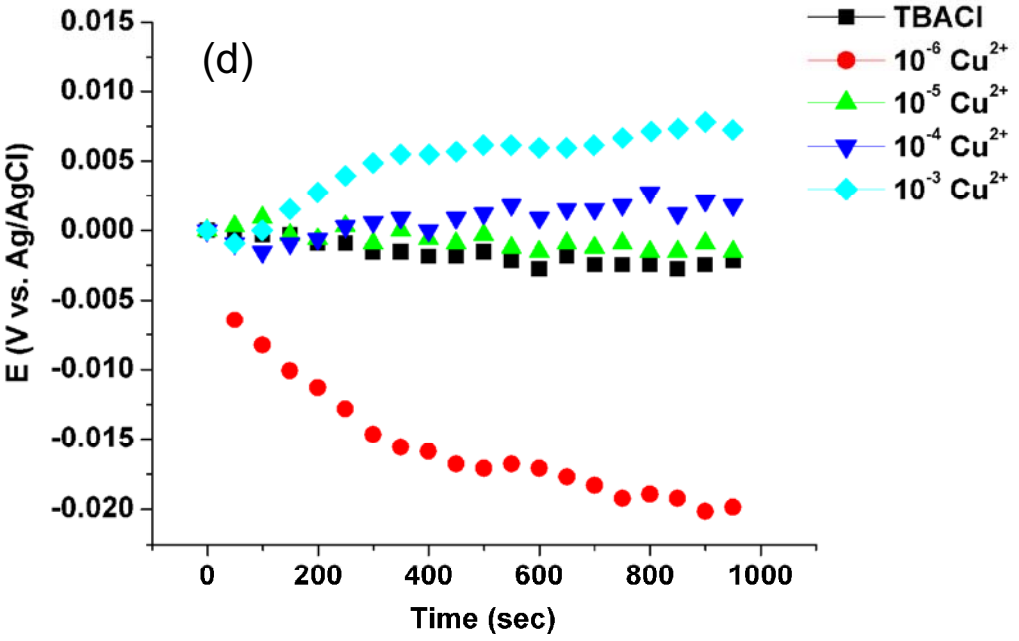
(d)
TBACl
10-6 Cu2+
10-5 Cu2+
10-4 Cu2+
10-3 Cu2+
E (V vs. Ag/AgCl)
Time (sec)
0.015
0.010
0.005
0.000
-0.005
-0.010
-0.015
-0.020
0
200
400
600
800
1000

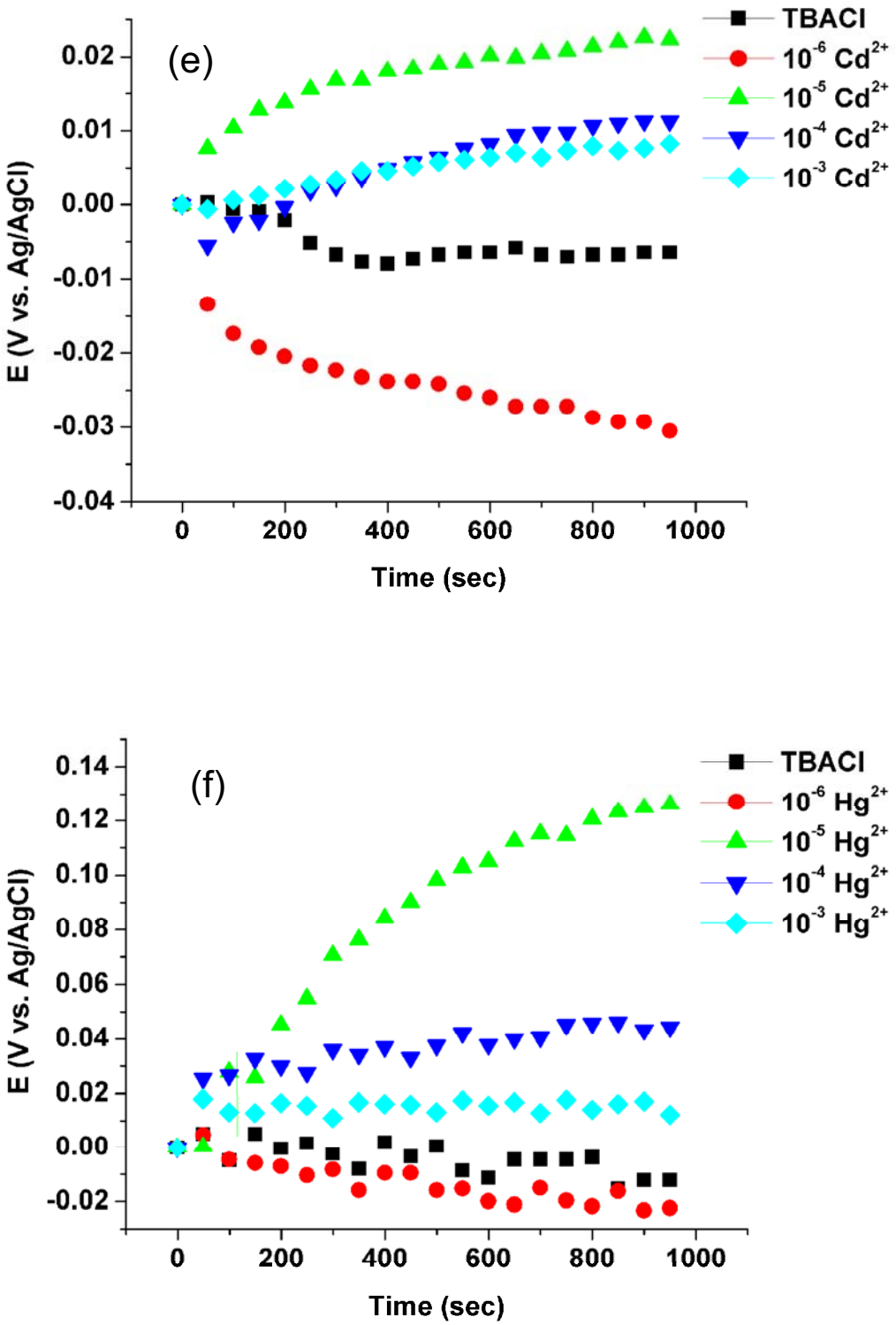

Figure S6. Potentiometric profiles of PCC-CBz on ITO in aqueous solution in different concentration of cations at 0 V: a) H^+, b) Ni^{2+}, c) Cd^{2+}, d) Co^{2+}, e) Cu^{2+}, f) Hg^{2+}.

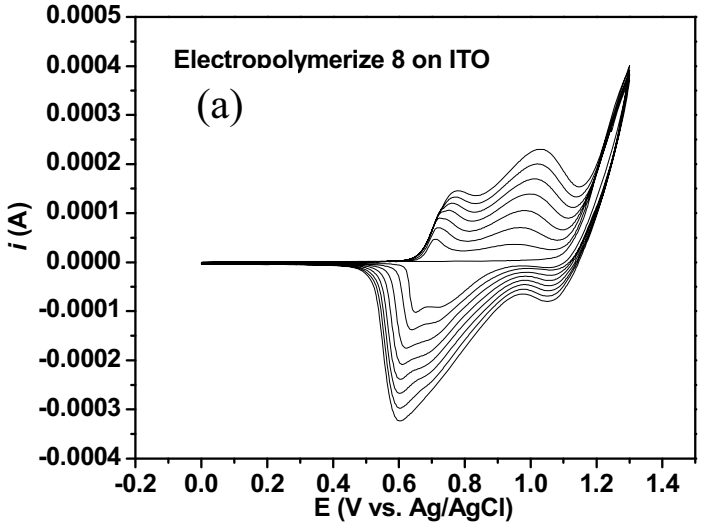
Electropolymerize 8 on ITO
(a)
i (A)
E (V vs. Ag/AgCl)
0.0005
0.0004
0.0003
0.0002
0.0001
0.0000
-0.0001
-0.0002
-0.0003
-0.0004
-0.2
0.0
0.2
0.4
0.6
0.8
1.0
1.2
1.4

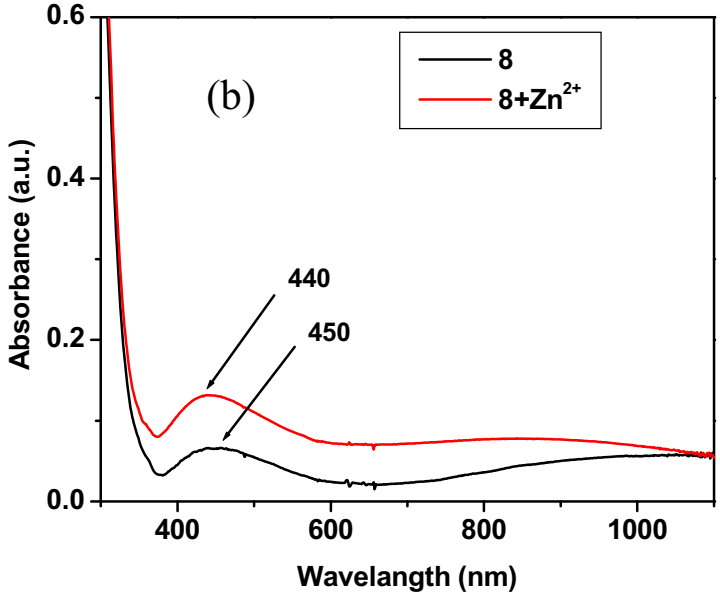
(b)
8
8+Zn2+
440
450
Absorbance (a.u.)
Wavelength (nm)
0.6
0.4
0.2
0.0
400
600
800
1000

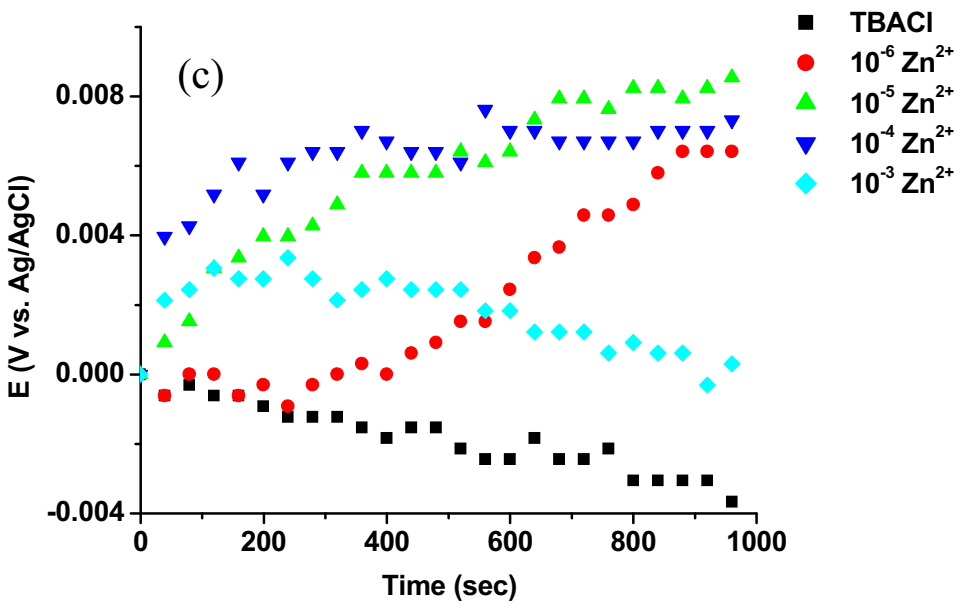

Figure S7. a) Cyclic voltammograms electrochemical cross-linking/deposition of **8** polymerization at a scan rate of 50 mv/s, 8 cycle deposited material on ITO substrates. b) The UV-Vis absorption spectrum of **8** films before and after addition of Zn^{2+}cations 10^{-3} M on ITO substrates c) Potentiometric profiles of **8** on ITO in aqueous solution in different concentration of Zn^{2+} at 0 V.

Supporting Information

Title: Conformation-selective Synthesis and Binding Properties of *N*-benzylhexahomotriaza-*p*-chlorocalix[3]-trinapthylamide

Authors: Chatthai Kaewtong,[1] Nongnuj Muangsin,[1] Narongsak Chaichit,[2] and Buncha Pulpoka*[1]

Content:

Experimental Section

NMR spectra were recorded on a Varian 400 MHz spectrometer in deuterated chloroform. MALDI-TOF mass spectra were recorded on a Biflex Bruker Mass spectrometer using 2-cyano-4-hydroxycinnamic acid (CCA) or 2,5-dihydroxy-benzoic acid (DHB) as a matrix. Elemental analyses were carried out on a CHNS/O analyzer (Perkin Elmer PE2400 series II). UV-vis absorption measurements were performed on a Hewlett Packard 8452A Diode Array Spectrometer. Infrared spectra were obtained on a Nicolet Impact 410 using KBr pellets. Column chromatography was carried out using silica gel (Kieselgel 60, 0.063 – 0.200 mm, Merck). All reagents were standard analytical grade and were used without further purification.

THF was distilled over sodium and benzophenone under nitrogen. Commercial grade solvents such as acetone, hexane, dichloromethane, methanol and ethyl acetate were distilled before used. Toluene and DMF were dried over CaH_2 and freshly distilled under nitrogen atmosphere prior to use.

X-ray data of compound 1 and 2a

X-ray data were collected on a Bruker SMART CCD area detector. The crystal structure was solved by direct methods and refined by full-matrix least-squares. All non-hydrogen atoms were refined anisotropically, and hydrogen atoms were refined using the riding model. All calculations were performed using a crystallographic software package, WinGX v1.64.05. Crystal data for **1**: $C_{84}H_{75}Cl_3N_6O_6 \bullet 3H_2O$, M_r = 1424.90, monoclinic, space group P-1, a = 16.1795(3) Å, b = 16.5809(3) Å, c = 16.6482(2) Å, α = 92.624(1)°, β = 105.880(1)°, γ = 112.174(1)°, V = 3921.97(11) Å^3, Z = 2, ρ_{calc} = 1.207 g cm^{-3}, $2\theta_{max}$ = 30.54°, Mo $K\alpha$ (λ = 0.71075 Å), μ = 0.176 mm^{-1}, θ-ω scans, T = 293(2)K, 28143 independent reflections, 20620 unique reflections ($I > 2.0\sigma(I)$), 924 refined parameters, $R1$ = 0.1276, Rw = 0.3142, $\Delta\rho_{max}$ = 1.204 e Å^{-3}, $\Delta\rho_{min}$ = -0.395 e Å^{-3}; CCDC 673516.

Crystal data for **2a** which 1 asymmetric unit contains 2 molecules: $C_{57}H_{60}Cl_3N_3O_9$, M_r = 1037.43, monoclinic, space group P-1, a = 13.3761(6)Å, b = 14.4152(7)Å, c = 28.8382(14)Å, α = 93.622 (1)°, β = 96.284(1)°, γ = 92.635(1)°, V = 5508.3(5) Å^3, Z = 4, ρ_{calc} = 1.251 g cm^{-3}, $2\theta_{max}$ = 30.55°, Mo $K\alpha$ (λ = 0.71075 Å), μ = 0.224 mm^{-1}, θ-ω scans, T = 293(2)K, 39,405 independent reflections, 28866 unique reflections ($I > 2.0\sigma(I)$), 1267 refined parameters, $R1$ = 0.0981, Rw = 0.2153, $\Delta\rho_{max}$ = 0.795 e Å^{-3}, $\Delta\rho_{min}$ = -0.389 e Å^{-3}; CCDC 673515.

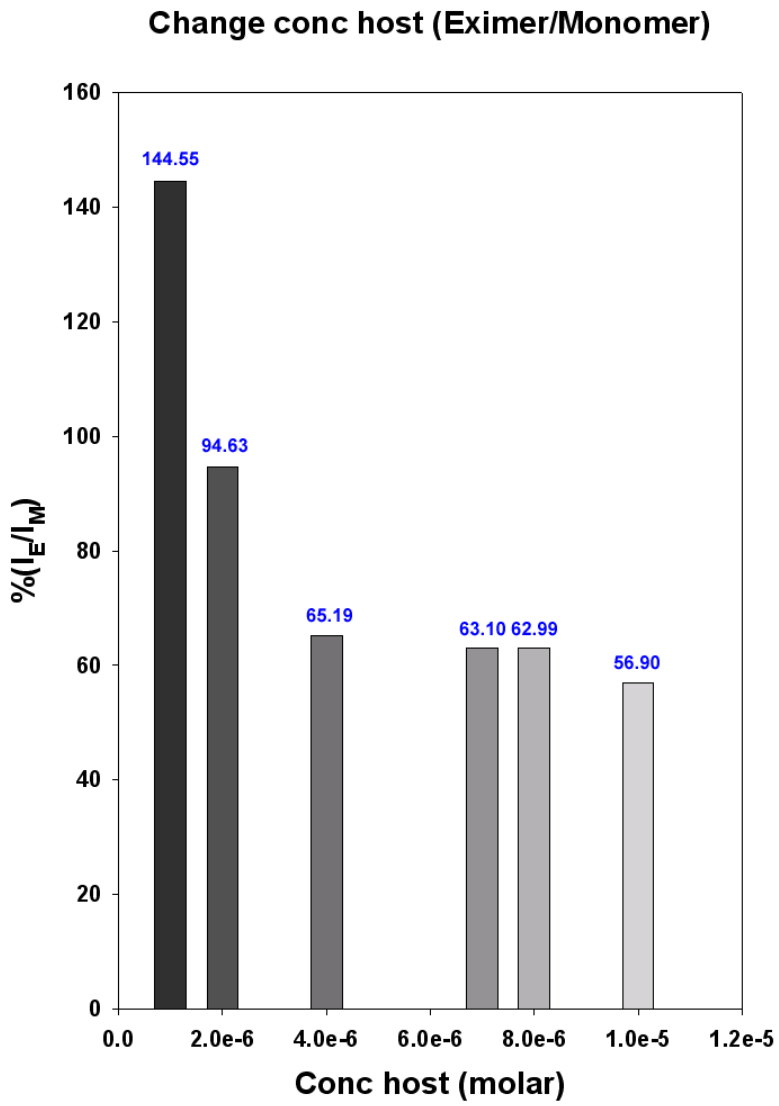

Figure S1. Plot of the ratio of excimer to monomer emission against concentration of ligand **1**.

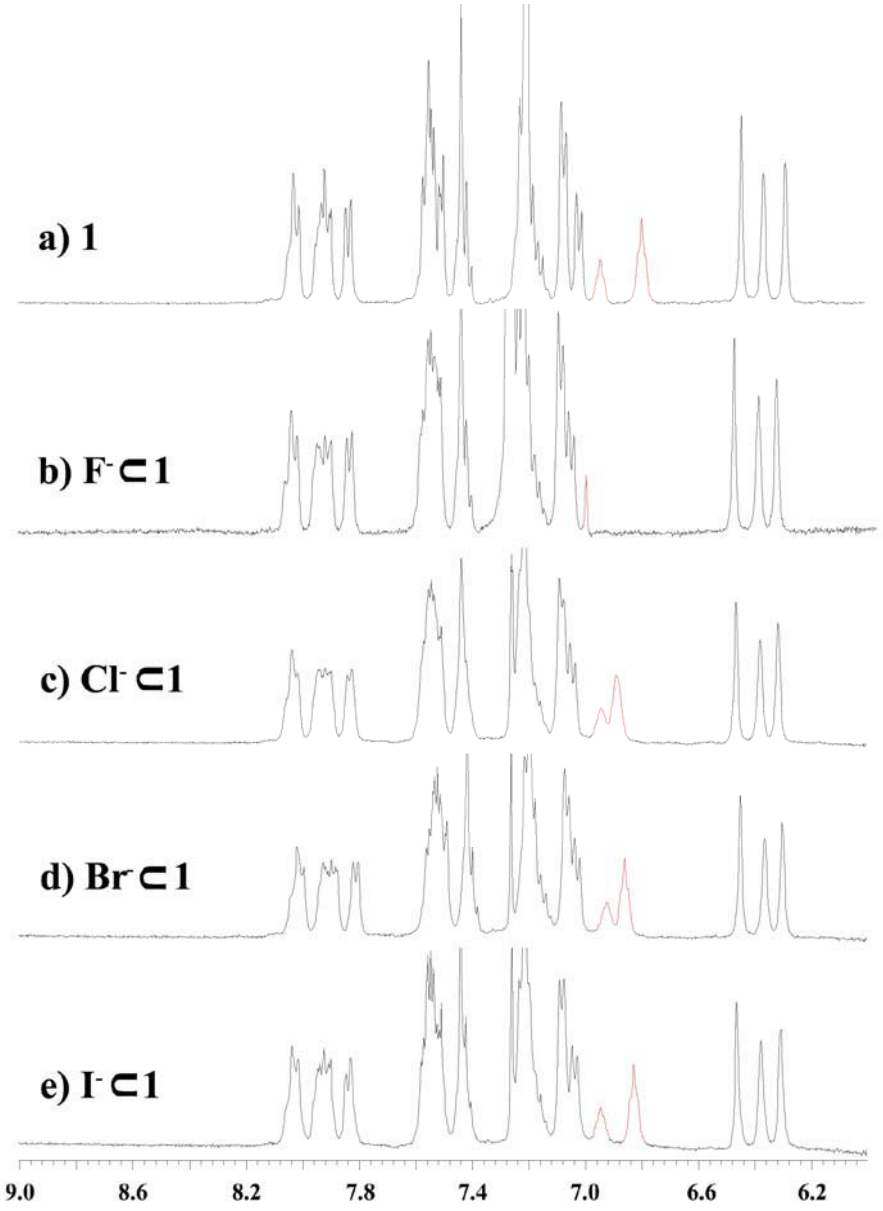
a) 1
b) F⁻⊂1
c) Cl⁻⊂1
d) Br⁻⊂1
e) I⁻⊂1
9.0
8.6
8.2
7.8
7.4
7.0
6.6
6.2

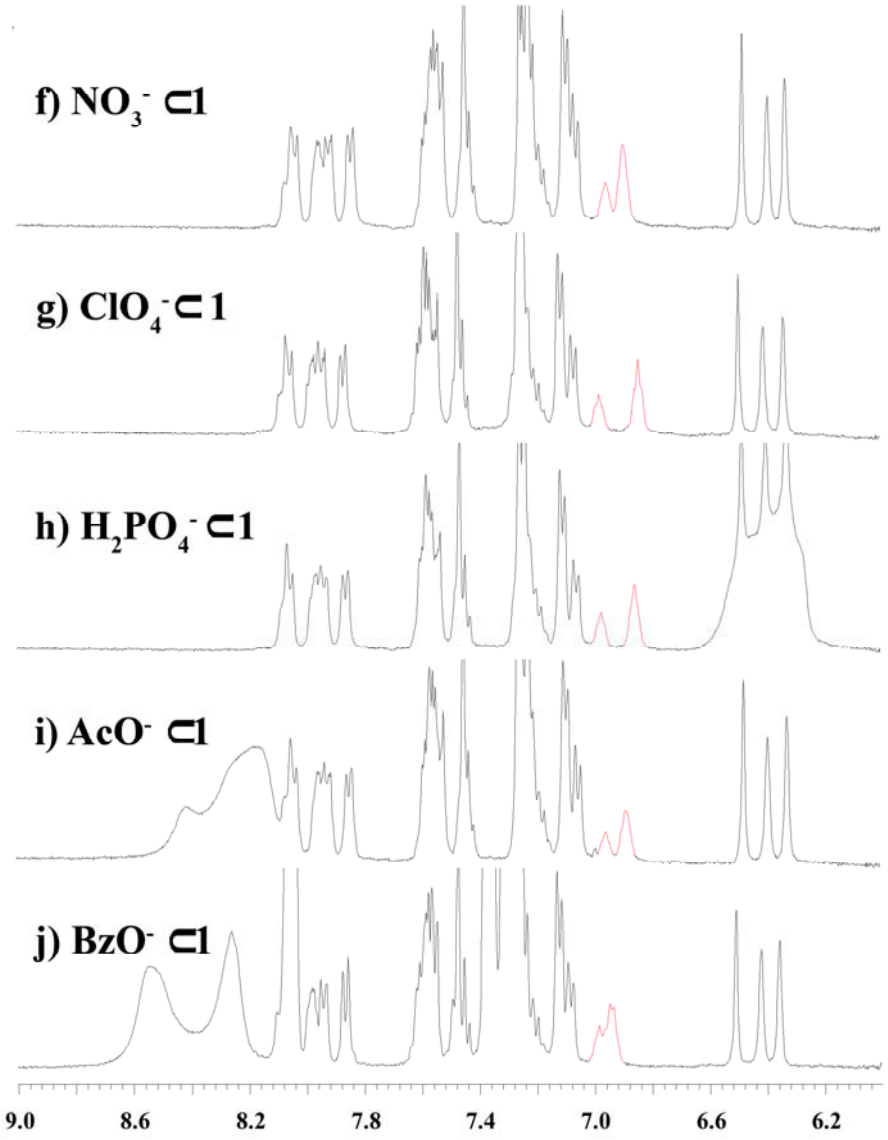

Figure S2. The ^{1}H-NMR spectra of **1** with 10 equivalents of TBAX in $CDCl_3$.

Complexation studies of ligand 1 by using UV-vis titrations

The complexation abilities of ligand **1** with cations and anions were investigated by using spectrophotometric titration in DMSO at 25°C. When necessary, Bu_4NPF_6 was employed to keep the ionic strength at 0.01 M.

2 mL of 0.03 nM ligand solution were placed in a spectrophotometric cell of 1cm path length. The spectrum was recorded from 260-360 nm. The solutions of a cation or an anion were added into the cell from a microburette. The mixture was stirred for 40 seconds after each addition and spectral variation was recorded. The stability constants were calculated from spectrometric data using the SIRKO program.[17]

Table S1. Variation in absorbances of compounds **1** in the absence or presence of various anions[a] (λ=293 nm).

Entry	Solution of ligand **1** with	A/A_0[b]
1.	free ligand **1**	1.00000
2.	TBA^+F^-	0.711418
3.	TBA^+Cl^-	1.027682
4.	TBA^+Br^-	0.835427
5.	TBA^+I^-	0.855821
6.	$TBA^+NO_3^-$	1.028281
7.	$TBA^+ClO_4^-$	1.012905
8.	$TBA^+H_2PO_4^-$	0.862922
9.	TBA^+AcO^-	0.723446
10.	TBA^+BzO^-	0.442596

[a]In DMSO, at 25°C, 0.03 mM of host and 1.2 mM of guests (in forms of tetrabutylammonium salts) were used. [b]A_0 and A are the absorbances of the host solution in the absence or presence of guests, respectively.

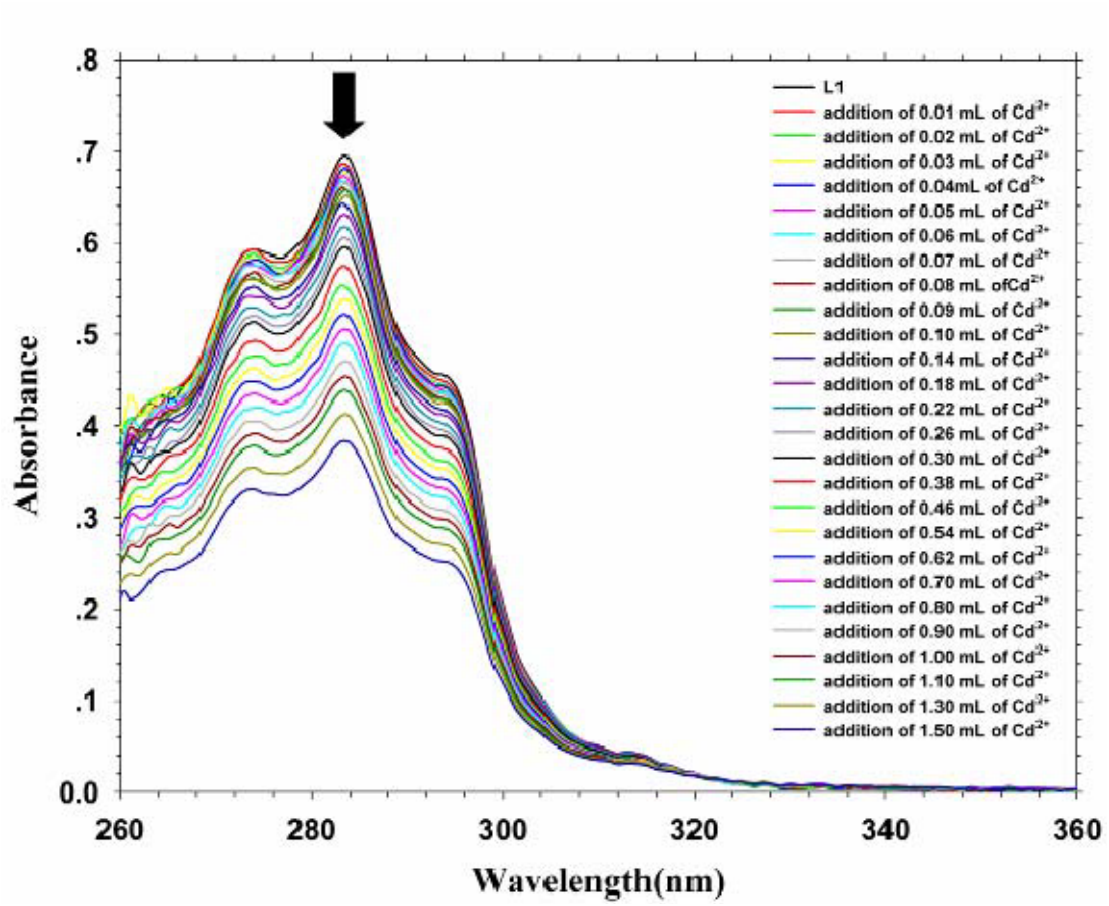

Figure S3. Spectral change in the UV-vis absorption of **1** ($C_L = 3\times10^{-5}$ M) upon addition of Cd^{2+} ($C_C = 1.2\times10^{-3}$ M) in DMSO ($0 \le C_A/C_L \le 30$).

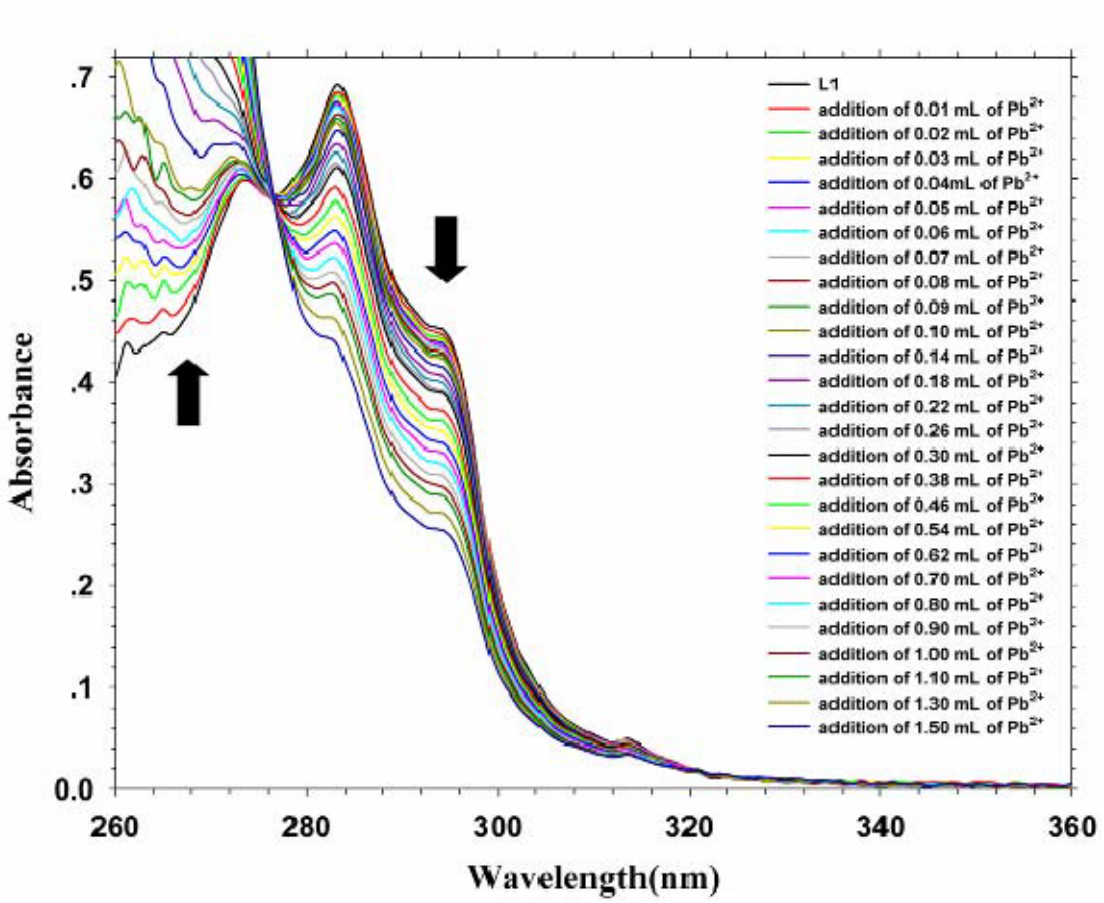

Figure S4. Spectral change in the UV-vis absorption of 1 ($C_L = 3\times10^{-5}$ M) upon addition of Pb^{2+} ($C_C = 1.2\times10^{-3}$ M) in DMSO ($0 \le C_A/C_L \le 30$).

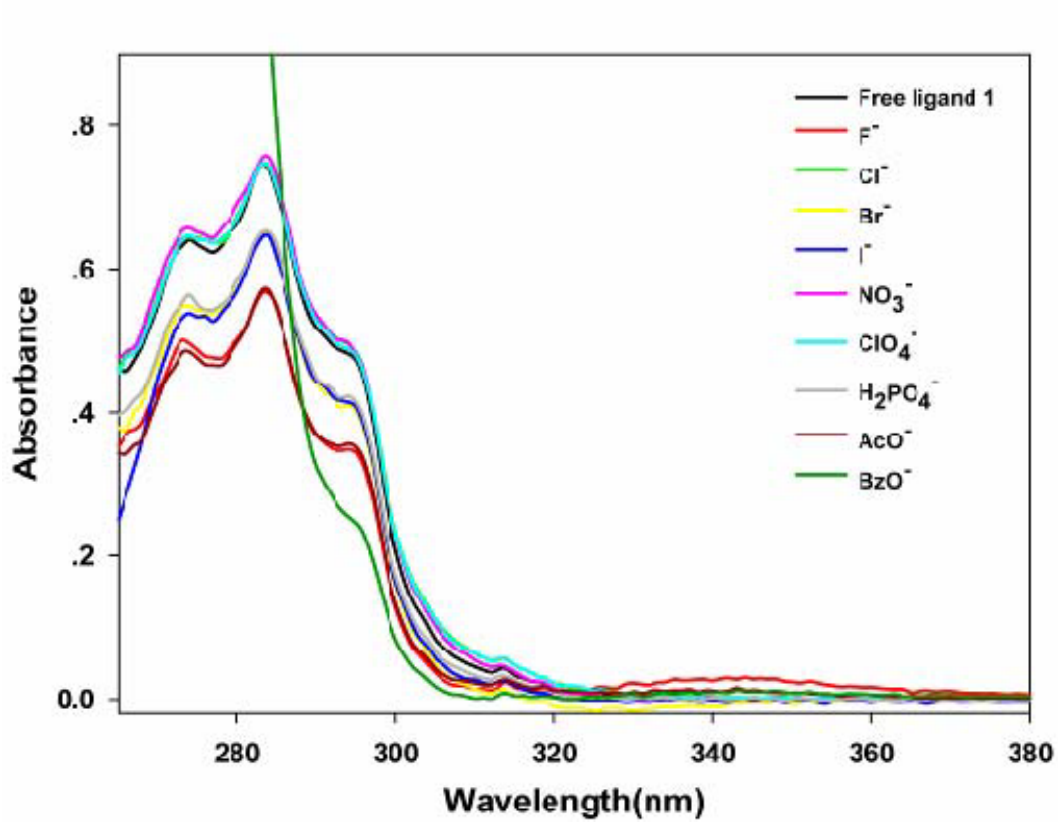

Figure S5. Spectral change of ligand **1** upon addition of 30 equivalents of TBAX.

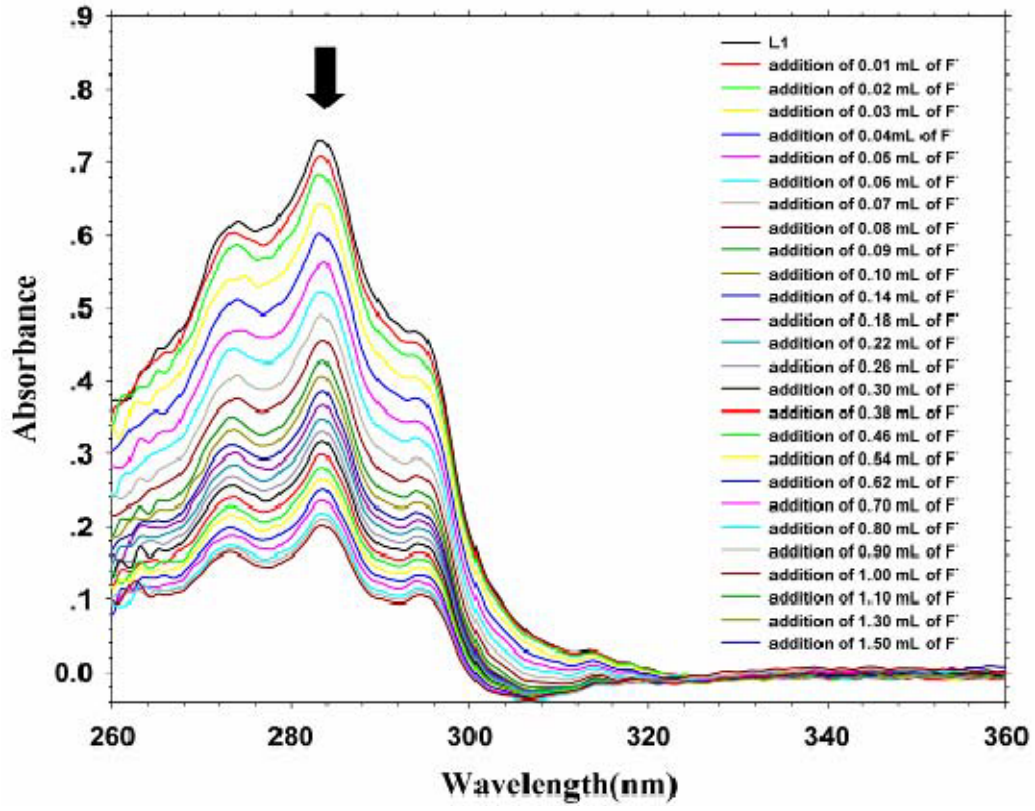

Figure S6. Spectral change in the UV-vis absorption of **1** ($C_L = 3\times10^{-5}$ M) upon addition of $NBu_4^+F^-$ ($C_A = 6\times10^{-4}$ M) in DMSO ($0 \le C_A/C_L \le 15$).

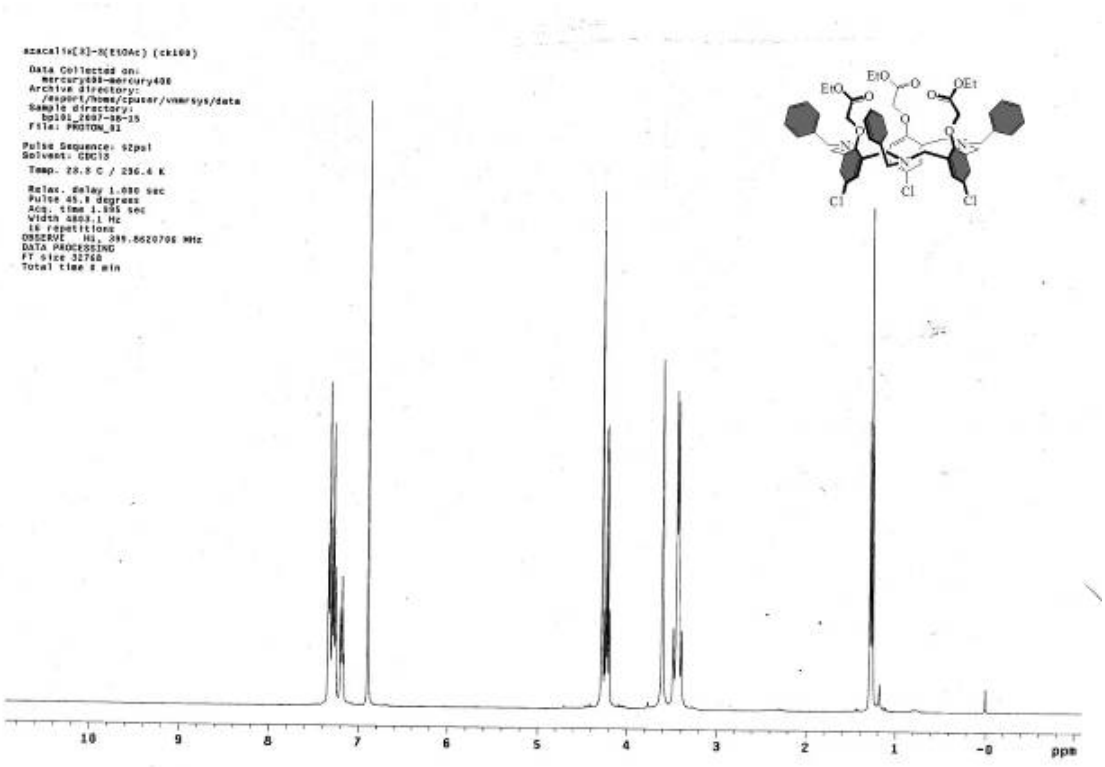

Figure S7. ^{1}H NMR spectrum of *N*-benzylhexahomotriaza-*p*-chloro-calix[3]-tri(ethyl acetate) (**2a**, cone) in $CDCl_3$ at 25 °C.

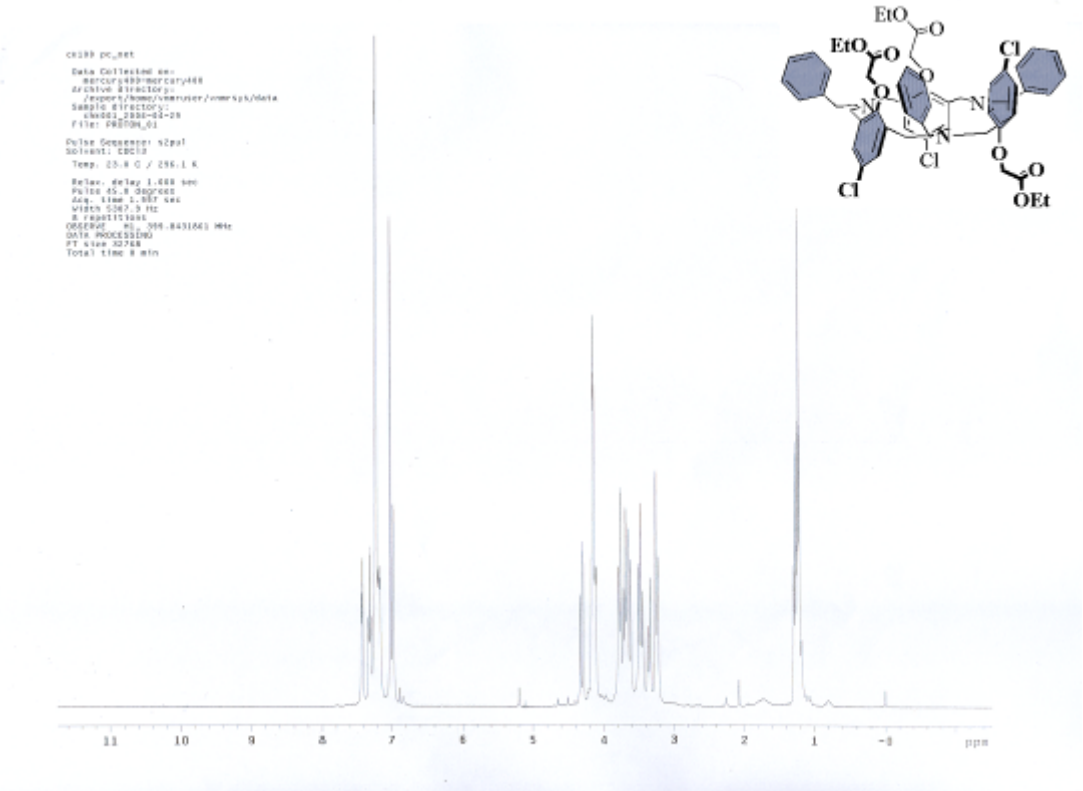

Figure S8. ^{1}H NMR spectrum of *N*-benzylhexahomotriaza-*p*-chloro-calix[3]-tri(ethyl acetate) (**2b**, partial cone) in $CDCl_3$ at 25 °C.

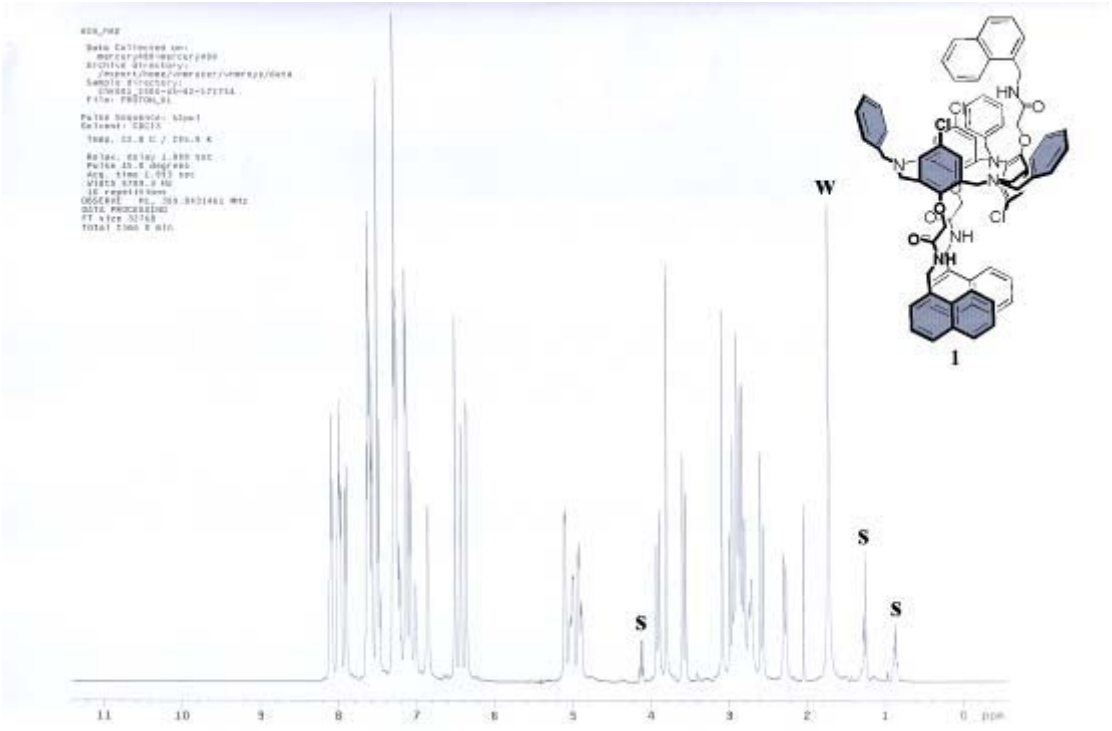

Figure S9. ^{1}H NMR spectrum of *N*-benzylhexahomotriaza-*p*-chlorocalix[3]-trinapthylamide (**1**) in $CDCl_3$ at 25 °C. Solvent and water peaks are labeled as "S" and "W", respectively.

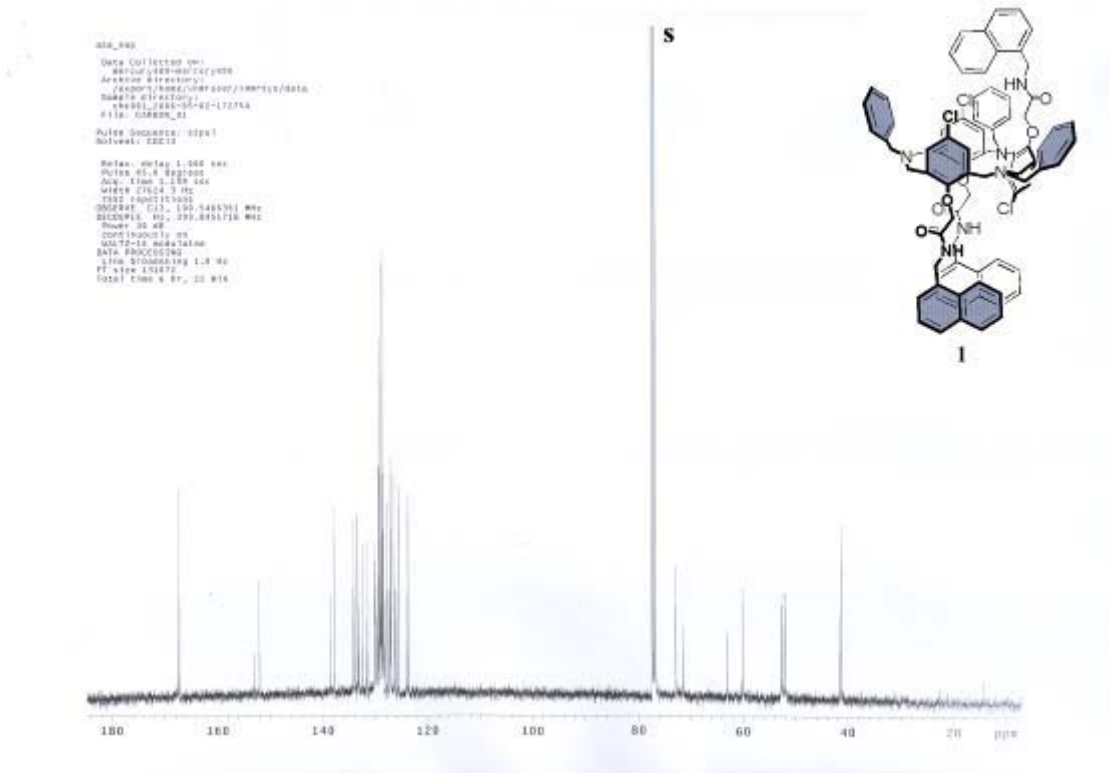

Figure S10. ^{13}C NMR spectrum of *N*-benzylhexahomo-triaza-*p*-chlorocalix[3]-trinapthylamide (**1**) in $CDCl_3$ at 25 °C.

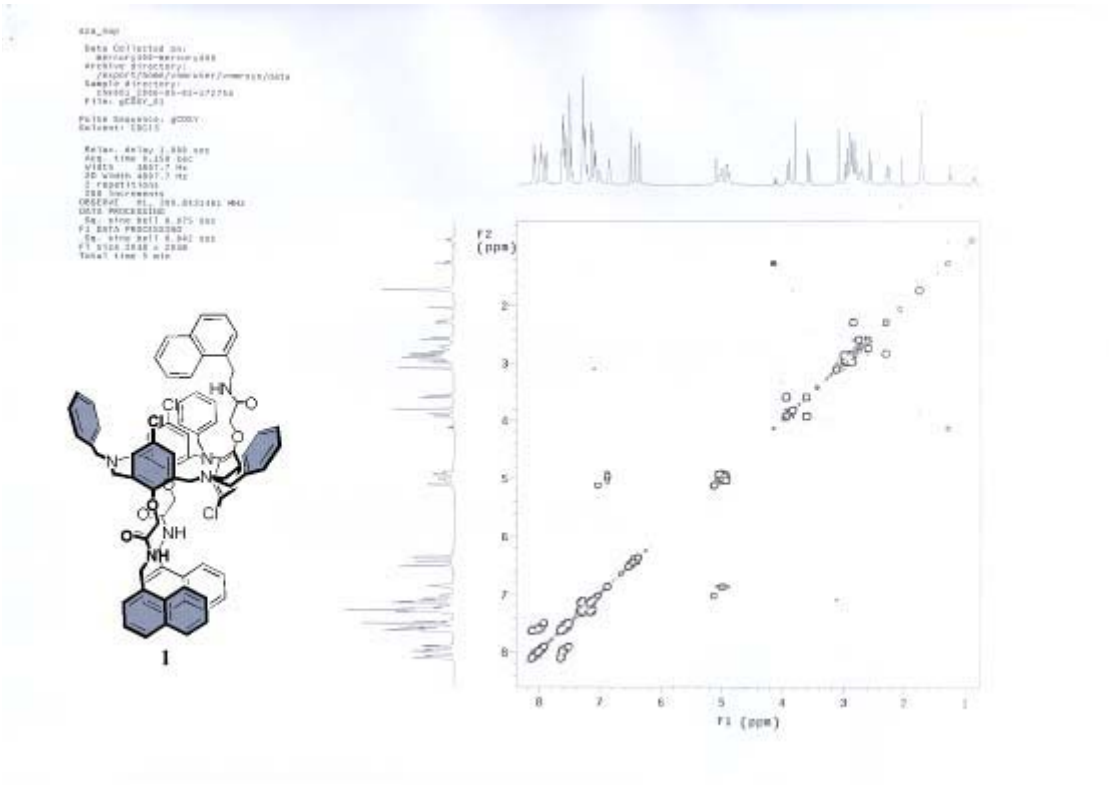

Figure S11. COSY spectrum of *N*-benzylhexahomotriaza-*p*-chlorocalix[3]-trinapthylamide (**1**) in $CDCl_3$ at 25 °C.

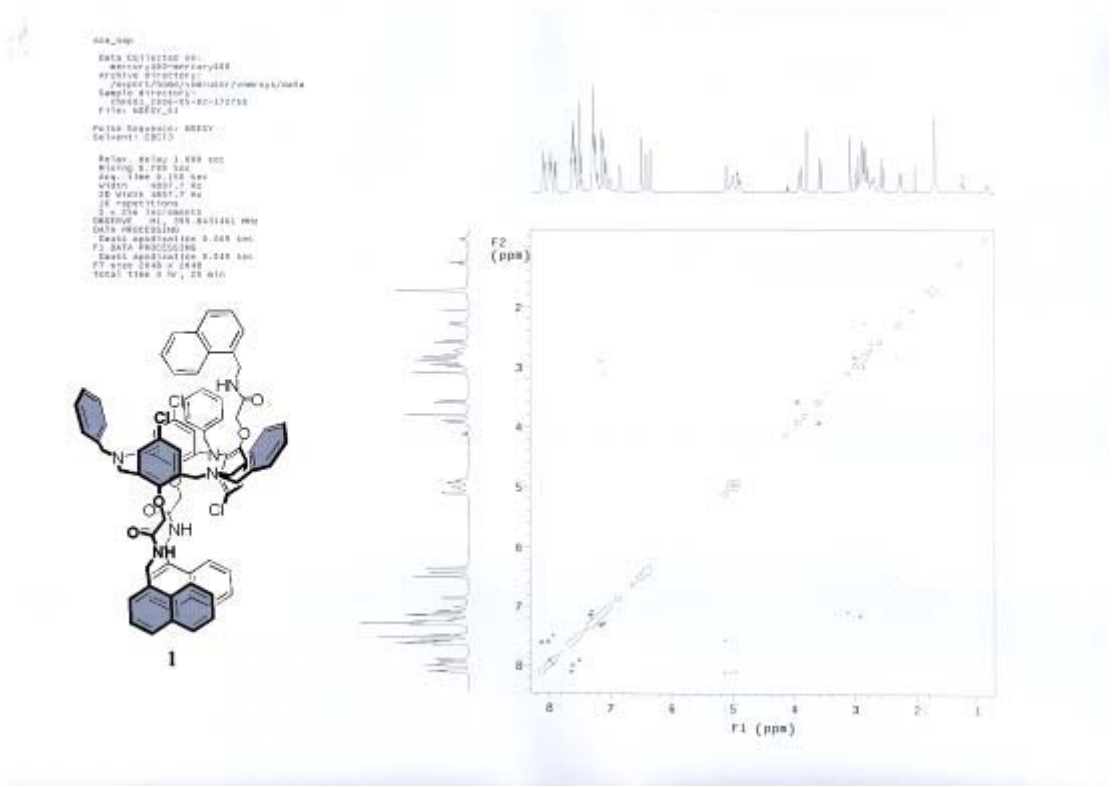

Figure S12. NOESY spectrum of *N*-benzylhexahomotriaza-*p*-chlorocalix[3]-trinapthylamide (**1**) in $CDCl_3$ at 25 °C.

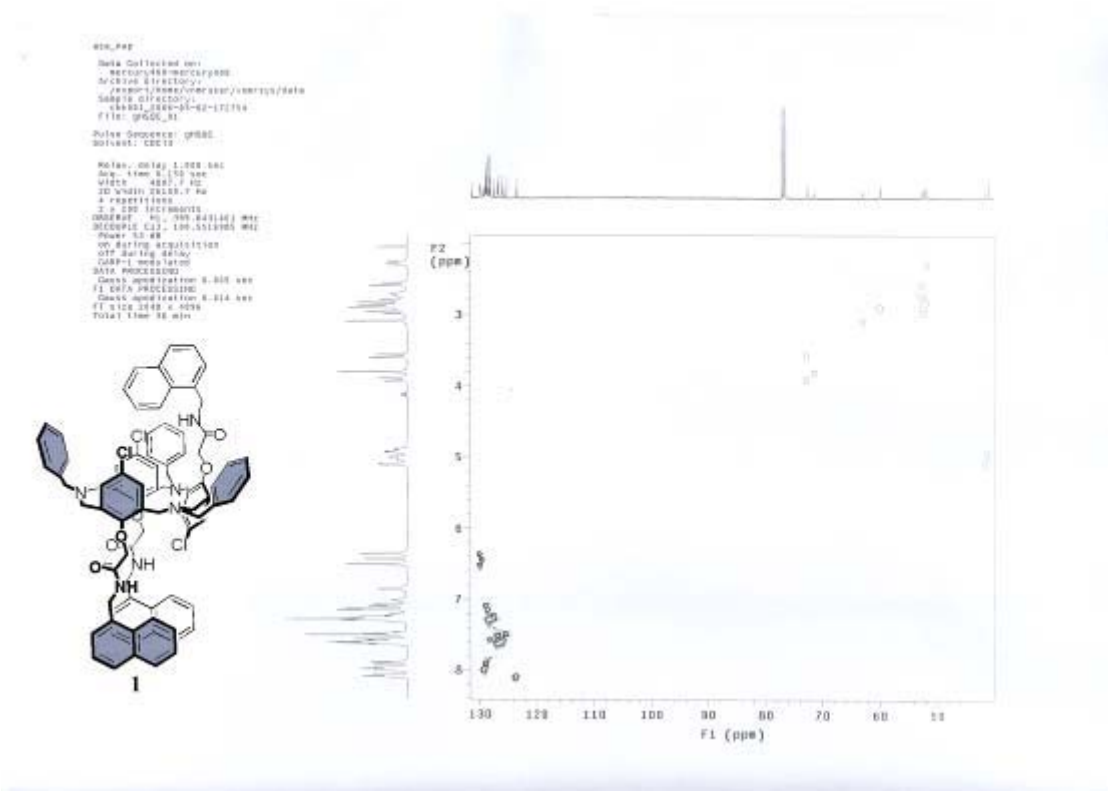

Figure S13. gHSQC spectrum of *N*-benzylhexahomotriaza-*p*-chlorocalix[3]-trinapthylamide (**1**) in $CDCl_3$ at 25 °C.

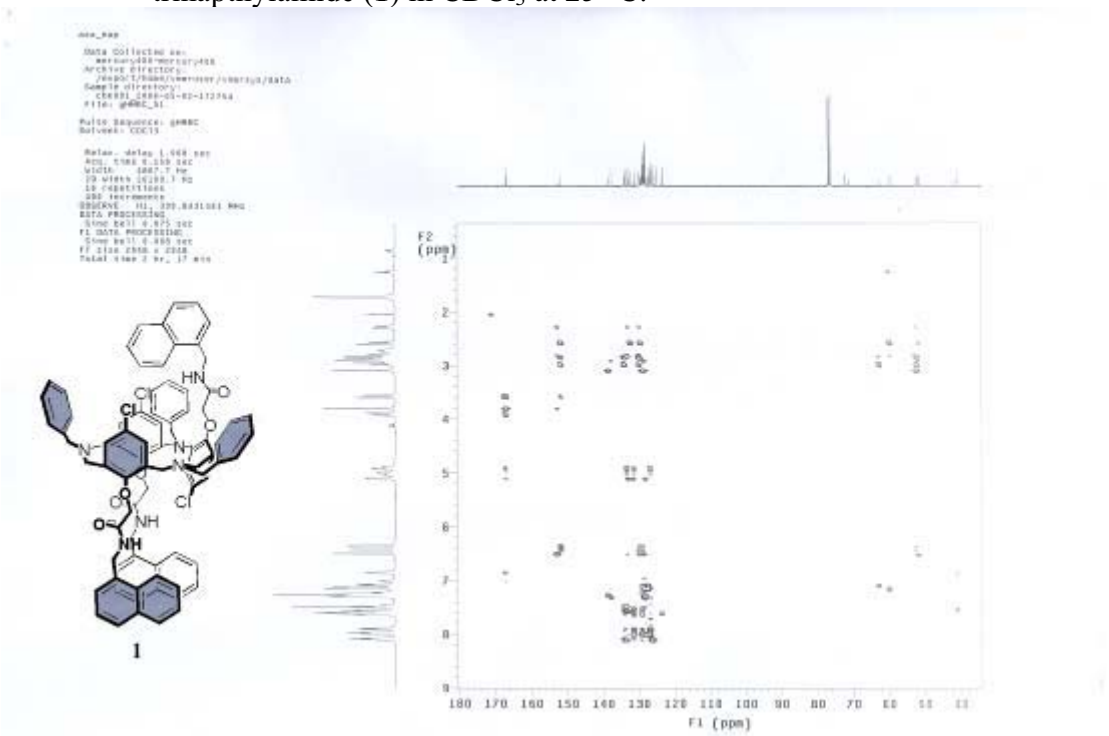

Figure S14. gHMBC spectrum of *N*-benzylhexahomotriaza-*p*-chlorocalix[3]-trinapthylamide (**1**) in $CDCl_3$ at 25 °C.

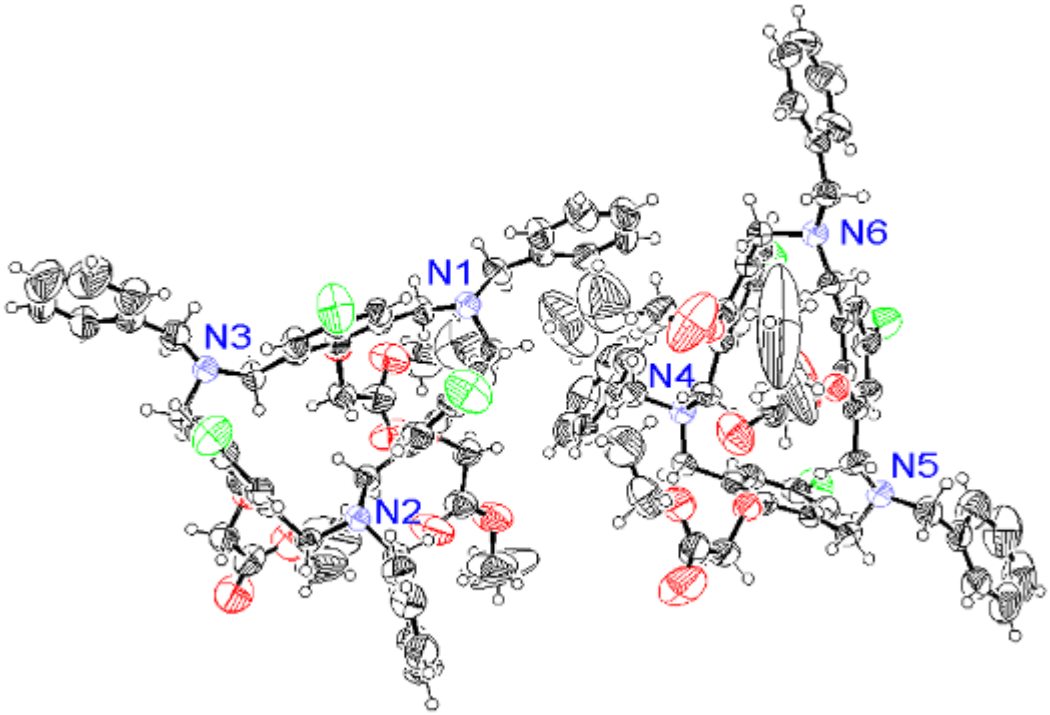

Figure S15. X-ray single crystal structure of *N*-benzylhexahomotriaza-*p*-chlorocalix[3]-tri(ethyl acetate) (**2a**)

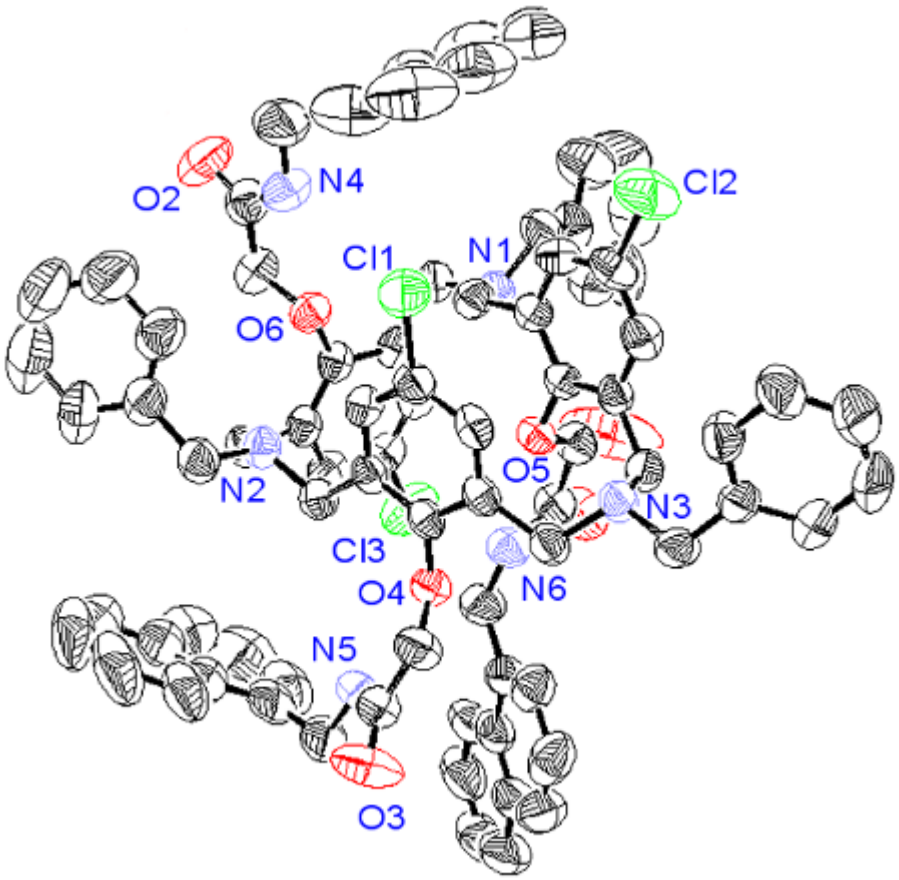

Figure S16. X-ray single crystal structure of *N*-benzylhexahomotriaza-*p*-chlorocalix[3]-trinapthylamide (**1**)

Subscriber access provided by CHULALONGKORN UNIV

Letter

Novel *C*-Symmetrical *N*-Hexahomotriazacalix[3]cryptand: A Highly Efficient Receptor for Halide Anions

Chatthai Kaewtong, Saowarux Fuangswasdi, Nongnuj Muangsin, Narongsak Chaichit, Jacques Vicens, and Buncha Pulpoka

Org. Lett., **2006**, 8 (8), 1561-1564• DOI: 10.1021/ol060052e • Publication Date (Web): 14 March 2006

Downloaded from http://pubs.acs.org on March 31, 2009

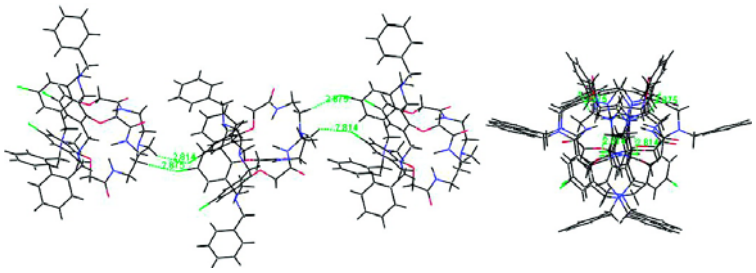

More About This Article

Additional resources and features associated with this article are available within the HTML version:

- Supporting Information
- Links to the 4 articles that cite this article, as of the time of this article download
- Access to high resolution figures
- Links to articles and content related to this article
- Copyright permission to reproduce figures and/or text from this article

View the Full Text HTML

ACS Publications
High quality. High impact.

Organic Letters is published by the American Chemical Society. 1155 Sixteenth Street N.W., Washington, DC 20036

ORGANIC LETTERS

2006
Vol. 8, No. 8
1561−1564

Novel C_{3v}-Symmetrical N_7-Hexahomotriazacalix[3]cryptand: A Highly Efficient Receptor for Halide Anions

Chatthai Kaewtong,[†] Saowarux Fuangswasdi,[†] Nongnuj Muangsin,[†] Narongsak Chaichit,[‡] Jacques Vicens,[§] and Buncha Pulpoka*,[†]

Supramolecular Chemistry Research Unit and Organic Synthesis Research Unit, Department of Chemistry, Faculty of Science, Chulalongkorn University, Bangkok 10330, Thailand, Department of Physics, Faculty of Science and Technology, Thammasat University at Rangsit, Pathumthani 12121, Thailand, and ECPM, Laboratoire de conception moléculaire (CNRS UMR 7512), 25 rue Becquerel, 67087 Strasbourg, France

buncha.p@chula.ac.th

Received January 9, 2006

ABSTRACT

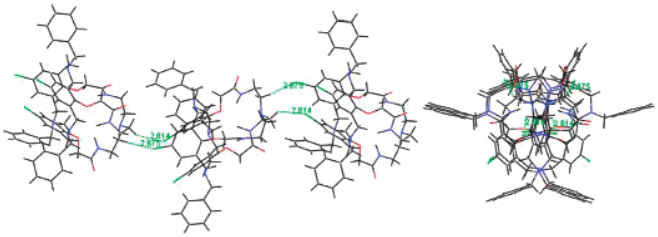

We report the synthesis of a novel C_{3v}-symmetrical N_7-hexahomotriazacalix[3]cryptand (1). Compound 1 was shown to be in a fixed cone conformation by ^{1}H NMR spectroscopy and X-ray single-crystal structure determination. Complexation studies showed that 1 is a selective receptor for halide ions. The effects of zinc metal cation on the receptor (1–Zn^{2+}) upon anion recognition are also shown.

Considerable attention has been paid to calixarenes and related compounds due to the molecular recognition properties they display.[1] The name homoazacalixarene (or azacalixarene) is currently used to indicate in a specific manner the calixarene analogues in which CH_2 groups are partly or completely replaced by CH_2NRCH_2.[2] The presence of soft nitrogen atoms in azacalixarenes is envisioned to bind soft cations such as transition metals according to the hard soft acid and base principle (HSAB) as well as other specific features such as building sophisticated receptors, metal ligand systems, etc.[2b,c] Indeed, such sophisticated ligands can be obtained by functionalization not only at the upper rim and/or lower rim, as usually done for calixarenes, but also within the macrocycle cup at the level of *N*-sidearms.[2]

Some examples have been given leading to an improvement of their ability to complex.[3] In this paper, we have

[†] Chulalongkorn University.
[‡] Thammasat University at Rangsit.
[§] ECPM.

(1) (a) *Calixarenes 2001*; Asfari, Z., Bhmer, V., Harrowfield, J., Vicens, J., Eds.; Kluwer Academic Publishers: Dordrecht, 2001. (b) *Calixarenes in Action*; Mandolini, L., Ungaro, R., Eds.; Imperial College: London, 2000. (c) Lumetta, G. J.; Rogers, R. D.; Gopalan, A. S. *Calixarenes for separation*; ACS Symposium Series; American Chemical Society: Washington, DC, 2000. (d) Gutsche, C. D. In *Calixarenes Revisited*; Stoddart, J. F., Ed.; The Royal Society of Chemistry: Cambridge, 1998. (e) *Calixarenes: a Versatile Class of Macrocyclic Compounds*; Vicens, J., Bhmer, V., Eds.; Kluwer Academic Publishers: Dordrecht, 1991. (f) Gutsche, C. D. In *Calixarenes*; Stoddart, J. F., Ed.; The Royal Society of Chemistry: Cambridge, 1989. (g) Pulpoka, B.; Vicens, J. *J. Nanobioechnol.* **2004**, *1*, 55.

(2) (a) Masci, B. In ref 1a, Chapter 12. (b) Takemura, H. *J. Inclusion Phenom. Macro.* **2002**, *42*, 1698. (c) Takemura, H.; Shimmyozu, T.; Inazh, T. *Coord. Chem. Rev.* **1996**, *156*, 183.

10.1021/ol060052e CCC: $33.50 © 2006 American Chemical Society
Published on Web 03/14/2006

addressed the problem of complexation of anions and, more generally, of ion pairs. Current efforts aim at developing supramolecular systems that simultaneously bind both a cation and an anion. Two strategies have been presented in the literature: (1) the so-called "dual receptor strategy" involving a binary mixture of a cation-receptor and an anion-receptor[4] and (2) the so-called "ditopic receptor strategy" consisting of a single ditopic receptor with defined cation- and anion-binding sites.[5] With this in mind, we have chosen azacalix[3]arene[1a,2b,c] to elaborate a novel ditopic receptor. This choice was in part due to the fact that not only does their chemistry have a high potential to be developed for ditopic receptors but also their structural C_{3v} symmetry accompanied by a hydrophobic cavity wider than that of calix[4]arene is also able to accept large substrates.

In this paper, we report the synthesis, the conformational analysis, the X-ray crystal structure, and the binding properties of C_{3v}-symmetrical N_7-hexahomotriazacalix[3]cryptand or N_7-azacalix[3]cryptand (**1**).

Scheme 1. Preparation of N_7-Azacalix[3]cryptand (**1**)

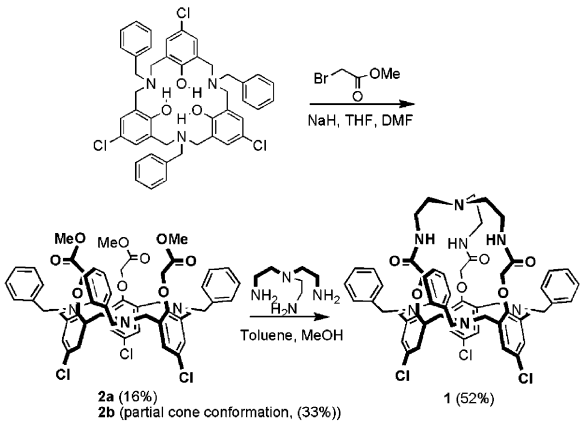

Our first idea was to design a preorganized receptor for anion binding. N_7-Azacalix[3]cryptand (**1**) combines a C_{3v}-symmetrical *N*-benzylhexahomotriaza-*p*-chlorocalix[3]arene element and a 3-fold symmetric tren residue[6] via an *amidation* reaction. This combination result is a system that can bind anions through hydrogen bonding with primary acetamide groups. The synthesis of **1** (Scheme 1) began by the reaction of *N*-benzylhexahomotriaza-*p*-chlorocalix[3]arene[3b] with 3 equiv of $BrCH_2CO_2Me$ and 7 equiv of NaH as base in THF for 2 days. Column chromatography (silica gel, 90/10 hexane/ethyl acetate) of the crude residue gave two *N*-benzylhexahomotriaza-*p*-chlorocalix[3]tri(methyl acetate) isomers: **2a** (deep yellow oil, 16%) and **2b** (pale yellow solid, 33%). Based on ^{1}H NMR, IR, and MS spectrocopies, **2a** was shown to be in a *cone conformation* while the *partial-cone conformation* was attributed to **2b**. Compound **2a** was refluxed with 3 equiv of $N(CH_2CH_2NH_2)_3$ or tren in a 1:1 mixture of methanol/toluene for 5 days to afford N_7-azacalix-[3]cryptand (**1**) in 52% yield.

MALDI TOF MS, ^{1}H NMR, ^{13}C NMR, 2D NMR (COSY, gHSQC and gHMBC), and elemental analysis fully confirmed the structure of N_7-azacalix[3]cryptand (**1**). The cone conformation was demonstrated by ^{1}H NMR and X-ray analysis. In its ^{1}H NMR spectrum (Figure 1a), the azacalix-[3] macroring was deduced to be in cone conformation due to the presence of only one singlet at 3.63 ppm for the

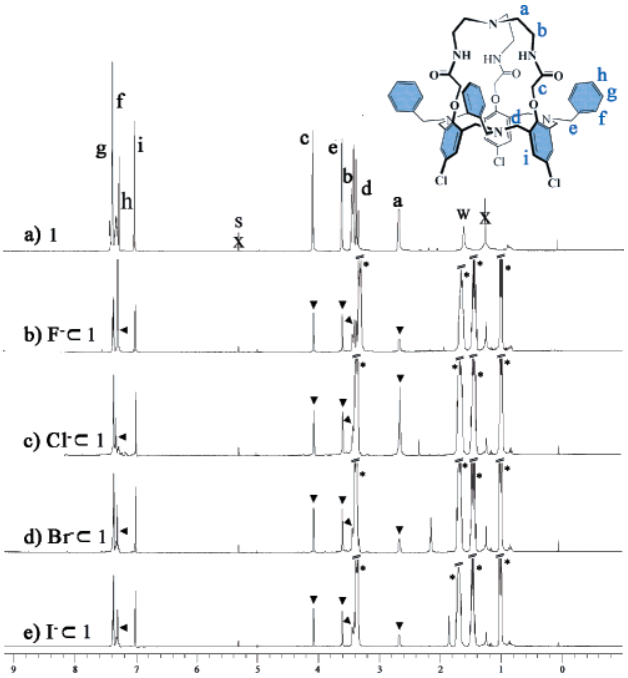

Figure 1. ^{1}H NMR spectra (400 MHz, $CDCl_3$): (a) N_7-azacalix-[3]cryptand (**1**), (b) **1**⊃F^-, (c) **1**⊃Cl^-, (d) **1**⊃Br^-, and (e) **1**⊃I^- complexes obtained upon addition of $NBu_4^+X^-$ (10 equiv) into a $CDCl_3$ solution of **1**. ▼: signals of **1**⊃X^-. *: signals of NBu_4^+. Residual solvents and partially protonated water are labeled as "S" and "W", respectively.

(3) (a) Hampton, P. D.; Tong, W.; Wu, S.; Duesler, E. N. *J. Chem. Soc., Perkin Trans. 2* **1996**, 1127. (b) Thury, P.; Nierlich, M.; Vicens, J.; Takemura, H. *J. Chem. Soc., Dalton Trans.* **2000**, 279. (c) Thury, P.; Nierlich, M.; Vicens, J.; Takemura, H. *Polyhedron* **2000**, *19*, 2673. (d) Thury, P.; Nierlich, M.; Vicens, J.; Takemura, H. *Polyhedron* **2001**, *20*, 3183.

(4) Recent examples of dual receptor systems: (a) Byriel, K. A.; Gasperov, V.; Gloe, K.; Kennard, C. H. L.; Leong, A. J.; Lindoy, L. F.; Mahinay, M. S.; Pham, H. T.; Tasker, P. A.; Thorp, D.; Turner, P. *J. Chem. Soc., Dalton Trans.* **2003**, 3034. (b) Cafeo, G.; Gargiulli, C.; Gattuso, G.; Kohnke, F. H.; Notti, A.; Occhipinti, S.; Pappalardo, S.; Parisi, M. F. *Tetrahedron Lett.* **2002**, *43*, 8103. (c) Cafeo, G.; Gattuso, G.; Kohnke, F. H.; Notti, A.; Occhipinti, S.; Pappalardo, S.; Parisi, M. F. *Angew. Chem., Int. Ed.* **2002**, *41*, 2122. (d) Qian, Q.; Wilson, G. S.; Bowman-James, K.; Girault, H. H. *Anal. Chem.* **2001**, *73*, 497. (e) Kavallieratos, K.; Moyer, B. A. *Chem. Commun.* **2001**, 1620. (f) Kavallieratos, K.; Sachleben, R. A.; Van Berkel, G. J.; Moyer, B. A. *Chem. Commun*. **2000**, 187.

(5) For recent papers that discuss ditopic salt-binding receptors, see the following: (a) Tumcharern, G.; Tuntulani, T.; Coles, S. J.; Hursthouse, M. B.; Kilburn, J. D. *Org. Lett.* **2003**, *5*, 4971. (b) Kotch, F. W.; Sidorov, V.; Lam, Y. F.; Kayser, K. J.; Li, H.; Kaucher, M. S.; Davis, J. T. *J. Am. Chem. Soc.* **2003**, *125*, 15140. (c) Bourgeois, J.; Fujita, M.; Kawano, M.; Sakamoto, S.; Yamaguchi, K. *J. Am. Chem. Soc.* **2003**, *125*, 9260. (d) Tongraung, P.; Chantarasiri, N.; Tuntulani, T. *Tetrahedron Lett.* **2003**, *44*, 29. (e) Zhou, L.; Sun, H.; Li, H.; Wang, H.; Zhang, X.; Wu, S.; Lee, S. *Org. Lett.* **2004**, *6*, 1071. (f) Plieger, P. G.; Tasker, P. A.; Galbraith, S. G. *J. Chem. Soc., Dalton Trans.* **2004**, 313.

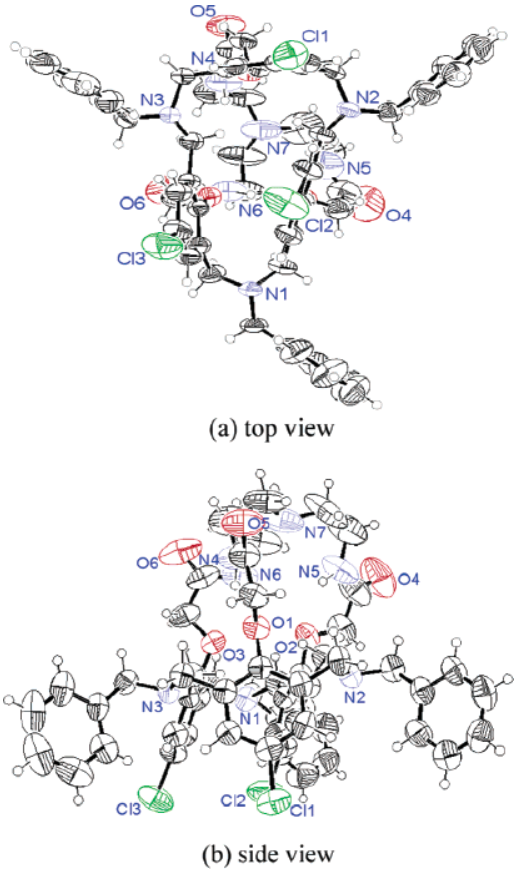

Figure 2. ORTEP drawing of N_7-azacalix[3]cryptand (**1**). The displacement ellipsoids are drawn at the 50% probability level.

ArCH_2N protons showing the retained C_{3v} symmetry of the molecule. X-ray single crystallographic analysis[7] clearly revealed that **1** was in a cone conformation (see Figure 2). They mutually interact outside the cavity to furnish a unique crytal structure stabilized by intermolecular CH/Cl hydrogen bond interactions (see Figure S11 in the Supporting Information).

The ability of **1** to include anions was investigated by ^{1}H NMR spectroscopy. $CDCl_3$ solutions of **1** were reacted with 10 equiv of tetrabutylammonium halides ($NBu_4^+X^-$). All of the resulting ^{1}H NMR spectra (see Figure 1b−e and Table S1 in the Supporting Information) displayed peaks shifts of OCH_2CO, NCH_2Ar, and NCH_2CH_2 toward downfield. This implies the formation of *endo* complexes while keeping the C_{3v} symmetry of the free ligand. Moreover, the signals of aromatic protons of benzyl moieties also displaced in the same manner, which may be due to a conformational organization.

The binding abilities of X^- by **1** were evaluated in DMSO by UV−vis spectroscopy (see Figure S1 in the Supporting Information). In all cases, hypochromic shifts were observed upon addition of $NBu_4^+X^-$ into solutions of **1**. The stoichiometries and stability constants of the complexes were refined by the SIRKO[8] program and are summarized in Table 1. It can be seen that **1** prefers to complex halide anions over CH_3COO^-, $PhCOO^-$, NO_3^-, PF_6^-, and ClO_4^- by forming 1:1 complexes.

Table 1. Stability Constants (log β)[a] of N_7-Azacalix[3]cryptand (1) Complexes with Anion in DMSO by UV−vis Titration Method (T = 25 °C, I = 0.01 M Bu_4NPF_6)

anions	log β (M^{-1})	% FA[b]
F^-	2.78 (0.01)[c]	40.80
Cl^-	4.55 (0.03)[c]	1.38
Br^-	3.97 (0.01)[c]	4.97
I^-	2.72 (0.01)[c]	43.87
NO_3^-	1.77 (0.01)[c]	89.87
ClO_4^-	undetermined	
CH_3COO^-	2.92 (0.01),[c] 6.06(0.01)[d]	0.03
$PhCOO^-$	2.36 (0.06),[c] 6.26(0.01)[d]	0.04

[a] Mean values of $n \geq 3$ independent determinations, with standard deviation σ_{n-1} on the mean in parentheses. [b] Percentage of various free halide anion at C_L, $C_A = 10^{-3}$ M. [c] 1:1 complex (AL). [d] 2:1 complex (A_2L).

Anion selectivity of **1** was obtained (as percentage of various free halide anion (% FA) (Table 1 and Figure S3 in the Supporting Information) by calculations using the Haltafall program.[9] For the halide ions, it may be concluded that **1** prefers to bind $Cl^- > Br^- > I^- > F^-$. This implies that the cavity size of receptor **1** is suitable for complexation with Cl^-. Though the NO_3^- ion (1.79 Å) has a similar size compared with the Cl^- ion (1.81 Å), the satibility constant of the NO_3^- complex is inferior to that of Cl^-. This can be explained by the ease of orientation of the anion inside the rigid cavity of receptor **1** to form hydrogen bonds with amide groups.

(6) Some examples are already known of "tripod-aza" receptor molecules combining calix units and tren: (a) Abidi, R.; Oueslati, I.; Amri, H.; Thuéry, P.; Nierlich, M.; Asfari, Z.; Vicens, J. *Tetrahedron Lett.* **2001**, *42*, 1685. (b) Tuntulani, T.; Thavornyutikarn, P.; Poompradub, S.; Jaiboon, N.; Ruangpornvisuti, V.; Chaicahit, N.; Asfari, Z.; Vicens, J. *Tetrahedron* **2002**, *58*, 10277. (c) Tuntulani, T.; Poompradub, S.; Thavornyutikarn, P.; Jaiboon, N., Ruangpornvisuti, V.; Chaicahit, N.; Asfari, Z.; Vicens, J. *Tetrahedron Lett.* **2001**, *42*, 5541. (d) Tuntulani, T.; Ruangpornvitusi, V.; Tantikunwatthara, N.; Ngampaboonsombut, O.; Seangprasertkij-Magee, R.; Asfari, Z.; Vicens, J. *Tetrahedron Lett.* **1997**, *38*, 3985. (e) Jabin, I.; Reinaud, O. *J. Org. Chem.* **2003**, *68*, 3416. (f) Darbost, U.; Zeng, X.; Rager, M.-N.; Giorgi, M.; Jabin, I.; Reinaud, O. *Eur. J. Inorg. Chem.* **2004**, 4371.

(7) X-ray data were collected on a Bruker SMART CCD area detector. The crystal structure was solved by direct methods and refined by full-matrix least-squares. All non-hydrogen atoms were refined anisotropically, and hydrogen atoms were refined using the riding model. All calculations were performed using a crystallographic sotware package, WinGX v1.64.05.[14] Crystal data for 1: M_r = 1095.3, monoclinic, space group $P2_1/n$, a = 13.297(2) Å, b = 19.191(3) Å, c = 23.602(5) Å, β = 97.599(1)°, V = 5969.82(8)^3, Z = 4, ρ_{calc} = 1.120 g cm^{-3}, $2\theta_{max}$ = 57.4°, Mo Kα (λ = 0.71075), μ = 0.71 cm^{-1}, $\theta-\omega$ scans, T = 293(2) K, 42, 269 independent reflections, 16,815 observed reflections ($I > 3.0\sigma(I)$), 340 refined paramaters, R_1 = 0.092, R_w = 0.136, $\Delta\rho_{max}$ = 2.38 e^{-3}, $\Delta\rho_{max}$ = −2.26 e^{-3}; CCDC 292414. See the Supporting Information for crystallographic data in CIF format.

(8) Vetrogon, V. I.; Lukyanenko, N. G.; Schwing-well, M. J.; Arnaud-Neu, F. *Talanta* **1994**, *41*, 2105.

(9) (a) Ingri, N.; Kakolowicz, W.; Sillen, L. G.; Warnqvist, B. *Talanta* **1967**, *14*, 1261. (b) Lamb, J. D.; Chrisstensen, J. L.; Izatt, S. R.; Bedke, K.; Astin, M.; Izatt, R. M. *J. Am. Chem. Soc.* **1980**, *102*, 3399.

Table 2. Stability Constants (log β')[a] of **1**·Zn^{2+} Complexes with Anion in DMSO by UV−vis Titration Method (T = 25 °C, I = 0.01 M Bu_4NPF_6)

anions	log β' (M^{-1})	% FA[b]
F^-	3.41 (0.08)[c]	15.31
Cl^-	3.58 (0.07)[c]	11.09
Br^-	4.33 (0.03)[c]	2.26
I^-	2.92 (0.05)[c]	33.94

[a] Mean values of $n \geq 3$ independent determinations, with standard deviation σ_{n-1} on the mean in parentheses. [b] Percentage of various free halide anion at C_L, $C_A = 10^{-3}$ M. [c] 1:1 complex (AL).

For CH_3COO^- and $PhCOO^-$ anions, two species of complexes (1:1 and 2:1 (anion/ligand)) were obtained leading to the lower percentages of free halide anion (% FA). This implies that the complexation may occur in an *exo* fashion.

As it was reported that the azacalix[3]arene can bind soft cations such as transition metals[2b,c] which can enhance anion binding by electrostatic force, we decided to check the effects of Zn^{2+} on anion complexation of **1**. In the presence of Zn^{2+}, hypochromic shifts increased in cases of F^-, Br^-, and I^- complexes while they decreased in the case of Cl^-, leading to incremental stability constants of halide complexation except for Cl^- (Table 2). This can be rationalized in the following manner: upon addition of Zn^{2+}, one can assume that the Zn^{2+} binds to the azacalix[3]arene part of **1** to give rise to a **1**·Zn^{2+} complex which is positively charged and thus increases the stability constants of **1**·Zn^{2+}/X^- by electrostatic interactions.[6b] In the case of Cl^-, the electronic interaction between $Zn^{2+}$and Cl^- may reduce the hydrogen bond interaction between **1** and Cl^-, which leads to a decrease of the stability constant.

Acknowledgment. We gratefully acknowledge the Thailand Research Fund (TRF) for financial support (RMU4880041 and RTA 4880008) and the Royal Golden Jubilee Ph.D. Program of TRF (PHD/0137/2546). We also thank Assistant Prof. Dr. Polkit Sangvanich for MALDI TOF MS results.

Supporting Information Available: Experimental procedures and characterization data for all new compounds (including NMR spectra and crystal structure for N_7-azacalix-[3]crytand (**1**) (CIF)). This material is available free of charge via the Internet at http://pubs.acs.org.

OL060052E

CHEMISTRY OF MATERIALS

Subscriber access provided by CHULALONGKORN UNIV

Article

Azacalix[3]arene#Carbazole Conjugated Polymer Network Ultrathin Films for Specific Cation Sensing

Chatthai Kaewtong, Guoqian Jiang, Yushin Park, Tim Fulghum, Akira Baba, Buncha Pulpoka, and Rigoberto Advincula

Chem. Mater., **2008**, 20 (15), 4915-4924• DOI: 10.1021/cm800284h • Publication Date (Web): 11 July 2008

Downloaded from http://pubs.acs.org on March 31, 2009

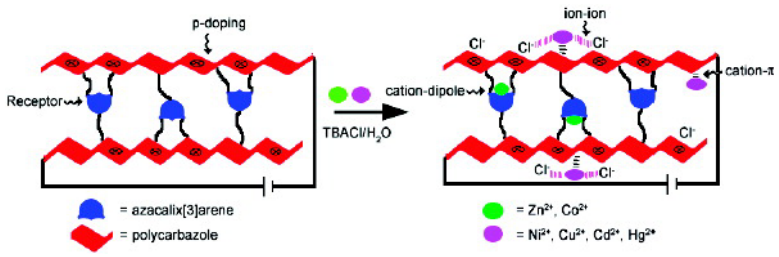

More About This Article

Additional resources and features associated with this article are available within the HTML version:

- Supporting Information
- Access to high resolution figures
- Links to articles and content related to this article
- Copyright permission to reproduce figures and/or text from this article

View the Full Text HTML

ACS Publications
High quality. High impact.

Chemistry of Materials is published by the American Chemical Society. 1155 Sixteenth Street N.W., Washington, DC 20036

Azacalix[3]arene−Carbazole Conjugated Polymer Network Ultrathin Films for Specific Cation Sensing

Chatthai Kaewtong,[†,‡] Guoqian Jiang,[†] Yushin Park,[†] Tim Fulghum,[†] Akira Baba,[†] Buncha Pulpoka,*[,‡] and Rigoberto Advincula*[,†]

Department of Chemistry and Department of Chemical Engineering, University of Houston, 136 Fleming Building, Houston, Texas 77204-5003, and Department of Chemistry, Faculty of Science, Chulalongkorn University, Bangkok 10330, Thailand

Received January 28, 2008. Revised Manuscript Received May 8, 2008

Developing highly selective and sensitive chemical sensors is a challenge with respect to new materials for chemical recognition. In this study, a new conjugated polymer network precursor, hexahomotriazacalix[3]arene−carbazole has been synthesized and electrochemically cross-linked to form ultrathin films using cyclic voltammetry. The incorporation of hexahomotriazacalix[3]arene moiety as a neutral cation-binding receptor into a conjugated polycarbazole network facilitates high selectivity and sensitivity for Zn^{2+}. The ultrathin films were characterized spectroscopically using UV−vis absorption and fluorescence spectroscopy. Surface morphology properties were examined by atomic force microscopy. Electrochemical deposition parameters and sensor transduction was studied by an electrochemical quartz crystal microbalance, surface plasmon resonance spectroscopy, and open-circuit potentiometry techniques. The results indicate that the high selectivity and sensitivity for Zn^{2+} compared to those of other cations is due to the combined size and dipole specificity of the azacalixarene unit and nonspecific ionic interaction with the redox couple of the conjugated polycarbazole units.

Introduction

The basic recognition element of a chemical sensor is essentially a molecular or macromolecular structure designed to recognize a specific analyte. The binding or complexation constant, K_{asso}, of the analyte is dependent on the strength of noncovalent interaction and accessibility to this structure. A high surface area is also a factor as it affects the diffusion kinetics of the analyte to the binding site. In the presence of a conducting (π-conjugated) polymer, a polymeric chemosensor system can be made electrochemically active, electrically conducting, and fluorescent, depending on the structure of the polymer, mode of electric field application, and wavelength excitation. Thus, it is not necessary for the receptor-analyte unit of the polymeric chemosensor to have an inherently high K_{asso}. Only partial occupancy of the recognition site may be required for signal transduction since the conjugated polymer also contributes to signal amplification and improved sensitivity.[1]

A number of well-investigated π-conjugated polymers such as polythiophenes, polypyrroles, polyanilines, etc. have been used successfully for sensor and device applications.[2] As a class of semiconducting polymers, polycarbazoles possess good electroactivity and useful thermal, electrical, and photophysical properties which have led to there use in redox catalysis, electrochromic displays, electroluminescent devices, and sensors.[3] For example, polycarbazole has been used to develop copper(II) ion-selective microelectrochemical transistors[4a] and L-dopa-selective sensors[4b] due to its negligible sensor response hysteresis and greater chemical and thermal stability compared to other conducting polymers.[4]

Calixarenes have received significant attention for the construction of molecular receptors due to their unique molecular recognition properties and ease of functionalization.[5] The size of the macrocyclic cavity and the presence of ion−dipole interactions with the heteroatoms can be made specific for a particular ion. Substituents to the calixarene can further control the size and specificity of the cavity through conformational change (torsional) and electronic effects. In recent years, oxacalixarenes and azacalixarenes have been developed as part of a class of compounds called expanded calixarenes.[6] The azacalixarenes, which have nitrogen atoms in the macrocyclic ring, could provide additional binding sites for many types of cations. Specifically, the azacalix[3]arenes have been shown to serve as

* Authors to whom correspondence should be addressed. E-mail: radvincula@uh.edu (R.A.); buncha.p@chula.ac.th (P.B.).
† University of Houston.
‡ Chulalongkorn University.

(1) (a) Swager, T. M. *Acc. Chem. Res.* **1998**, *31*, 201. (b) Dimitriev, O. P. *Macromolecules* **2004**, *37*, 3388. (c) Ferguson, G.; Gallagher, J. F.; Lough, A. J.; Notti, An.; Pappalardo, S.; Parisi, M. F. *J. Org. Chem.* **1999**, *64*, 5876.
(2) (a) Richard, D. M. *Adv. Mater.* **1998**, *10*, 93. (b) Roncali, J. *J. Mater. Chem.* **1999**, *9*, 1875. (c) Janata, J.; Mira, J. *Nat. Mater.* **2003**, *2*, 19. (d) Bobacka, J.; Ivaska, A.; Lewenstam, A. *Electroanalysis* **2003**, *15*, 366.
(3) (a) Mallouk, T. E.; Gavin, J. A. *Acc. Chem. Res.* **1998**, *31*, 209. (b) Crooks, R. M.; Ricco, A. J. *Acc. Chem. Res.* **1998**, *31*, 219.
(4) (a) Rani, V.; Santhanam, K. S. V. *J. Solid State Electrochem.* **1998**, *2*, 99. (b) Kawde, R. B.; Laxmeshwar, N. B.; Santhanam, K. S. V. *Sens. Actuators B* **1995**, *23*, 35. (c) Choudhury, S.; Saxena, V.; Gupta, S. K.; Yakhmi, J. V. *Thin Solid Films* **2005**, *493*, 267.
(5) (a) *Calixarenes in Action*; Mandolini, L., Ungaro, R., Eds.; Imperial College Press: London, U. K., 2000. (b) Ikeda, A.; Shinkai, S. *Chem. Rev.* **1997**, *97*, 1713. (c) Vigalok, A.; Zhu, Z.; Swager, T. M. *J. Am. Chem. Soc.* **2001**, *123*, 7917. (d) Vigalok, A.; Swager, T. M. *Adv. Mater.* **2002**, *14*, 368.

10.1021/cm800284h CCC: $40.75 © 2008 American Chemical Society
Published on Web 07/11/2008

Scheme 1. Synthesis and Electrochemical Polymerization (Cross-linking) of *p*-Chloro-*N*-benzylhexahomotriazacalix[3]-tri(buthyl carbazole) or Monomer

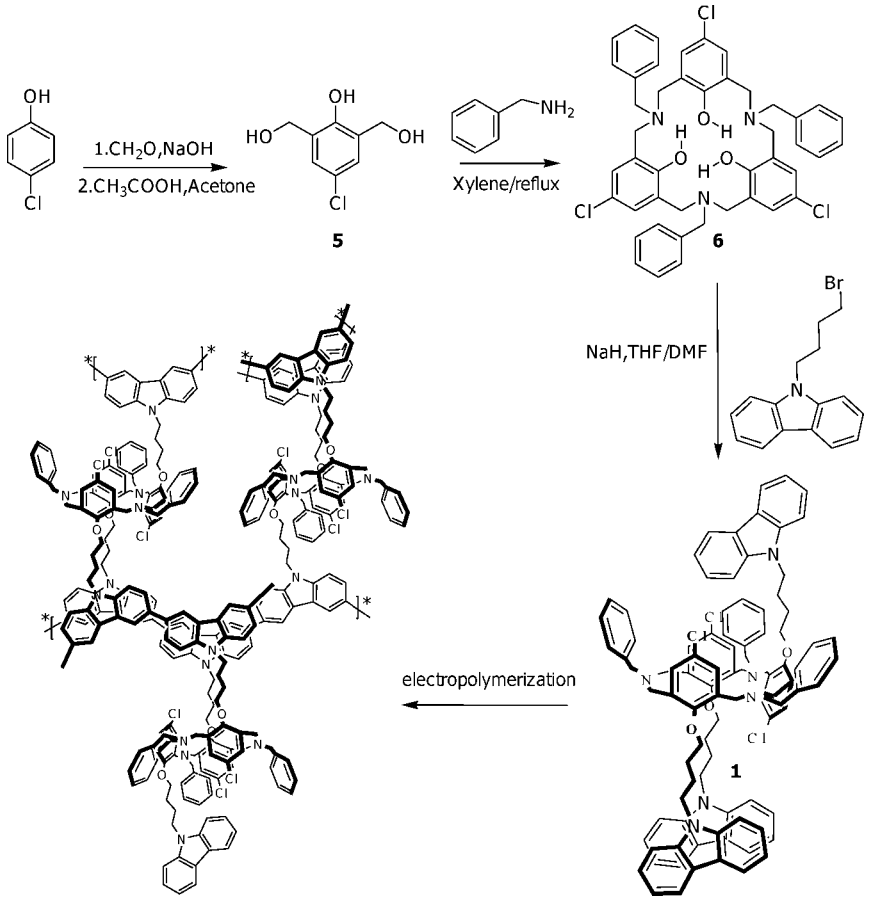

highly selective receptors for both cations[6d,e] and anions.[7] Halide anion selectivity can be tuned by first complexing a cation with bridged nitrogen atoms inside the macrocycle.[7]

With the aim of preparing a new class of chemical recognition elements for sensors, we have synthesized hexahomotriazacalix[3]arene-carbazole as a precursor for the formation of conjugated polymer networks (CPN). To the best of our knowledge, there has been no report on the use of azacalix[3]arene in partial-cone conformation combined with polycarbazoles in a chemical sensor material system. By electropolymerization, these precursors can be deposited as ultrathin films on Au and indium tin oxide (ITO) electrode substrates. This electrochemical process results in the formation of a CPN due to the inherent intermolecular and intramolecular reactivity of pendant carbazole units.[8] The films were characterized by UV−vis spectroscopy, fluorescence spectroscopy, and atomic force microscopy (AFM). The electrochemical and sensing properties were investigated in conjunction with various electrochemically hyphenated optical and acoustic techniques, e.g., electrochemical quartz crystal microbalance (EC-QCM), electrochemical surface plasmon spectroscopy (EC-SPR), and open-circuit potentiometry. It is believed that the partial-cone conformation of azacalix[3]arene allows a gain in the kinetic binding property, with its selectivity remaining intact with electropolymerization, leading to a high specificity for Zn^{2+}.

Results and Discussion

Synthesis. The synthesis of monomer **1** Scheme 1 was completed by reacting *N*-benzylhexahomotriaza-*p*-chlorocalix[3]arene[6e] with 3.5 equiv of 9-(4-bromobutyl)-9*H*-carbazole and 3.5 equiv of NaH as base in THF/DMF solution for 2 days. Column chromatography (silica gel, 90/10 hexane/ethyl acetate) was used to afford monomer **1** in 10% yield. The carbazole-functionalized hexahomotriazacalix[3]arene monomer was then characterized by FT-IR, ^{1}H NMR, ^{13}C NMR, and MALDI-TOF MS as summarized in the Experimental Section.

It was found that hexahomotriazacalix[3]-tricarbazole **1** was fixed as a partial-cone conformation as evidenced by the presence of two triplet $-CH-_{azacalix}$ aromatic peaks at 7.04 ppm (J = 7.2 Hz) and 7.01 ppm (J = 7.2 Hz) and multiplet peaks of $-NCH_2Ar-$ at 3.78−3.00 ppm in the ^{1}H NMR spectrum. The ^{13}C NMR spectrum also gave evidence of the changes,

(6) (a) *Calixarenes 2001*; Asfari, Z., Bhmer, V., Harrowfield, J., Vicens, J., Eds.; Kluwer Academic Publishers: Dordrecht, 2001. (b) Takemura, H. *J. Inclusion Phenom. Macro.* **2002**, *42*, 1698. (c) Takemura, H.; Shimmyozu, T.; Inazh, T. *Coord. Chem. Rev.* **1996**, *156*, 183. (d) Hampton, P. D.; Tong, W.; Wu, S.; Duesler, E. N. *J. Chem. Soc., Perkin Trans.* **1996**, *2*, 1127. (e) Thury, P.; Nierlich, M.; Vicens, J.; Takemura, H. *J. Chem. Soc., Dalton Trans.* **2000**, 279.

(7) Kaewtong, C.; Fuangswasdi, S.; Muangsin, N.; Chaichit, N.; Vicens, J.; Pulpoka, B. *Org. Lett.* **2006**, *8*, 1561.

(8) (a) Taranekar, P.; Baba, A.; Fulghum, T. M.; Advincula, R. *Macromolecules* **2005**, *38*, 3679. (b) Baba, A.; Onishi, K.; Knoll, W.; Advincula, R. *J. Phys. Chem. B* **2004**, *108*, 18949. (c) Taranekar, P.; Fulghum, T. M.; Baba, A.; Patton, D.; Advincula, R. *Langmuir* **2007**, *23*, 908.

consistent with the previous study from a cone conformation spectrum,[7] i.e., $-OCH_2CH_2-$ showed two peaks (75.0, 74.7 ppm) and the −C− of the aromatic azacalix split into three peaks (135.0, 134.0, and 133.5 ppm).

Electropolymerization of *p*-Chloro-*N*-benzylhexahomotriazacalix[3]-tri(buthyl carbazole). Electropolymerization by cyclic voltammetry (CV) is a widely used method for preparing polycarbazole (PCBz) films.[9,10] To test the ability to form network ultrathin films, monomer **1** was electropolymerized and deposited on three working electrodes: plain gold-coated glass substrate, CBzC11SH (thiol-undec-9*H*-carbazole) (**4**) self-assembled monolayer (SAM) coated gold substrate, and ITO substrate. All the CV trace diagrams of monomer **1** deposited onto the different substrates are also shown in Figure S3 (Supporting Information). Deposition on a bare gold-coated slide was first attempted. The current increase was low and the CV was not well-behaved. When the **4** SAMs coated gold substrate was used (Figure 1a), the monomer was shown to be electropolymerized anodically at 1.0 V. After several cycles, the oxidation and reduction peaks were observed at 0.85 and 0.77 V, respectively. The current was low on the first cycle but increased in the second and slightly changed with further cycles. Thus, compared to the bare−Au electrode, more material was deposited on this **4** coated gold substrate based on a higher current increase at 0.85 V. On the other hand, the best films were obtained when ITO was used as the electrode−substrate with an applied potential window from 0 to 1.3 V (Figure 1b) (electropolymerization was initially attempted with applied potential up to 1.5 V, Figure S3). The linear increase in the oxidation current and high cyclic reversibility is indicative of uniform film growth. The anodic current trace splits into two peaks with further cycles. At the first cycle, the broad anodic peak is centered at 0.90 V and the reduction peak is at 0.75 V. When the eighth cycle was reached, two consecutive anodic peaks centered at 0.85 and 0.96 V became more pronounced. The two anodic current peaks can be assigned to the doping with anions into the polymerized carbazole from the electrolyte solution and oxidation of the remaining carbazole monomer, leading to radical cation species.[8] This is reasonable because only one reduction peak is observed, which decreases from 0.75 to 0.71 V. Thus, the reduction from the previously oxidized but un-cross-linked species may be the source of this peak. Dedoping may also be involved in this reduction process but is not favored considering polycarbazole is a p-type semiconductor polymer.

Morphology Studies. The morphology before and after electropolymerization on the ITO, gold-coated slides and **4** SAM coated gold substrates were characterized by AFM

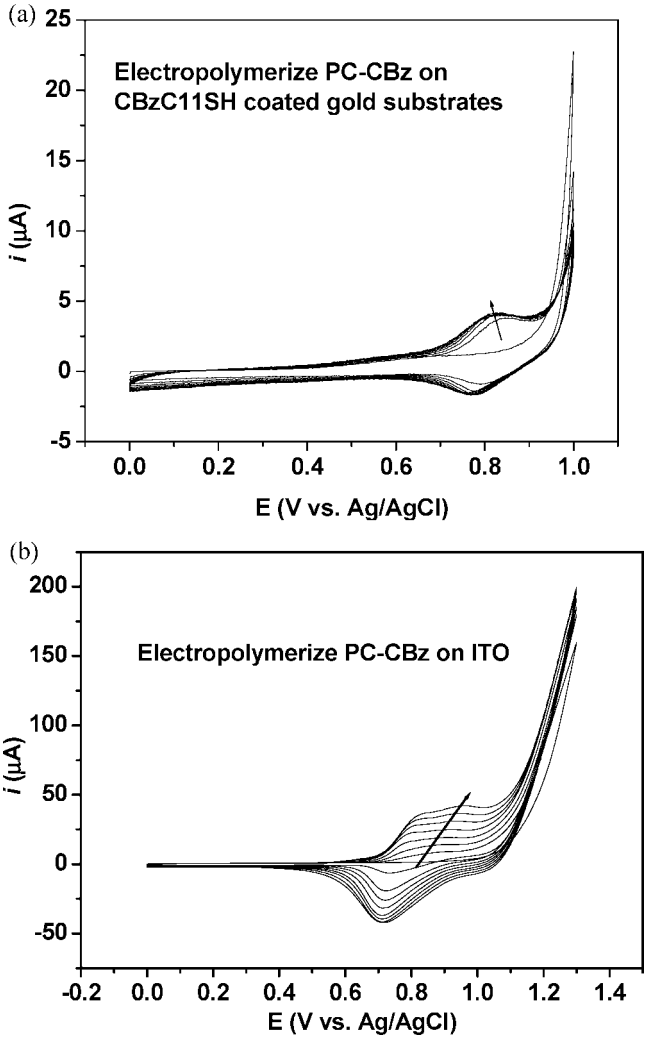

Figure 1. Cyclic voltammograms of the electrochemical cross-linking/deposition of PC-CBz at a scan rate of 50 mV/s, 8 cycles: (a) deposited material on **4** coated gold substrates and (b) deposited material on ITO substrates.

(Figure 2). All the other AFM images are shown in Figures S4 and S5 (Supporting Information). PC-CBz was electropolymerized for 8 cycles at a range of 0−1.0 V with a scan rate of 50 mV/s in 0.1 M $TBAPF_6$/anhydrous CH_2Cl_2 as electrolyte (WE, gold-coated slide; CE, Pt wire; RE, Ag/AgCl wire). In the case of direct deposition on unfunctionalized gold substrate, the morphology was found to be more similar to that of bare gold, indicating a very small quantity was deposited. When **4** SAM coated gold was used, the morphologies are relatively rough (rms roughness = 15 nm) (Figure 2a, b). It implied that the deposition of the precursor material was achieved better on **4** coated gold substrates but were not as uniform as expected. The nucleation of **4** SAM may play a very important role during the polymerization, as suggested from a previous report on polythiophene electrodeposition.[11] For the ITO substrates, a highly uniform morphology (rms roughness = 7 nm) was observed with applied potentials from 0 to 1.3 V (Figure 2c, d). However, in the case of higher applied potential (up to 1.5 V), the polymer films tended to give a rougher and patchy film (but

(9) (a) Kuwabara, Y.; Ogawa, H.; Inada, H.; Nona, N.; Shirota, Y. *Adv. Mater.* **1994**, *6*, 667. (b) O'Brien, D. F.; Burrows, P. E.; Forrest, S. R.; Koene, B. E.; Loy, D. E.; Thompson, M. E. *Adv. Mater.* **1998**, *10*, 1108. (c) Koene, B. E.; Loy, D. E.; Thompson, M. E. *Chem. Mater.* **1998**, *10*, 2235. (d) Thomas, K. R. J.; Lim, J. T.; Tao, Y. T.; Ko, C. W. *J. Am. Chem. Soc.* **2001**, *123*, 9404. (e) Li, J.; Liu, D.; Li, Y.; Lee, C. S.; Kwong, H. L.; Lee, S. *Chem. Mater.* **2005**, *17*, 1208.

(10) (a) Liu, B.; Yu, W. L.; Lai, Y. H.; Huang, W. *Chem. Mater.* **2001**, *13*, 1984. (b) Xia, C.; Advincula, R. C. *Macromolecules* **2001**, *34*, 5854. (c) Stephen, O.; Vial, J.-C. *Synth. Met.* **1999**, *106*, 115.

(11) Kang, J. F.; Perry, J. D.; Tian, P.; Kilbey, S. M. *Langmuir* **2002**, *18*, 10196.

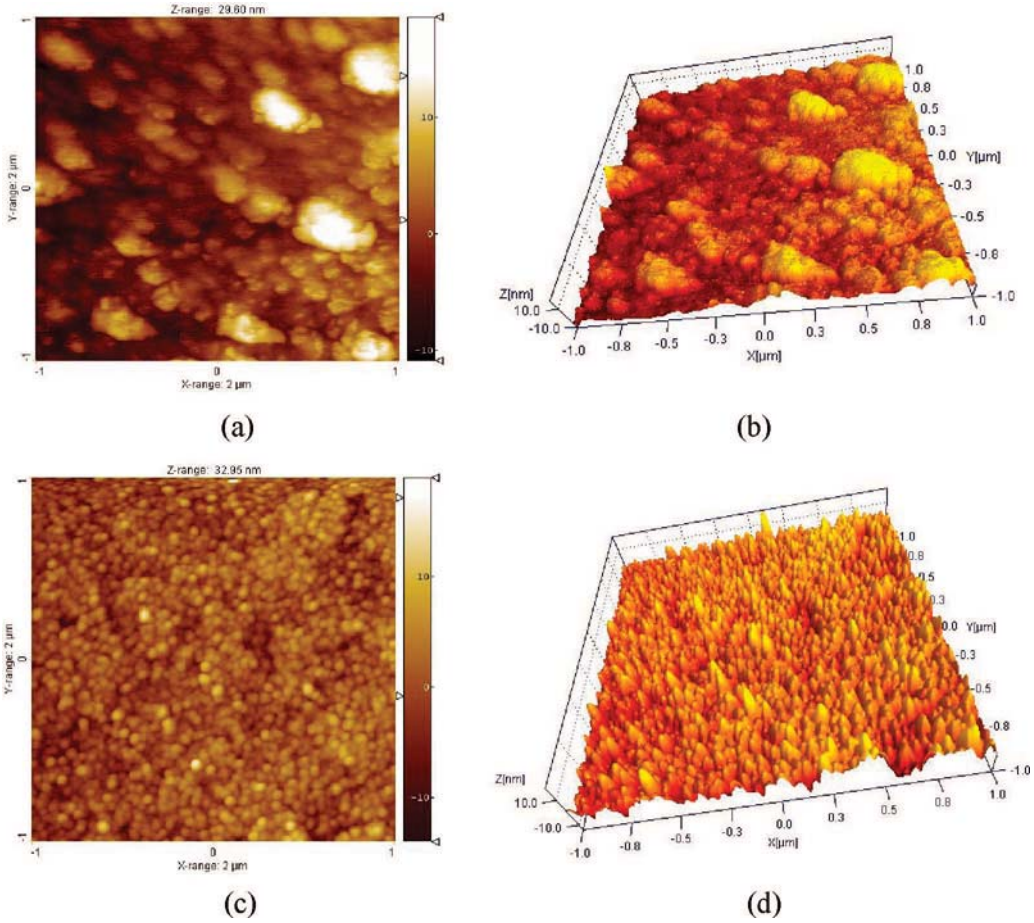

Figure 2. 2D (a, c) and 3D (b, d) AFM images of PPC-CBz electropolymerized at 50 mV/s in $TBAPF_6/CH_2Cl_2$ electrolyte (CE, Pt wire; RE, Ag/AgCl wire): on the **4** coated gold substrate (WE) (rms roughness = 15 nm) (a, b) and on the ITO substrate (WE) (rms roughness = 7 nm) (c, d).

complete coverage) as shown in Figure S5 (Supporting Information).

Spectroelectrochemistry. Spectroelectrochemical measurements were performed using a previously described setup.[12] The spectroelectrochemical measurement of PPC-CBz was performed to investigate the cross-linking polymerization process in situ and the presence of polaronic states associated with the formation of a more conjugated polymer. The in situ UV−vis absorption spectra of PC-CBz were measured simultaneously with electropolymerization in a 0.1 M $TBAPF_6/CH_2Cl_2$ solution as electrolyte (WE, ITO; CE, Pt wire; RE, Ag/AgCl) at a scan rate of 50 mV/s. Figure 3 shows the extended appearance of the $\pi-\pi^*$ transition peak and a shoulder at 445 nm, which is attributed to polycarbazole.[13] The broad peak centered at 950 nm can be assigned to the polaronic and bipolaronic bands originating from the formation of the conjugated polycarbazole species and their complexed ion redox couple with hexafluorophosphate ions. From the spectra, the peaks at 445 and 950 nm were tracked and showed a linear increase with increasing CV cycles, indicating an even deposition of the polymer.

In addition to the electronic absorption properties, the fluorescence emission properties of polycarbazole further confirmed the cross-linking reaction.[14] It was found that the azacalix[3]arene−carbazole precursor shows different fluorescence spectra before and after cross-linking. The fluorescence peak of the carbazole units present on PC-CBz was observed at 370 nm (Figure 3b) (film). After electropolymerization, this peak is quenched in the case of the solid state PPC-CBz film, where a new peak arises at 390 nm attributed to the formation of polycarbazole. This was also observed previously as in the case of CBz functionalized polybenzyl ether dendrimers in solution and solid-state carbazole containing polystyrenic CPN films.[14]

Sensing Selectivity and Sensitivity: Potentiometric Measurements. The sensing selectivity and sensitivity studies were first investigated by open-circuit potentiometry (an electrochemical cell potential set at zero current). The changes in potential (ΔE) were recorded simultaneously as a function of time at constant zero-current voltage. The experiment also tracks the redox state of the polymer since it can be influenced by either introducing an electric charge or adding a reagent (analyte) which interferes with the redox equilibrium. The selectivity studies by potentiometry were first performed using the electrochemically cross-linked PPC-CBz film on ITO against 10^{-6} M of the various cations (0.01 M TBACl is present as supporting electrolyte).

(12) Tran-Van, F.; Chevrot, C. *Electrochim. Acta* **2002**, *47*, 2927.
(13) (a) Buttry, D. A. In *Electroanalytical Chemistry*; Bard, A. J., Ed.; Marcel Dekker: New York, 1991; Vol. 17, p 1. (b) Taranekar, P.; Baba, A.; Fulghum, T.; Advincula, R. *Macromolecules* **2005**, *38*, 3679.
(14) Taranekar, P.; Park, J.-Y.; Patton, D.; Fulghum, T.; Ramon, G. J.; Advincula, R. *Adv. Mater.* **2006**, *18*, 2461.

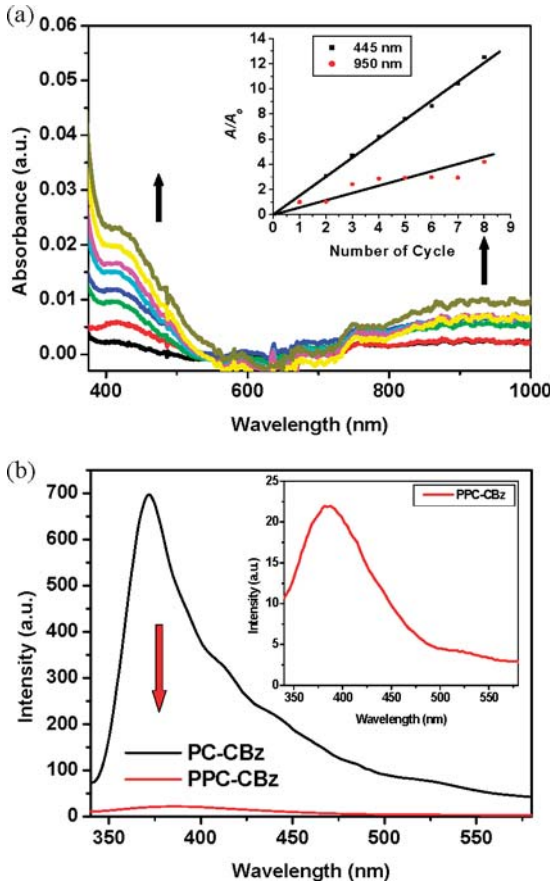

Figure 3. (a) Spectroelectrochemical analysis performed in 0.1 M $TBAPF_6$/CH_2Cl_2 of PC-CBz, growth of the 445 and 950 nm peaks during electrodeposition of PPC-CBz, spectra taken in situ at 0 V during each CV cycle and (b) fluorescence spectra before and after electropolymerization of PC-CBz which are taken at the excitation wavelength $\lambda = 320$ nm.

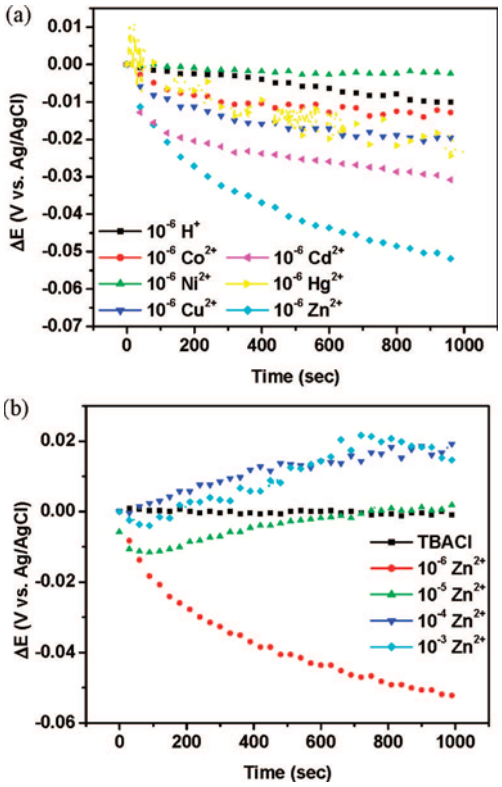

Figure 4. Potentiometric profiles of PPC-CBz on ITO in 0.01 M TBACl aqueous solution: (a) various cation analytes and (b) various concentrations of Zn^{2+}. Plotted data are within 5% deviation from several measurements.

As shown in Figure 4a, the highest selectivity (biggest change in ΔE of up to −0.06 V) was observed from Zn^{2+} compared with those of other cations. A priori, this may be due to the exact size and fit of the Zn^{2+} cation on the azacalix[3]arene, steric effect from the polymer backbone and hard–soft acid and base principle (HSAB).[6] The presence of the nitrogen atoms (soft) in azacalix[3]arenes allows them to bind soft cations (such as transition metals).[6e,7] However, our previous work[7] has shown that the azacalix[3]arene template can be made specific for Zn^{2+} ions in organic solution. Thus, by design, the hexahomotriazacalix[3]-tri(buthylcarbazole) was made to be specific for the Zn^{2+} cations compared to the other transition metals. In this case, the conductivity of the cross-linked polymer may increase with binding of the Zn^{2+} cations to the azacalix[3]arene pocket. This seemed to be readily achieved at 10^{-6} M where the other cations have little effect on the potential change since they did not have an exact fit on the azacalix[3]arene units and thus showed little deviation from the zero-current potential.

In general for the Zn^{2+} cations, after the lowest concentration (10^{-6} M), the ΔE did not decrease much over time (Figure 4b). For the other concentrations, the potential decreases in the first 100 s, followed by a gradual increase until it reaches a steady state. This is generally observed for all the other cations at higher concentrations (10^{-5} to 10^{-3} M) (see Figure S6, Supporting Information). This indicates that the decrease of potential at 10^{-6} M of the cations over time is primarily due to the first cations being encapsulated in the cavity of azacalix[3]arene through cation−dipole interaction. With increasing concentrations, the limited amount of the cavities does not allow further encapsulation and therefore cations are free to complex with other species in the polymer backbone, i.e., driven by the interaction between the cations with doped anions (Cl^- and PF_6^-) along the extended π-conjugated polymer backbone. Thus, the potentiometric changes can be attributed to the increasing interference of the Zn^{2+} on charged species in the polymer such as polarons and bipolarons along with their neutralizing counterions which are independent species.

Clearly, on the basis of the potentiometric measurements in the presence of 10^{-6} M cations, the Zn^{2+} showed the best performance in terms of selectivity and sensitivity compared to the other cations. However, there is a need to further explain this phenomenon of the ΔE change beyond the HSAB principle and the presence of other independent ionic species in the polymer. The basic premise is that the other ions when not bound to the azacalix[3]arene cavity via a cation−dipole interaction are primarily involved with ion pairing on the doped conjugated polymer, i.e., cation−π interaction between cations and π-extended conjugated polymer.

To begin with, the observed behavior can be correlated with the effect of charge-carrier properties on a conjugated polymer, i.e., hole transport and electron transfer properties of the polycarbazole to the cations. There are two explana-

Scheme 2. Two Explanations for the Potential Changes after the Addition of Different Cations[a]

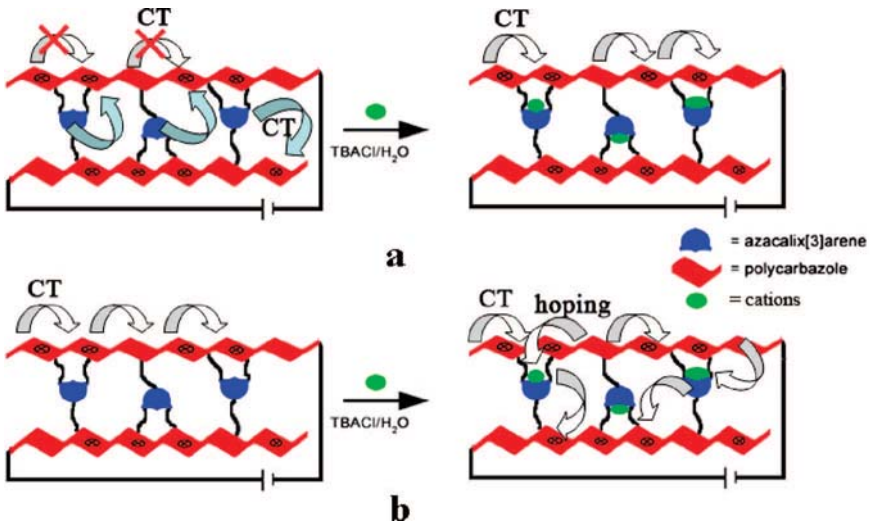

[a] (a) Cations can be protected from electron transfer to the conjugated polymer backbone and (b) cations complexation can be a hole to improve the hole transport pathways between chains.

tions for the potential changes after the addition of different cations along with different concentrations: (1) One can first consider the contribution of electron transfer from the lone pair of nitrogen on the azacalix[3]arene moiety to the conjugated polymer backbone. This was confirmed by studying the complexation of protons with the azacalix[3]arene (see Figure S6a, Supporting Information). As shown in Scheme 2a, protonation of nitrogen (ammonium formation) induces less efficiency for electron transfer to the polycarbazole. As a consequence, fewer holes can be generated and thus less conductivity enhancement or a smaller potential decrease would be expected, which is indeed the case. (2) The other consideration is based on hole transport throughout the whole polymer network in a three-dimensional manner. Since the Zn^{2+} are complexed in the azacalix[3]arene cavities by ion−dipole interaction as shown in Scheme 2b, the holes not only move along the polymer backbones but also hop through the cations to improve the hole transport pathways between chains.[15a] The other effect to consider is the competition with the free ions (overall ionic strength) and the ions bound on the doped polymer. With increasing concentration of the cations, the ion−ion and cation−π interactions increases and begin to reside proximal to the polymer backbones, pairing with the anions (Cl^- and PF_6^-) on the doped sequences of the polymer. Thus, they tend to decrease the doping level of the polymer films by removing the anions paired to the polymer backbone and thus the stabilization of π-extended conjugated polymer chains.

Consequently, the net potential shift is attributed to the competition of these two effects. The flux of the cations into the polymer films may proceed in two steps: at first they diffuse into the polymer and selectively bind with the azacalix[3]arene cavities, which enhances the conductivity. If all the cavities have been filled up, the cations would slowly disperse to the sequences occupied by the dopants, which interrupts the polymeric conjugation and decreases the hole mobility.

In principle, the conductivity of conjugated polymers can be fine-tuned by changing charge transport pathways. Previous studies[15] correlated that the three-dimensional connectivity for bipolaron migration was caused by the close contact between planar π-extended polymers which efficiently promote an interstrand charge hopping mechanism and consequently facilitates charge delocalization. On the other hand, the minimization of cross-communication of the conjugated polymer backbones can remarkably change the conductivity profile by reducing the dimensionality of charge-transporting pathways.[16] As a control experiment, 9-(4-(9*H*-carbazol)-9*H*-carbazole (**8**) was used. The data showed only a little change in ΔE as shown in Figure S7 (Supporting Information) at −0.004 V compared to −0.06 V in the absence of the azacalix[3]arene units.

Spectroelectrochemical studies were also performed to support the order of cation sensitivity and selectivity. As expected, the addition of 10^{-3} M cations into the cell containing the films resulted in different changes in the absorption spectra. The blue shift (≈45 nm) from 455 nm to 405 nm and 950 nm to 910 nm upon the addition of Ni^{2+}, Cu^{2+}, Cd^{2+}, and Hg^{2+} suggests that conjugation of the polycarbazole indeed decreased, consistent with the above discussion in the potentiometric measurements. However, little change in the absorption spectra of **1** was observed upon the addition of Zn^{2+} and Co^{2+} and can be attributed primarily to an allosteric effect. This suggests that the Zn^{2+} and Co^{2+} ions are primarily bound in the cavity of azacalix[3]arene by cation−dipole interaction. This was also confirmed by the addition of protons. As can be seen from Figure 5, there is a slight blue shift with protons primarily bound on the nitrogen of azacalix[3]arene, but the interference is much weaker than the metal ions, maintaining the polymeric

(15) (a) Zhu, S. S.; Swager, T. M. *J. Am. Chem. Soc.* **1997**, *119*, 12568. (b) Lee, D.; Swager, T. M. *J. Am. Chem. Soc.* **2003**, *125*, 6870.
(16) (a) Miller, L. L.; Mann, K. R. *Acc. Chem. Res.* **1996**, *29*, 417. (b) Cornil, J.; Beljonne, D.; Calbert, J.-P.; Brédas, J.-L. *Adv. Mater.* **2001**, *13*, 1053.

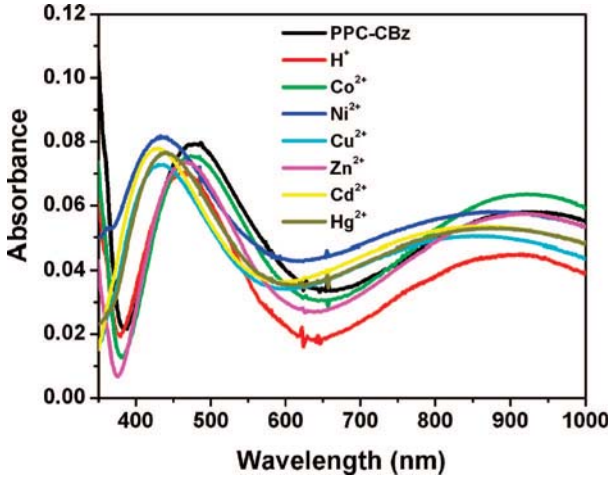

Figure 5. UV−vis absorption spectrum of PPC-CBz films upon the addition of different cations with the concentration 10^{-3} M on ITO substrates.

conjugation to a large extent. From the Co^{2+} spectrum, this may imply that Co^{2+} ion may compete with Zn^{2+} for the azacalix[3]arene specificity. However, the blue shift (∼10 nm) from 450 to 440 nm occurred upon the addition of Zn^{2+} in the control experiment (Figure S7b). From this data, the blue shift can be explained by cation−π interactions between the cations and the conjugated polymers.

Additionally, we used a combined electrochemistry and quartz crystal microbalance method (EC-QCM) to confirm the sensitivity and selectivity of PPC-CBz. This method is very informative for probing mass-transport processes in thin films.[12] The mass deposition per cycle was measured during electropolymerization and showed a general decrease in frequency with each cycle over time, indicating a continuous deposition on the substrate (Figure 6a). After the deposition of PPC-CBz on the EQCM probe, aqueous solutions of the cations were added. In general, the Butterworth−van Dyke (BD) equation provides a method for relating the electrical properties of the quartz resonator to the mechanical properties of the deposited film.[17] The relationship between ΔR and ΔF under liquid loading was derived from the BD equation.[18] The increase in ΔR is correlated with an increase in the viscoelasticity of the layer adjacent to the crystal surface while a small change in ΔR is indicative of a more rigid adsorbed layer. From Figures 6a and 6b, the resistance increased with each cycle, indicating increasing rigidity (viscoelastic behavior) of the films with more layers deposited. In general, with oxidation and reduction, the change in resistance indicates the transport of the ions in and out of the cross-linked film. After cross-linking, the addition of Zn^{2+} caused a rapid increase of the mass of the deposited polymer (Figure 6c). This was the highest for the Zn^{2+} as compared to the other ions. Analysis of the mass−concentration relationship, according to the Langmuir equation ($1/\Gamma = 1 + 1/KC_M$, where $\Gamma = \Delta m/\Delta m_{max}$, C_M is the metal ion concentration and K the complexation constant) was made.[19] The binding ability of PPC-CBz toward cations thus varies

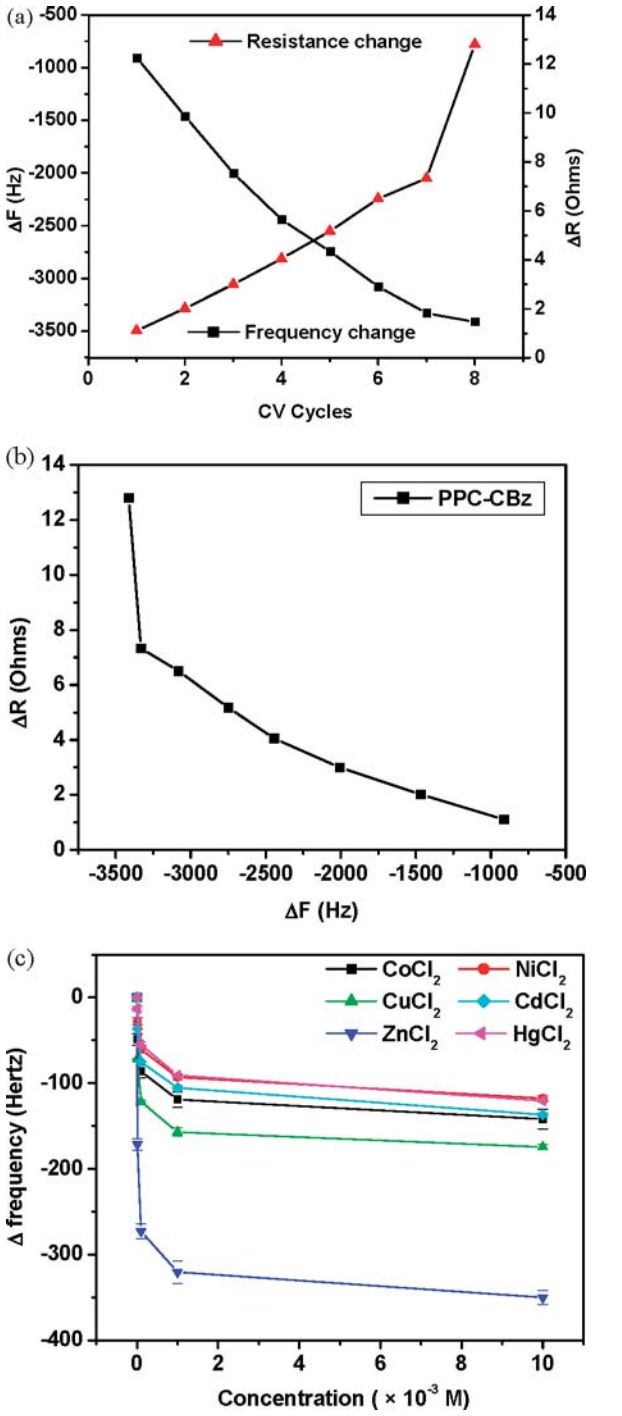

Figure 6. Electrochemical quartz crystal microbalance studies the following: (a) ΔF, frequency change, and ΔR, resistance change during the CV cycling. (b) Changes in the viscoelastic behavior in the polymers. (c) ΔF, frequency change as a function of different cations concentration.

as follows: Zn^{2+} ($K = 1.1 \times 10^6$ M^{-1}) > $Cu^{2+} \approx Co^{2+}$ ($K = 9.0 \times 10^5$ M^{-1}) > $Ni^{2+} \approx Hg^{2+}$ ($K = 3.3 \times 10^5$ M^{-1}) > Cd^{2+}($K = 2.5 \times 10^5$ M^{-1}).

Finally, SPR spectroscopy was combined with an electrochemistry setup to study the efficiency of transport and sensitivity of Zn^{2+} ions with PPC-CBz films. As shown in the EC-SPR measurements (Figure 7), the reflectivity increases with increasing CV cycles, indicating the continuous deposition of the film onto the **4** SAM coated gold substrates. Again, the subsequent doping and dedoping of the films with oxidation and reduction cycles are shown in

(17) Buttry, D. A.; Ward, M. D. *Chem. Rev.* **1992**, *92*, 1355.
(18) Muramatsu, H.; Tamiya, E.; Karube, I. *Anal. Chem.* **1988**, *60*, 2142.
(19) Sannicolo, F.; Brenna, E.; Benincori, T.; Zotti, G.; Zecchin, S.; Schiavon, G.; Pilati, T. *Chem. Mater.* **1998**, *10*, 2167.

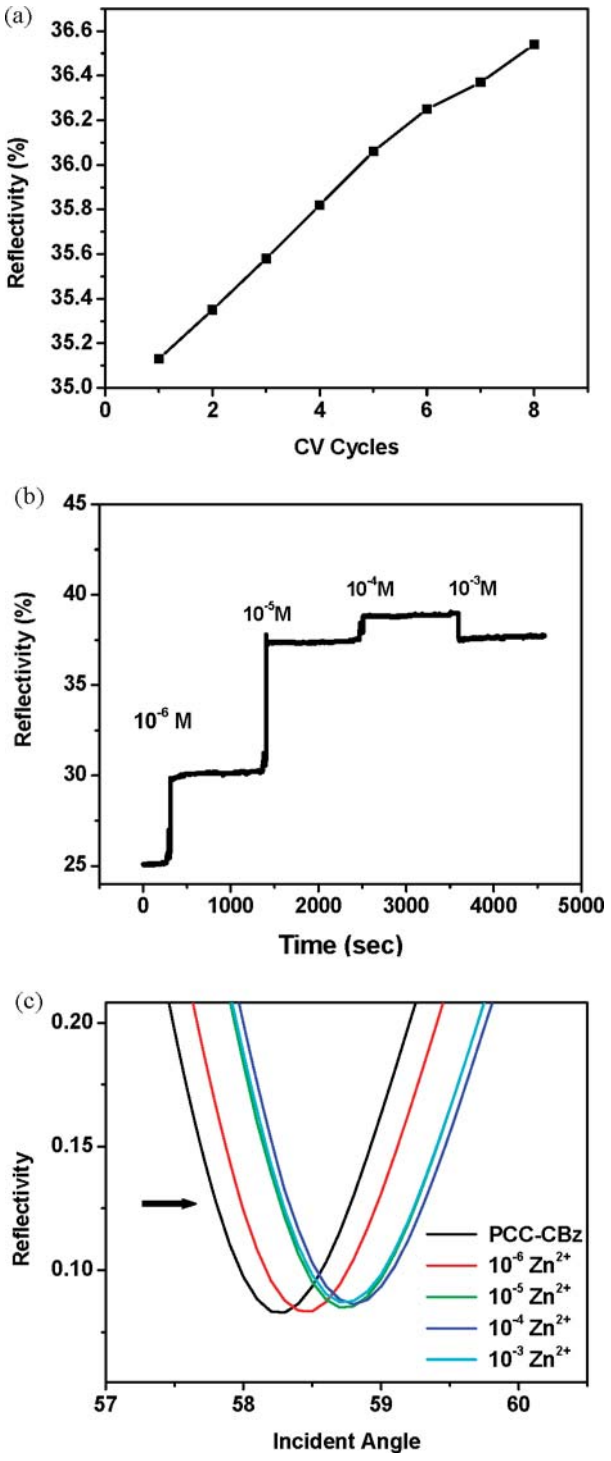

Figure 7. EC-SPR and SPR studies of PPC-CBz on **4** coated gold substrates: (a) kinetic measurement during deposited film, (b) kinetic sensorgram at different concentrations of Zn^{2+}, and (c) angular sensorgram at different concentrations of Zn^{2+}.

the reversible reflectivity change which consists of either a change in dielectric constant or thickness.[20]

The sensing experiment was conducted by injecting different concentrations of Zn^{2+} into the SPR cell embedded with the as-deposited polymer film on a Au working electrode. From the SPR sensorgram (Figure 7b), a sudden change was observed on the reflectivity upon injection of 10^{-6} and 10^{-5} M Zn^{2+} and a peak saturation was observed upon injection of 10^{-4} M and higher concentrations. The concentrations at this level are not expected to give a measurable change in reflectivity.[21] This indicated that the association of Zn^{2+} with the film induced primarily the dielectric constant change assuming the thickness was constant. It is also interesting to note that the highest change was observed with 10^{-6} and 10^{-5} M Zn^{2+} concentrations, indicating that at these concentrations the azacalix[3]arene units are fully bounded and that excess ions do not participate in a significant dielectric constant change to the film, similar to the results with open-circuit potentiometry. This confirms that the allosteric effect is mostly observed only at lower concentrations of the Zn^{2+} cation and that, at higher concentrations, the excess ion does not participate in binding to the azacalix[3]arenes.

Conclusion

In summary, we have successfully developed a new class of chemosensor recognition elements based on conjugated polymer network ultrathin films by electrochemical cross-linking of hexahomotriazacalix[3]arene−carbazole and demonstrated its selectivity and sensitivity toward Zn^{2+} by various techniques: potentiometry, QCM, and SPR combined with electrochemistry. The results of this investigation have shown that cation interaction with the film might increase charge carrier transport properties on a conjugated polymer through azacalix[3]arene-bound cations, reduce the doping states by interfering ions through ion−ion interaction, and perturbing the π-extended conjugated polymer through $\pi-\pi$ interaction. Specifically, these observed changes in the electrical and spectroelectrochemical properties of the films are related to the cation−dipole interaction between Zn^{2+} and azacalix[3]arene, resulting in a higher binding constant and its subsequent specificity for chemical sensing.

Experimental Section

Chemicals and Methods. All chemical reagents were purchased from Aldrich Chemical Co. unless otherwise stated. Solvents were purchased from Fisher. Tetrahydrofuran (THF) was distilled over sodium/benzophenone ketyl, and *N*,*N*-dimethylformamide (DMF) was purchased in anhydrous form or was otherwise dried over Linde type 4 Å molecular sieves.

Instrumentation. Nuclear magnetic resonance (NMR) spectra were recorded on a Varian 400 MHz spectrometer in deuterated chloroform or a General Electric QE-300 spectrometer at 300 MHz. Chemical shifts (δ) are reported in parts per million and the residual solvent peak was used as an internal standard.

UV−vis spectra were recorded using an HP-8453 spectrometer. Spectroelectrochemical UV−vis measurements of the films were carried out in situ on ITO substrates. This was done using a Teflon flow cell fabricated with a modified ITO window and microscope slide window that was placed in the path of an HP-8453 diode array spectrometer.

MALDI-TOF mass spectra were recorded on a Biflex Bruker Mass spectrometer with 2-cyano-4-hydroxycinnamic acid (CCA) or 2,5-dihydroxy-benzoic acid (DHB) as matrix.

(20) (a) Taranekar, P.; Baba, A.; Park, J. Y.; Fulghum, T. M.; Advincula, R. *Adv. Funct. Mater.* **2006**, *16*, 2000. (b) Kang, X.; Jin, Y.; Cheng, G.; Dong, S. *Langmuir* **2002**, *18*, 10305. (c) Georgiadis, R.; Peterlinz, K. A.; Rahn, J. R.; Peterson, A. W.; Grassi, J. H. *Langmuir* **2000**, *16*, 6759. (d) Bund, A.; Baba, A.; Berg, S.; Johannsmann, D.; Lubben, J.; Wang, Z.; Knoll, W. *J. Phys. Chem. B* **2003**, *107*, 6743.

(21) Neumann, T.; Johansson, M.-L.; Kambhampati, D.; Knoll, W. *Adv. Funct. Mater.* **2002**, *12*, 575.

All FTIR measurements were performed using a Digilab FTS 7000 step scan spectrometer.

The cyclic voltammetry (CV) experiments were carried out on a Princeton Applied Research Parstat 2263 with a modified ITO substrate as the working electrode coupled with a Pt plate counter and Ag/AgCl reference electrode. Cyclic voltammetry was utilized to prepare the cross-linked films from a 0.1 wt % of the precursor polymer solution of 0.1 M $TBAPF_6/CH_2Cl_2$.

The QCM apparatus, probe, and crystals are available from Maxtek Inc. The data acquisition was done using a RQCM (Research Quartz Crystal Microbalance, Maxtek, Inc.) system equipped with a built-in phase lock oscillator and the RQCM Data-Log Software. This was coupled with the Amel potentiostat to generate EC-QCM results. A 5 MHz AT-cut CBzC11SH modified on Au-coated quartz crystal with an effective area of 1.327 cm^2 was used as a working electrode. Platinum as a counter electrode and Ag/AgCl as a reference were used to measure in situ polymerization during cyclic voltammetry. To initiate the experiment, an inert probe was first immersed in methylene chloride until a stable frequency was obtained.

Surface plasmon resonance spectroscopy (SPR) on Au-coated glass (∼45 nm) was performed using a commercially available instrument (Multiskop) with a Kretschmann configuration and attenuated total reflection (ATR) conditions.[14] The reflectance was monitored with a p-polarized He−Ne laser (632.8 nm) as a function of angle of incidence.

Electrochemical surface plasmon resonance spectroscopy (EC-SPR) measurements were performed using a SPR setup combined with a three-electrode electrochemical cell in a Kretschmann configuration for the excitation of surface plasmons. The details of this setup are described in the Supporting Information. Surface plasmons were excited by reflecting p-polarized laser light off the Au-coated base of the prism. The excitation source employed was a He−Ne laser: $\lambda = 632.8$ nm. Kinetic measurements were performed to monitor the formation of the film. Reflectivity-angular measurements were also performed by scanning an incident angle range before and after in situ polymerization. For these experiments, the gold film thickness (∼45 nm) was chosen for optimum excitation of the surface plasmons. The electrode surface area was 0.785 cm^2.

Atomic force microscopy (AFM) imaging was examined in ambient conditions with a PicoSPM II (PicoPlus System, Molecular Imaging (now Agilent Technologies) Tempe, AZ) in tapping mode (AAC mode).

Synthesis. *Synthesis of 9-(Undec-10-enyl)-9*H*-carbazole (**2**).* To a stirred solution of 6.00 g (36.00 mmol) of carbazole in 15 mL of dimethylformamide (DMF), NaH 1.83 g (39.6 mmol) was added in portions, and after complete addition the mixture was heated to 60 °C for 2 h. After the mixture was cooled, a solution of 11-bromoundec-1-ene (9.40 g, 40.00 mmol) in 5 mL of DMF was added dropwise to the reaction mixture and was allowed to stir for 48 h at room temperature. The reaction mixture was then poured into water, extracted using methylene chloride, and dried over anhydrous Na_2SO_4. After the solvent was evaporated, the crude product was purified by column chromatography; using hexane as an eluent gave 9.50 g (3%) of the product. ^{1}H NMR (300 MHz, $CDCl_3$): δ 8.14 (d, $J = 7.8$ Hz, 2H, Ar*H*), 7.53−7.42 (m, 4H, Ar*H*), 7.27 (t, $J = 7.4$ Hz, 2H, Ar*H*), 5.84–5.63 (m, 1H, $CH_2CH{=}CH_2$), 4.99–4.82 (m, 2H, $CH_2CH{=}CH_2$), 4.29 (t, $J = 6.6$ Hz, 2H, NCH_2CH_2), 2.17–1.93 (m, 2H, CH_2CH_2CH), 1.96–1.67 (m, 2H, $CH_2CH_2CH_2$), 1.35−1.22 (m, 12H, $CH_2CH_2CH_2$). ^{13}C NMR (75 MH_Z, $CDCl_3$): 140.6, 139.3, 125.7, 123.1, 120.3, 118.9, 114.3, 109.9, 43.4, 34.2, 29.8, 29.7, 29.4, 29.3, 29.2, 27.7.

*Synthesis of 11-(9*H*-Carbazol-9-yl)undecyl Ethanethioate (**3**).* A solution of **2** (1.91 g, 6.00 mmol) in dry tetrahydrofuran (THF, 20 mL) containing thioacetic acid (0.63 g, 8.32 mmol) and 2,2′-azobis(2-methylpropionitrile) (AIBN) (56 mg, 0.172 mmol) was refluxed at 60 °C for 12 h under nitrogen. After cooling of the reaction flask, 20 mg of AIBN and 0.30 g of thioacetic acid were added and the mixture was refluxed for another 4 h. Concentration of the reaction mixture followed by flash column chromatography (4:1 hexane/CH_2Cl_2) gave 2.10 g (89%) of the product. ^{1}H NMR (300 MHz, $CDCl_3$): δ 8.14 (d, J=7.8Hz, 2H, Ar*H*), 7.53−7.42 (m, 4H, Ar*H*), 7.27 (t, $J = 7.8$ Hz, 2H, Ar*H*), 4.29 (t, $J = 6.8$ Hz, 2H, NCH_2CH_2), 2.70 (t, $J = 6.8$ Hz, 2H, CH_2CH_2CO), 2.35 (s, 3H, $COCH_3$), 1.92−1.88 (m, 2H, $CH_2CH_2CH_2$), 1.74−1.69 (m, 2H, $CH_2CH_2CH_2$), 1.38−1.26 (m, 14H, $CH_2CH_2CH_2$). ^{13}C NMR (75 MH_Z, $CDCl_3$): 196.0, 140.6, 125.7, 123.1, 120.3118.6, 108.9, 43.0, 39.1, 35.1, 32.1, 30.5, 29.4, 29.3, 29.1, 28.9, 27.3.

*Synthesis of 11-(9*H*-Carbazol-9-yl)-undecane-1-thiol (**4**).* In a 100 mL round-bottomed flask, **3** (1.00 g, 2.52 mmol) was dissolved in 10 mL of methanol, and CH_2Cl_2 was added dropwise to make the suspension clear. To this solution was added 1 mL of 50 wt % NaOH under nitrogen and the resulting mixture was allowed to stir overnight. The reaction mixture was neutralized by the addition of acetic acid. The neutralized solution was then poured into 25 mL of water and the organic phase was extracted using methylene chloride. The organic phase was then washed with brine and dried over Na_2SO_4. After filtration and concentration under vacuum, the crude product was further washed with hexane to give the pure product as 0.78 g (87%) of slightly yellowish oil. ^{1}H NMR (300 MHz, $CDCl_3$): δ 8.14 (d, $J = 7.8$ Hz, 2H, Ar*H*), 7.53−7.42 (m, 4H, Ar*H*), 7.27 (t, 2H, Ar*H*), 4.29 (t, 2H, NCH_2CH_2), 2.68 (t, 2H, CH_2CH_2SH), 1.92−1.88 (m, 2H, $CH_2CH_2CH_2$), 1.74−1.69 (m, 2H, $CH_2CH_2CH_2$), 1.38−1.26 (m, 15H, $CH_2CH_2CH_2$ and S*H*). ^{13}C NMR (75 MH_Z, $CDCl_3$): 140.6, 125.7, 123.1, 120.3, 118.6, 108.9, 43.0, 39.1, 35.1, 32.1, 29.3, 29.1, 29.0, 28.9, 28.4, 27.3.

*Synthesis of 4-Chloro-2,6-bis(hydroxymethyl)phenol (**5**).*[6e] To a solution of *p*-chlorophenol were added formaldehyde and sodium hydroxide and the resulting mixture was stirred for 7−10 days. The sodium salts of **5** were isolated by removal of the solvent under reduced pressure. Acidification of the sodium salts with acetic acid in acetone, removal of sodium acetate by filtration, and recrystallization from ethyl acetate resulted in 72% yield. ^{1}H NMR (400 MHz, CD_3OD): 7.178 (s, 2H, Ar*H*), 7.3 (m, 6H, Ar*H*). IR (KBr): ν 3412, 3300, 2967, 2914, 2888, 1478, 1456, 1211, 1068, 1010 cm^{-1}. MS (MALDI-TOF) Calcd for $[C_8H_9ClO_3]^+$: *m*/*z* 188.02. Found: *m*/*z* 189 $[M + H]^+$.

Synthesis of p-*Chloro*-N-*benzylhexahomotriazacalix[3]arene (**6**).*[6e] To a solution of **5** (6.00 g, 32.52 mmol) was added benzylamine (3.39 g, 31.67 mmol) in 150 mL of xylene; the resulting mixture was refluxed for 72 h, and the water generated was removed during the course of the reaction with a Dean-Sturk condenser. The mixture was evaporated to dryness as deep yellow oil. Chromatography on silica gel (hexane:EtOAc = 9:1, v/v) gives **6** (2.73 g, 33% yield). ^{1}H NMR (400 MHz, CD_2Cl_2): δ 7.29 (br s, g 15H, Ar*H*), 7.01 (s, 6H, Ar*H*), 3.69 (s, 6H, NCH_2Ar), 3.64 (s, 12H, NCH_2Ar). ^{13}C NMR (100 MH_Z, $CDCl_3$): δ 155.5, 136.4, 129.6, 129.4, 128.1, 127.3, 125.0, 122.7, 58.0, 56.7. IR (KBr): ν 3054, 3023, 2832, 2805, 1738, 1602, 1470, 1372, 1240, 1116, 863, 738, 699, 485 cm^{-1}. MS (MALDI-TOF) Calcd for $[C_{45}H_{42}C_{l3}N_3O_3]^+$: *m*/*z* 777.23. Found: *m*/*z* 778.69 $[M + H]^+$. Anal. Calcd for $C_{45}H_{42}C_{l3}N_3O_3$: C, 69.36; H, 5.43; N, 5.39. Found: C, 65.48; H, 5.78; N, 9.38.

*Synthesis of 9-(4-Bromobutyl)-9*H*-carbazole (**7**).* A solution of 59.1 g (237.7 mmol) of 1,4-dibromobutane, 1.00 g of tetrabutylammonium bromide, 5.16 g (30.86 mmol) of carbazole, 50 mL of

aqueous 50% sodium hydroxide, and 50 mL of benzene was stirred at 40 °C for 6 h. The organic layer was separated, and the aqueous layer was extracted three times with chloroform (3 × 30 mL). The combined organic layer was washed three times with water (3 × 40 mL) and dried over Na_2SO_4. The organic solvent was distilled over a water bath, the unreacted 1,4-dibromobutane was removed by vacuum distillation, and the residue was recrystallized from ethanol to give a white needle-like solid. Yield: 5.8 g (62%). ^{1}H NMR (300 MHz, $CDCl_3$): δ 8.06 (d, 2H, Ar*H*), 7.11−7.47 (m, 6*H*, Ar*H*), 4.29 (t, J = 5.4 Hz, 2H, NCH_2), 3.32 (t, J = 5.8 Hz, 2H, CH_2CH_2Br), 1.98 (m, 4H, ArCH_2CH_2). IR (KBr): ν 3045, 2939, 2925, 2855, 1620, 1593 cm^{-1}.

Synthesis of p-*Chloro*-N-*benzylhexahomotriazacalix[3]-tri(butylcarbazole) (***1***).* To a solution of **6** (0.50 g, 0.64 mmol), NaH (0.11 g, 4.42 mmol) in THF (20 mL), and DMF (5 mL) was added a solution of **7** (0.68 g, 2.25 mmol) in THF (10 mL). After being stirred for 2 days at 80 °C, the reaction mixture was evaporated, extracted with CH_2Cl_2, and washed with saturated $NaHCO_3$. The organic layer was dried over anhydrous Na_2SO_4, filtered, and evaporated under vacuum. Column chromatography on siliga gel (hexane/EtOAc = 9:1, v/v) afforded **1** (0.09 g, 0.06 mmol) in 10% yield as deep white oil. ^{1}H NMR (300 MHz, $CDCl_3$): δ 8.13–8.11 (m, 6H, ArH_{cbz}), 7.52–7.48 (m, 12H, ArH_{cbz}), 7.31 (m, 15H, ArH_{calix}), 7.04 (s, 4H, ArH_{calix}), 7.01 (s, 2H, ArH_{calix}), 4.13 (t, J = 7.2 Hz, 2H, OCH_2CH_2), 3.74 (t, J = 7.2 Hz, 4H, OCH_2CH_2), 3.78–3.00 (m, 24H, NCH_2Ar and $CH_2CH_2N_{cbz}$), 1.76−1.18 (m, 12H, CH_2CH_2 CH_2). ^{13}C NMR (75 MH_Z, $CDCl_3$): δ 157.5, 155.5, 141.0, 140.9, 139.8, 139.7, 135.0, 134.0, 133.6, 131.4, 129.9, 129.5, 129.4, 129.1, 128.9, 127.9, 127.7, 126.2, 123.4, 121.0, 120.9, 119.5, 119.4, 119.3, 109.3, 109.2, 75.0, 74.7, 63.4, 62.8, 60.4, 53.2, 52.2, 51.4, 43.50, 43.3, 30.2, 28.2, 28.1, 26.3, 26.2. IR (KBr): ν 2977, 2937, 2880, 1470, 1386, 1320, 1243, 1168, 1107, 1059, 1035, 929, 879, 817, 738 cm^{-1}. MS (MALDI-TOF) Calcd for $[C_{93}H_{87}Cl_3N_6O_3]^+$: *m*/*z* 1443.08. Found: *m*/*z* 1443.70 $[M + H]^+$.

*Synthesis of 9-(4-(9*H*-carbazol-9-yl)butyl)-9*H*-carbazole (***8***).* A solution of carbazole (5.00 g, 30.00 mmol) and KOH (1.68 g, 30.00 mmol) in acetone (20 mL) was added dropwise into a solution of dibromobutane (2.60 g, 12.00 mmol) in acetone (5 mL). After being stirred for 24 h at RT, the reaction mixture was evaporated, then extracted with CH_2Cl_2, and finally washed with EtOH and THF. The filter was dried in vacuum to afford **3** (3.26 g, 8.39 mmol) in 70% yield as a white solid. ^{1}H NMR (300 MHz, $CDCl_3$): δ 8.10 (d, J = 7.7 Hz, 4H, Ar*H*), 7.45–7.43 (m, 4H, Ar*H*), 7.23 (m, 4H, Ar*H*), 4.24 (t, J = 7.2 Hz, 4H, NC$H_2$$CH_2$), 2.13–1.88 (m, 4H, CH_2CH_2 CH_2).

Electrochemical Synthesis of Cross-linked Polymers (PPC-CBZ). The precursor polymers were synthesized using the cyclic voltammetry (CV) technique. In a three-electrode cell, 0.1 M tetrabutylammonium hexafluorophosphate ($TBAPF_6$) was used as a supporting electrolyte along with 0.1 wt % precursor **1** dissolved in anhydrous methylene chloride in separate cells. The electropolymerization of each precursor **1** was performed by sweeping the voltage at a scan rate of 50 mV/s from 0 to 1.0, 1.3, 1.5 V against Ag/AgCl as a reference electrode and platinum as a counter electrode. The ITO, gold-coated slides, and **4** coated gold substrates were used both as a working electrode and as a substrate.

Sensitivity and Selectivity Studies of PPC-CBz by Using Potentiometry. Polymerized on ITO substrates by sweeping the voltage at a scan rate of 50 mV/s from 0 to 1.3 V, **1** was studied as a sensor using 0.01 M TBACl as electrolyte. With use of a Teflon cell, 0.01 M TBACl was injected, until the potential signal was kept constant. To study sensitivity and selectivity of the polymer, different concentrations of cations were held constant for 1000 s. The change in potential (ΔE), [(ΔE) = observed potential (E_0) − initial potential (E_i)] was recorded simultaneously as a function of time.

Sensitivity and Selectivity Studies of PPC-CBz by Using EC-QCM and QCM. EC-QCM was used to polymerize PC-CBz on **4** coated gold substrates. The electropolymerization was performed by sweeping the voltage at the scan rate of 50 mV/s from 0 to 1.0 V. The sensitivity and selectivity were monitored in aqueous solution. From Figure S1, we injected water into the sample cell and kept this cell constant at room temperature for 1000 s. After that, such cell was dried in a vacuum oven for 10 min, and each delta frequency shown in Figure S1 was measured in air by QCM each time for 20 min as a function of cations' concentration: 10^{-6}, 10^{-5}, 10^{-4}, and 10^{-3} M.

Sensitivity and Selectivity Studies of PPC-CBz by Using EC-SPR and SPR. The details of this setup are described in Figure S2. Electropolymerization was done by EC-SPR (WE, **4** coated gold substrates; CE, Pt wire; RE, Ag/AgCl) at a scan rate of 20 mV/s (0 to 1.0 V). The sensing experiment was performed by injecting different concentrations of cations and each concentration stood for 1000 s at room temperature. Kinetic and angular measurements were observed as a function of time.

Acknowledgment. . The authors gratefully acknowledge financial support from NSF-DMR (05-04435), NSF-DMR-(06-02896), NSF-CTS (0330127), and the Robert A. Welch Foundation. C.K. and B.P. acknowledge support from the Thailand Research Fund (TRF) (RMU4880041) and the Royal Golden Jubilee Ph.D Program of TRF (PHD/0137/2546). We also acknowledge Prof. Akira Baba for his assistance in setting up the surface plasmon resonance spectrometer. Technical support from Maxtek Inc. and Optrel GmBH is also acknowledged.

Supporting Information Available: Experimental details and results for electrochemistry and AFM analysis on other substrates and control experiments for sensing (PDF). This material is available free of charge via the Internet at http://pubs.acs.org.

CM800284H

JOC The Journal of Organic Chemistry

Subscriber access provided by CHULALONGKORN UNIV

Note

Conformation-Selective Synthesis and Binding Properties of *N*-Benzylhexahomotriaza-*p*-chlorocalix[3]trinaphthylamide

Chatthai Kaewtong, Nongnuj Muangsin, Narongsak Chaichit, and Buncha Pulpoka

J. Org. Chem., **2008**, 73 (14), 5574-5577• DOI: 10.1021/jo800461r • Publication Date (Web): 25 June 2008

Downloaded from http://pubs.acs.org on March 31, 2009

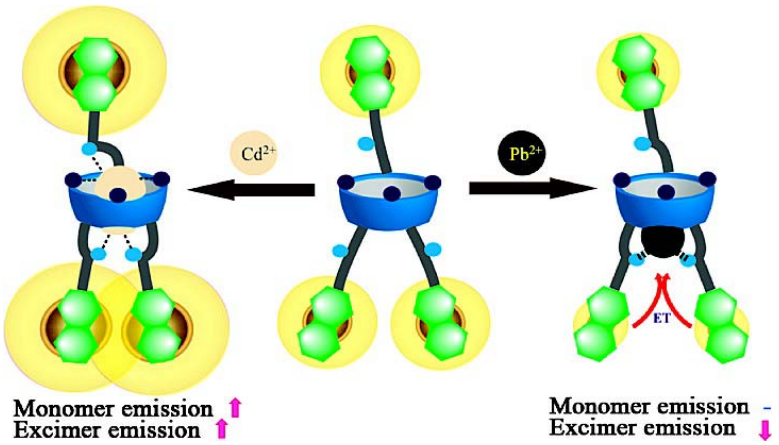

More About This Article

Additional resources and features associated with this article are available within the HTML version:

- Supporting Information
- Links to the 1 articles that cite this article, as of the time of this article download
- Access to high resolution figures
- Links to articles and content related to this article
- Copyright permission to reproduce figures and/or text from this article

View the Full Text HTML

ACS Publications
High quality. High impact.

The Journal of Organic Chemistry is published by the American Chemical Society.
1155 Sixteenth Street N.W., Washington, DC 20036

JOC*Note*

Conformation-Selective Synthesis and Binding Properties of *N*-Benzylhexahomotriaza-*p*-chlorocalix[3]trinaphthylamide

Chatthai Kaewtong,[†] Nongnuj Muangsin,[†] Narongsak Chaichit,[‡] and Buncha Pulpoka*,[†]

Supramolecular Chemistry Research Unit and Organic Synthesis Research Unit, Department of Chemistry, Faculty of Science, Chulalongkorn University, Bangkok 10330, Thailand, and Department of Physics, Faculty of Science and Technology, Thammasat University (Rangsit Campus), Pathumthani 12121, Thailand

buncha.p@chula.ac.th

Received March 5, 2008

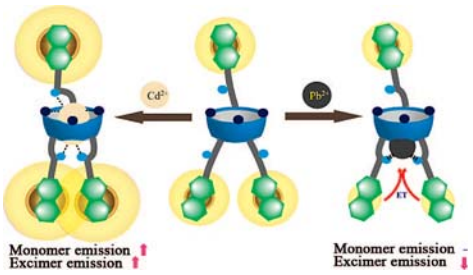

N-Benzylhexahomotriaza-*p*-chlorocalix[3]trinaphthylamide in partial cone conformation was selectively synthesized by appropriately controlling the steric effect during the amidation reactions of *N*-benzylhexahomotriaza-*p*-chlorocalix[3]tri-(ethyl acetate) in cone or partial cone conformations with use of 1-aminomethylnaphthalene. The conformation was confirmed by ^{1}H, ^{13}C, and 2D NMR and X-ray single-crystal analysis. Analyses of the complexes revealed that recognition is strongly affected by Cd^{2+}, Pb^{2+}, and F^{-} ions.

On the basis of the concepts provided by host−guest chemistry, cation and anion sensing has recently risen to a dominant position in research devoted to the detection of designated species.[1] This rapid growth is derived from the realization of the diverse roles played by cations and anions in biological and environmental systems.[2,3]

Calixarenes and the related macrocycles have received a lot of recent attention due to their molecular recognition properties.[3,4] In recent years, the homocalixarenes, hexahomotrioxacalixarenes (or oxacalix[3]arenes),[5] hexahomotrithiacalixarenes (or thiacalix[3]arenes),[6] and hexahomotriazacalixarenes (or azacalix-[3]arenes), have been synthesized as parts of a class of compounds called expanded calixarenes.[7] From a structural point of view, they are of a similar size to 18-crown-6. However, their topology provides 3-D cavities which can better envelop the substrates. It is well-known that the more coordinating sites that are present then, generally, the higher the complex stability.[8] Therefore, to optimize the number of such binding sites, oxygen and sulfur atoms on oxa- and thiacalix[3]arenes are typically replaced with nitrogen in the azacalixarenes. Nevertheless, the azacalixarenes have received relatively little attention, mainly because they can only be synthesized in relatively low overall yields. Thus, there are only a limited number of studies of the solution conformations, solid-state structures, and complex formation properties of these molecules and, unlike calixarenes, the conditions for functionalization to provide a specific conformation have rarely been reported. Previously, Hampton and co-workers[9] showed that the conformations of azacalix[3]arenes were cone and partial cone, based on NMR and X-ray single-crystal studies, but most research has focused on studying only the cone conformations.[7−9] Metal complexes of the cone conformation with an extraction method, such as UO_2^{2+} in the presence of a high concentration of NaCl,[7a] lanthanide ions,[7b] and alkali metals,[7c] have been reported. Moreover, Thuéry et al.[10] prepared UO_2^{2+}, Nd^{3+}, and Yb^{3+} complexes of azacalixarenes without using any bases and obtained crystals of the complexes suitable for crystallographic analyses.

Recently, we reported that the cone conformation of N_7-hexahomotriazacalix[3]cryptand (**3**) can serve as a highly selective receptor for chloride ions.[11] Its selectivity can be altered to preferentially bind bromide ions over other halide ions by complexing with zinc ions, presumably due to allosteric and ion-pair effects as illustrated in Scheme 1. However, partial cone conformation was not reported in this study. To further

[†] Chulalongkorn University.
[‡] Thammasat University (Rangsit Campus).

(1) (a) Lehn, J.-M. *Supramolecular Chemistry, Concepts and Perspectives*; WCH:Weinheim, Germany, 1995. (b) Inoue,Y.; Gokel, G. W. *Cation Binding by Macrocycles, Complexation of Cationic Species by Crown Ether*; Marcel Dekker: New York, 1990.
(2) (a) Gutsche, C. D. *Calixarenes, Monographs in Supramolecular Chemistry*; Stoddart, J. F., Ed.; Royal Society of Chemistry: Cambridge, U.K., 1989; Vol. 1. (b) Anslyn, E. V. *J. Org. Chem.* **2007**, *72*, 687.
(3) Lumetta, G. J.; Rogers, R. D.; Gopalan, A. S. *Calixarenes for Separations*; American Chemical Society: Washington, DC, 2000.
(4) Asfari, Z.; Böhmer, V.; Harrowfield, J. *Calixarenes 2001*; Kluwer Academic Publishers: Dordretch, The Netherlands, 2001.
(5) (a) Dhawan, B.; Gutsche, C. D. *J. Org. Chem.* **1983**, *48*, 1536. (b) Zerr, P.; Mussrabi, M.; Vicens, J. *Tetrahedron Lett.* **1991**, *32*, 1879. (c) Hampton, P. D.; Bencze, Z.; Tong, W.; Daitch, C. E. *J. Org. Chem.* **1994**, *59*, 4838. (d) Ashram, M.; Mizyed, S.; Georghiou, P. E. *J. Org. Chem.* **2001**, *66*, 1473. (e) Ashram, M. *J. Inclusion Phenom.* **2006**, *54*, 253. (f) Tsubaki, K.; Otsubo, T.; Tanaka, K.; Fuji, K. *J. Org. Chem.* **1998**, *63*, 3260. (g) Tsubaki, K.; Mukoyoshi, K.; Otsubo, T.; Fuji, K. *Chem. Pharm. Bull.* **2000**, *48* (6), 882. (h) Tsubaki, K.; Morimoto, T.; Otsubo, T.; Kinoshita, T.; Fuji, K. *J. Org. Chem.* **2001**, *66*, 4083.
(6) Masci, B.; Nierlich, M.; Thuéry, P. *New J. Chem.* **2002**, *26*, 766.
(7) (a) Takemura, H.; Yoshimura, K.; Khan, I. U.; Shinmyozu, T.; Inazu, T. *Tetrahedron Lett.* **1992**, *33*, 5775. (b) Takemura, H.; Shinmyozu, T.; Miyura, H. *J. Inclusion Phenom. Macrocyclic Chem.* **1994**, *19*, 193. (c) Hampton, P. D.; Tong, W. D.; Wu, S.; Duesler, E. N. *J. Chem. Soc., Perkin Trans. 2.* **1996**, 1127.
(8) Schneider, H-J.; Yatsimirsky, A. K. *Principle and methods in Supramolecular Chemistry*; Wiley: New York, 2000.
(9) Chirakul, P.; Hampton, P. D.; Duesler, E. N. *Tetrahedron Lett.* **1998**, *39*, 5473.
(10) (a) Thuéry, P.; Nierlich, M.; Vicens, J.; Takemura, H. *J. Chem. Soc., Dalton Trans.* **2000**, *42*, 279. (b) Thuéry, P.; Nierlich, M.; Vicens, J.; Masci, B.; Takemura, H. *Eur. J. Inorg. Chem.* **2001**, 637. (c) Thuéry, P.; Nierlich, M.; Vicens, J.; Takemura, H. *Polyhedron* **2000**, *19*, 2673.
(11) Kaewtong, C.; Fuangswasdi, S.; Muangsin, N.; Chaichit, N.; Vicens, J.; Pulpoka, B. *Org. Lett.* **2006**, *8*, 1561.

10.1021/jo800461r CCC: $40.75 © 2008 American Chemical Society
Published on Web 06/25/2008

SCHEME 1. Cone Conformation of N_7-Hexahomotriazacalix[3]cryptand (3) Can Serve As a Highly Selective Receptor for Chloride Ions or Be Adapted to Preferentially Bind Bromide Ions in the Present Zinc Ions

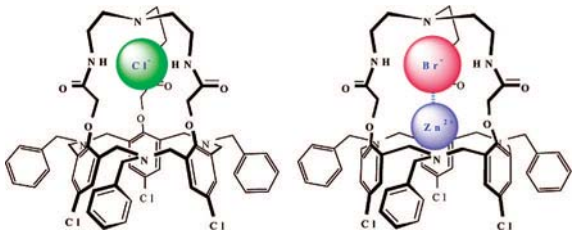

SCHEME 2. Synthesis of 1[a]

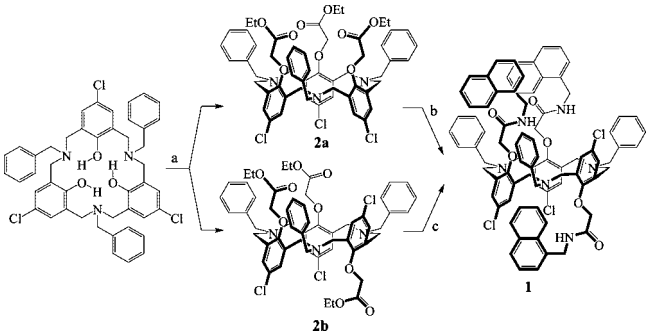

[a] Reagents and conditions: (a) ethyl bromoacetate, NaH, THF, DMF, reflux, 72 h, **2a** (21%) and **2b** (31%); (b) 1-aminomethylnaphthalene, toluene:MeOH (1:1), rt, 3 d, **1** (41%); (c) 1-aminomethylnaphthalene, toluene:MeOH (1:1), rt, 7 d, **1** (42%).

understand the properties of azacalix[3]arenes, this work reports a conformational selective synthesis, the X-ray crystal structures, and the binding properties of *N*-benzylhexahomotriaza-*p*-chlorocalix[3]trinaphthylamide (**1** in Scheme 2). To the best of our knowledge, this is the first example showing the complex formation ability of a partial cone azacalix[3]arene.

The synthesis of *N*-benzylhexahomotriaza-*p*-chlorocalix[3]-trinaphthylamide (**1**) was carried out as schematically shown in Scheme 2. Alkylation of *N*-benzylhexahomotriaza-*p*-chlorocalix[3]arene with ethyl bromoacetate in the presence of NaH in THF/DMF produced compound **2a** (*cone conformation*, 21% yield) and compound **2b** (*partial cone conformation*, 31% yield). The reactions between **2a** and **2b** with 1-aminomethyl-naphthalene afforded only the partial cone conformer of *N*-benzylhexahomotriaza-*p*-chlorocalix[3]trinaphylamide (**1**) with 41% and 42% yields, respectively. More interestingly, during the preparation of **1** by starting with **2a**, the conformation changed from cone to partial cone. This may be due to the small energetic barrier of aromatic flipping by passing the para position through the cavity for cone-to-partial cone inversion of azacalix[3]arene, which provides a more stable partial cone conformer as a result of the steric effect and solvent polarity.[12] The structure of compound **2a** was confirmed by X-ray single-crystal analysis, as shown in Figure 1a.

The proposed partial cone conformation of *N*-benzylhexaho-motriaza-*p*-chlorocalix[3]trinaphylamide (**1**) was confirmed by ^{1}H, ^{13}C, 2D NMR and X-ray single crystal studies (Supporting Information). In the ^{1}H NMR spectrum of **1**, the methylene protons of the $Ar_{calix}CH_2N$ bridges are presented as two AB doublets at 3.91 (J_{H-H} = 15.0 Hz), 3.58 (J_{H-H} = 15.0 Hz), 2.57 (J_{H-H} = 13.4 Hz), and 2.28 (J_{H-H} = 13.4 Hz) ppm and as a signal in a multiplet at 2.99−2.71 ppm. The other doublets for the methylene protons of $Ar_{nap}CH_2NH$ appear at 5.11, 5.04, 5.00, 4.93, and 4.89 ppm with germinal coupling constants of 4.8, 5.6, 4.8, 4.8, and 5.2 Hz, respectively. In the parent hexahomotriazacalix[3]arene, which adopts a regular C_{3v} cone conformation, the six protons of $Ar_{calix}H$ exists as a singlet at δ 7.01 ppm.[10] In this case, the three singlets of $Ar_{calix}H$ are observed at 6.51, 6.44, and 6.36 ppm. The ^{13}C NMR spectrum also confirms the partial cone conformation of the azacalix[3]arene macroring of **1**. $Ar_{nap}CH_2NH$ appears as two peaks (41.6, 41.2 ppm) and $Ar_{calix}CH_2N$ splits into four peaks (72.8, 52.7, 52.5, and 52.0 ppm). ^{13}C signals of Ar_{calix} connected with hydrogen also have three peaks, at 130.2, 130.1, and 129.5 ppm. These findings suggest that the three O-substituents have different environments, which implies that **1** is in a stable partial cone conformation. The X-ray single-crystal structure of **1**[13] also strongly supports the partial cone conformation, as shown in Figure 1b. The results show the cavity of azacalix[3]arene macroring (7.92 × 4.92 Å^2) for cation and free N−H for anion binding sites of **1**.

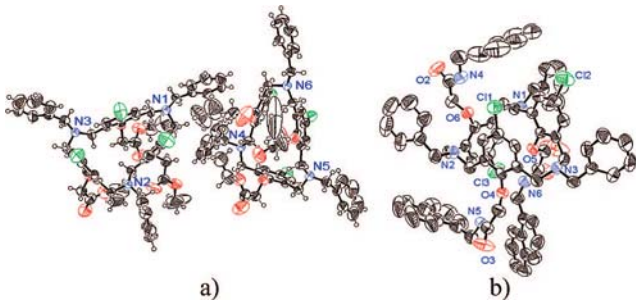

FIGURE 1. ORTEP drawing of (a) *N*-benzylhexahomotriaza-*p*-chlorocalix[3]tri(ethyl acetate) (**2a**) and (b) *N*-benzylhexahomotriaza-*p*-chlorocalix[3]trinaphthylamide (**1**). The displacement ellipsoids are drawn at the 50% probability level.

It is well-known that hexahomotriazacalix[3]arene is a strong metal ion complexing agent[7,10] and an amide derivative that can complex anions.[11] Generally, a naphthylene-based fluorophore can form a monomer and excimer[13] that can be observed in a fluorescent spectrum at wavelengths of 336 and 423 nm, respectively. However, the excimer formation of fluorophores that contain more than one fluorogenic unit can be either inter- or intramolecular, in which the former depends on the concentration and solvent polarity. The ratio of excimer to monomer can be observed by the ratio of intensities of excimer to monomer ($I_{excimer}/I_{monomer}$ or I_e/I_m). From the fluorescent spectrum, it was observed that ligand **1** exhibits a strong monomer emission at 336 nm and an excimer emission at 423 nm, suggesting that the two naphthalene units are in a face-to-face π-stack so as to form a dynamic excimer.[14] The ratio of I_e/I_m increases when the concentration of fluorophore **1** decreases (Figure S1, Supporting Information). This may be because, at low concentra-

(12) Iwamoto, K.; Ikeda, A.; Araki, K.; Harada, T.; Shinkai, S. *Tetrahedron Lett.* **1993**, *49*, 9937.

(13) X-ray data were collected on a Bruker SMART CCD area detector. The crystal structure was solved by direct methods and refined by full-matrix least-squares. All non-hydrogen atoms were refined anisotropically, and hydrogen atoms were refined by using the riding model. All calculations were performed with a crystallographic software package, WinGX v1.64.05. Crystal data for **1**: $C_{84}H_{75}Cl_3N_6O_6 \cdot 3H_2O$, M_r = 1424.90, monoclinic, space group $P\bar{1}$, a = 16.1795(3) Å, b = 16.5809(3) Å, c = 16.6482(2) Å, α = 92.624(1)°, β = 105.880(1)°, γ = 112.174(1)°, V = 3921.97(11) Å^3, Z = 2, ρ_{calc} = 1.207 g cm^{-3}, $2\theta_{max}$ = 30.54°, Mo Kα (λ = 0.71075 Å), μ = 0.176 mm^{-1}, $\theta-\omega$ scans, T = 293(2) K, 28143 independent reflections, 20620 unique reflections ($I > 2.0\sigma(I)$), 924 refined parameters, R_1 = 0.1276, Rw = 0.3142, $\Delta\rho_{max}$ = 1.204 e Å^{-3}, $\Delta\rho_{min}$ = −0.395 e Å^{-3}; CCDC 673516. See the Supporting Information for crystallographic data in CIF format.

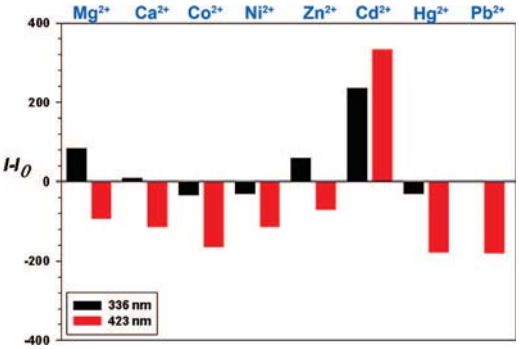

FIGURE 2. Fluorescence changes ($I - I_o$) of **1** upon addition of various metal ions. Conditions: **1** (1 μM) in DMSO, excitation at 285 nm, metal nitrate and chloride (300 equiv) in DMSO. I is the fluorescence emission intensity of complexes **1**. I_o is the fluorescence emission intensity of free **1**.

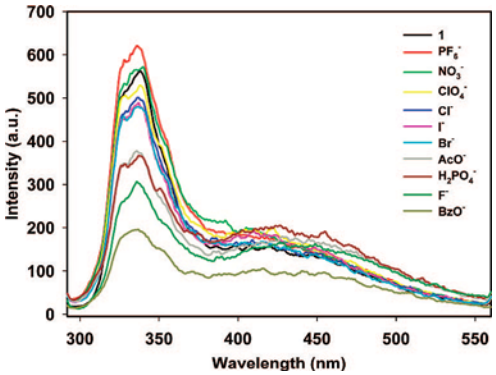

FIGURE 3. Fluorescence emission spectra of **1** upon addition of various anions. Conditions: **1** (0.1 μM) in DMSO, excitation at 285 nm, TBAX (300 equiv) in DMSO.

tions where there is a low percentage of intermolecular interaction, the two naphthyl groups which are on the same side of the azacalix[3]arene platform form an intramolecular excimer and give an excimer emission at 423 nm.

The other naphthyl moiety, where no intermolecular interaction occurs, remains a monomer, but its monomer emission at 336 nm is quenched because the nitrogen atoms are sharing electrons with PET. At higher concentrations, the intermolecular interaction increases, leading to the formation of a hydrogen bond between the amide groups from a side containing a single residue. This hydrogen bond formation prevents the face-to-face stacking of naphthyl moieties and the PET process, leading to increased monomer emission.

The fluorescence intensity changes of **1** were investigated to determine the cation (Figure 2) and anion (Figure 3) binding abilities. In the case of cations, it was found that **1** exhibits Pb^{2+}, Hg^{2+} and Co^{2+} (strong quenching), and Cd^{2+} (strong enhancing) selectivity over the other metal cations studied, as shown in Figure 2. These data imply that **1** binds metal ions with different modes. In the case of Pb^{2+}, only excimer fluorescence is strongly quenched, which is likely to be due not only to the reverse PET from the naphthyl groups to the electron-deficient carbonyl oxygen atoms but also to a heavy-metal ion effect.[15] This may then suggest that Pb^{2+} is strongly bound in a cavity on the side containing two naphthylamide units.

In the case of Cd^{2+}, both monomer and excimer emissions increased with its presence, strongly suggesting that the Cd^{2+} ion preferentially binds by nitrogen atoms of the azacalix[3]arene macroring and is weakly chelated by the carbonyl groups from both sides of azacalix[3]arene, and that consequently the PET and heavy metal effects are excluded. The azacalix[3]arene template, which has a similar structure to that of azacrown ether,[16] exhibits excellent binding with Cd^{2+} and shows, for the first time, the advantage of the azacalixarene framework over the parent calixarene.[7] UV−vis spectroscopy was employed to determine the stoichiometry and stability constants for the complexes with use of the SIRKO program.[17] According to the extent of the observed absorption spectra changes, the association constants of **1** were obtained, and are summarized in Table 1. The data indicate that ligand **1** binds strongly with Pb^{2+} (log β = 4.68 M^{-1}) and Cd^{2+} (log β = 4.53 M^{-1}). The titration profiles of absorption changes of **1** with Cd^{2+} and Pb^{2+} are shown in Figures S3 and S4 (Supporting Information) which show the different patterns. The absorptions of the azacalix[3]arene unit in receptor **1** at wavelengths of 285 and 296 nm strongly decrease upon an addition of Cd^{2+}. In case of Pb^{2+}, the decreases of absorption of these two wavelengths are less pronounced, while the absorption at a wavelength around 265 nm strongly increases. This result confirms that both cations were bound with different modes.

TABLE 1. Stability Constants (log β)[a] of 1:1 Complexes of 1 with Cations and Anions in DMSO by the UV−Vis Titration Method (T = 25 °C, I = 0.01 M Bu_4NPF_6)

cation	log β (M^{-1})	anion	log β (M^{-1})
Mg^{2+}	2.13 (0.01)[b]	F^-	4.21 (0.09),[b] 9.71 (0.01)[c]
Ca^{2+}	2.01 (0.04)[b]	Cl^-	2.37 (0.05)[b]
Co^{2+}	4.08 (0.09)[b]	Br^-	not determined
Ni^{2+}	1.83 (0.04)[b]	I^-	not determined
Cu^{2+}	2.06 (0.08)[b]	NO_3^-	2.03 (0.01)[b]
Zn^{2+}	3.23 (0.09)[b]	ClO_4^-	2.20 (0.01)[b]
Cd^{2+}	4.53 (0.04)[b]	$H_2PO_4^-$	not determined
Hg^{2+}	2.12 (0.01)[b]	AcO^-	2.43 (0.02),[b] 9.29 (0.03)[c]
Pb^{2+}	4.68 (0.04)[b]	BzO^-	2.83 (0.01),[b] 9.43 (0.03)[c]

[a] Mean values of $n \geq 3$ (for cations) and $n \geq 2$ (for anions) of independent determinations with standard deviation σ_{n-1} on the mean in parentheses. [b] 1:1 complex (AL). [c] 2:1 complex (A_2L).

For the anion sensor study, the fluorescence reveals a quenching effect from a PET mechanism on the monomer peak. The excimer peak, however, has a much lower effect, indicating that allosteric effect-induced conformation changes do not favor the binding of anions. The ^1H MNR spectra of **1** anions also strongly support this notion revealing that only the signals of amide protons shift (Figure S2, Supporting Information), and thus that anions were likely bound by hydrogen bonds with the amide groups.

To obtain an insight into the selectivity of anion binding, UV−vis spectroscopy was employed to study the interaction

(14) (a) Galindo, F.; Becerril, J.; Burguete, M. I.; Luis, S. V.; Vigara, L. *Tetrahedron Lett.* **2004**, *45*, 1659. (b) Roy, M. B.; Samanta, S.; Chattopadhyay, G.; Ghosh, S. *J. Lumin.* **2004**, *106*, 141.

(15) (a) Kim, J. S.; Quang, D. T. *Chem. Rev.* **2007**, *107*, 3780. (b) Kim, S. K.; Kim, S. H.; Kim, H. J.; Lee, S. H.; Lee, S. W.; Ko, J.; Bartsch, R. A.; Kim, J. S. *Inorg. Chem.* **2005**, *44*, 7866. (c) Choi, J. K.; Kim, S. H.; Yoon, J.; Lee, K.-H.; Bartsch, R. A.; Kim, J. S. *J. Org. Chem.* **2006**, *71*, 8011. (d) Kim, J. S.; Kim, H. J.; Kim, H. M.; Kim, S. H.; Lee, J. W.; Kim, S. K.; Cho, B. R. *J. Org. Chem.* **2006**, *71*, 8016.

(16) (a) Cakir, U.; Cicek, B. *Transition Metal. Chem.* **2004**, *29*, 263. (b) Costero, A. M.; Salvador Gil, S.; Sanchis, J.; Peransí, S.; Sanz, V.; Williams, J. A. G. *Tetrahedron* **2004**, *60*, 6327. (c) Liang, X.; Parkinson, J. A.; Parsons, S.; Weishäupl, M.; Sadler, P. J. *Inorg. Chem.* **2002**, *41*, 4539. (d) Costero, A. M.; Monrabal, E.; Sanjuan, F. *Tetrahedron* **1999**, *55*, 15141. (e) Nelson, J.; Mckee, V.; Morgan, G. *Prog. Inorg. Chem.* **2007**, *47*, 167–316.

(17) Vetrogon, V. I.; Lukyanenko, N. G.; Schwing-well, M. J.; Arnaud-Neu, F. *Talanta* **1994**, *41*, 2105.

of compounds **1** with anionic guests. Upon the addition of anions, the absorption spectra of **1** changed (see Table S1, Supporting Information). From the derived stability constants (Table 1) of compound **1** complexes with anions, it can be concluded that **1** prefers to complex F^- over the other anions tested by forming 1:1 complexes.

In summary, the partial-cone conformation of *N*-benzylhexahomotriaza-*p*-chlorocalix[3]trinaphthylamide (**1**) was selectively synthesized from both cone and partial-cone triester intermediates coupling with 1-aminomethylnaphthalene. The crystal structures of **1** and **2a** were confirmed by X-ray crystallography. On the basis of fluorescent, UV−vis, and ^{1}H NMR spectra changes upon cation and anion complex formation, it has been noted that **1** displays strong binding with Cd^{2+} (by using nitrogen at the azacalix[3]arene framework), Pb^{2+} and Co^{2+} (by using the carbonyl of amide groups from the side of azacaliz[3]arene containing two naphthyl groups), and F^- (by using hydrogen bonds between the NH part of the amide with anions).

Experimental Section

Synthesis of *N*-Benzylhexahomotriaza-*p*-chlorocalix[3]tri(ethyl acetate) (2). The synthetic procedures of **2a** and **2b** have been modified from our previous work[11] by replacing the methyl bromoacetate with ethyl bromoacetate. Column chromatography on silica gel (hexane/EtOAc = 9:1, v/v) of crude product afforded a 21% yield of **2a** (X-ray data demonstrated in the Supporting Information) (0.135 g, 0.130 mmol) as a deep yellow oil. **2a**: ^{1}H NMR (400 MHz, $CDCl_3$) δ 7.34−7.26 (m, 12H, Ar*H*), 7.18 (t, 3H, J_{H-H} = 7.2 Hz, Ar*H*), 6.90 (s, 6H, Ar*H*), 4.28 (s, 6H, OCH_2CO), 4.22 (q, 6H, J_{H-H} = 7.6 Hz, OCH_2CH$_3$), 3.61 (s, 6H, NCH_2Ar), 3.44 (dd, 12H, J_{H-H} = 14.4, 7.6 Hz, NCH_2Ar), 1.28 (t, 9H, J_{H-H} = 7.2 Hz, OCH$_2$CH_3); ^{13}C NMR (100 MH$_Z$, $CDCl_3$) δ 169.1, 152.3, 139.2, 133.9, 130.1, 129.0, 128.9, 128.9, 128.6, 127.3, 71.0, 62.4, 52.5, 52.1, 14.4; IR (KBr) ν 3063, 3028, 2981, 2929, 2803, 1757, 1448, 1372, 1292, 1188, 1118, 1065, 1030, 879, 743, 701 cm^{-1}; MS (MALDI-TOF) calcd for $[C_{57}H_{60}Cl_3N_3O_9]^+$ *m*/*z* 1035.34, found 1036.92 $[M + H]^+$. Anal. Calcd for $C_{57}H_{60}Cl_3N_3O_9$: C, 65.99; H, 5.83; N, 4.05. Found: C, 65.95; H, 5.71; N, 4.00. **2b** (pale yellow solid, 31%): ^{1}H NMR (400 MHz, $CDCl_3$) δ 7.57 (d, J = 7.6 Hz, 2H, Ar*H*), 7.31 (t, J = 7.6 Hz, 3H, Ar*H*), 7.38−7.30 (m, 10H, Ar*H*), 7.02 (s, 4H, Ar*H*), 6.98 (s, 2H, Ar*H*), 4.31 (br d, 2H, OCH_2CO), 4.15 (s, 4H, OCH_2CH$_3$), 4.13 (s, 2H, OCH_2CH$_3$), 4.11 (br d, 2H, OCH$_2$CO), 3.79−3.22 (m, 20H, OCH$_2$CO and NCH$_2$Ar), 1.24 (m, 9H, OCH$_2$CH$_3$); ^{13}C NMR (100 MHz, $CDCl_3$) δ 169.1, 169.0, 155.8, 154.1, 139.4, 138.6, 134.8, 133.4, 132.9, 131.6, 130.4, 129.6, 129.3, 129.2, 128.8, 128.5, 128.4, 128.1, 127.4, 127.3, 70.8, 70.3, 63.0, 60.9, 59.4, 53.0, 52.7, 52.4, 14.4, 14.3; IR (KBr) ν 3063, 3028, 2981, 2922, 2852, 2804, 1756, 1446, 1376, 1291, 1187, 1121, 1063, 1030, 891, 743, 700 cm^{-1}; MS (MALDI-TOF) calcd for $[C_{54}H_{54}Cl_3N_3O_9]^+$ *m*/*z* 1035.34, found 1036.92 $[M + H]^+$. Anal. Calcd for for $C_{57}H_{60}Cl_3N_3O_9$: C, 65.99; H, 5.83; N, 4.05. Found: C, 65.82; H, 5.92; N, 3.93.

Synthesis of *N*-Benzylhexahomotriaza-*p*-chlorocalix[3]trinaphthylamide (1). A solution of **2a** (0.135 g, 0.130 mmol) was charged with a solution of 1-napthymethylamine (0.072 g, 0.456 mmol) in 1:1 methanol:toluene mixture (10 mL). The solution was refluxed for 3 days. After removing the solvents, the crude mixture was purified by column chromatography of the precipitate on silica gel (hexane/EtOAc = 3:2, v/v), which gave **1** (0.073 g, 0.053 mmol, 41%) as a white solid. A solution of **2b** (0.207 g, 0.200 mmol) was charged with a solution of 1-napthymethylamine (0.207 g, 0.700 mmol) in 1:1 methanol:toluene mixture (10 mL). The solution was refluxed for 7 days. After removing the solvents, the crude mixture was purified by column chromatography of the precipitate on silica gel (hexane/EtOAc = 3:2, v/v), which gave **1** (0.114 g, 0.087 mmol, 42%) as a white solid: ^{1}H NMR (400 MHz, CDCl3) δ 8.10−8.08 (m, 3H, ArH_{nap}), 8.01−7.97 (m, 4H, ArH_{nap}), 7.91 (d, J_{H-H} = 7.2 Hz, 2H, ArH_{nap}), 7.64−7.57 (m, 8H, ArH_{nap}), 7.64−7.57 (m, 4H, ArH_{nap}), 7.32−7.21 (m, 9H, ArH_{calix}), 7.14 (d, J_{H-H} = 6.8 Hz, 2H, ArH_{calix}), 7.09 (d, J_{H-H} = 7.6 Hz, 4H, ArH_{calix}), 7.02 (s, 1H, CH$_2$N*H*CO), 6.86 (s, 2H, CH$_2$NHCO), 6.51 (s, 2H, ArH_{calix}), 6.44 (s, 2H, ArH_{calix}), 6.36 (s, 2H, ArH_{calix}), 5.11 (d, J_{H-H} = 4.8 Hz, 2H, ArCH_2NH), 5.04 (d, J_{H-H} = 5.6 Hz, 1H, ArCH_2NH), 5.00 (d, J_{H-H} = 4.8 Hz, 1H, ArCH_2NH), 4.93 (d, J_{H-H} = 4.8 Hz, 1H, ArCH_2NH), 4.89 (d, J_{H-H} = 5.2 Hz, 1H, ArCH_2NH), 3.91 (d, J_{H-H} = 15.2 Hz, 2H, ArCH_2N), 3.80 (s, 2H, OCH_2CO), 3.58 (d, J_{H-H} = 14.8 Hz, 2H, ArCH_2N), 3.09 (s, 2H, OCH_2CO), 2.99−2.71 (m, 12H, ArCH_2N and OCH_2CO), 2.57 (d, J_{H-H} = 12.8 Hz, 2H, ArCH_2N), 2.28 (d, J_{H-H} = 14.0 Hz, 2H, ArCH_2N); ^{13}C NMR (100 MH$_Z$, $CDCl_3$) δ 167.3, 167.2, 153.1, 152.0, 138.6, 137.8, 134.2, 134.1, 133.5, 133.3, 133.1, 132.5, 131.7, 131.5, 130.2, 130.1, 129.7, 129.5, 129.3, 129.2, 129.1, 129.0, 128.8, 128.7, 128.5, 128.4, 128.3, 127.7, 127.5, 127.1, 127.0, 126.4, 126.3, 126.0, 125.5, 123.9, 123.6, 72.8, 71.4, 63.0, 60.0, 52.7, 52.5, 52.0, 41.6, 41.2; IR (KBr) ν 3419, 3059, 2921, 2837, 2810, 1679, 1594, 1524, 1436, 1364, 1251, 1193, 1124, 1041, 884, 797, 789, 745, 701 cm^{-1}; MS (MALDI-TOF) calcd for $[C_{84}H_{75}Cl_3N_6O_6]^+$ *m*/*z* 1368.48, found 1369.67 $[M + H]^+$. Anal. Calcd for $C_{84}H_{75}Cl_3N_6O_6$: C, 73.59; H, 5.51; N, 6.31. Found: C, 73.56; H, 5.53; N, 6.14.

Acknowledgment. The authors gratefully acknowledge the Thailand Research Fund (TRF) for financial support (RMU4880041 and RTA4880008) and the Royal Golden Jubilee Ph.D. Program of TRF (PHD/0137/2546).

Supporting Information Available: Experimental procedures and spectroscopic data for all new compounds including NMR spectra and crystal structures of *N*-benzylhexahomotriaza-*p*-chlorocalix[3]trinaphthylamide (**1**) (CIF) and *N*-benzylhexahomotriaza-*p*-chlorocalix[3]tri(ethyl acetate) (**2a**) (CIF). This material is available free of charge via the Internet at http://pubs.acs.org.

JO800461R

ACS NANO

Subscriber access provided by CHULALONGKORN UNIV

Articles

Self-Assembly and Electrochemical Oxidation of Polyamidoamine#Carbazole Dendron Surfmer Complexes: Nanoring Formation

Chatthai Kaewtong, Guoqian Jiang, Mary Jane Felipe, Buncha Pulpoka, and Rigoberto Advincula

ACS Nano, **2008**, 2 (8), 1533-1542• DOI: 10.1021/nn800098j • Publication Date (Web): 25 July 2008

Downloaded from http://pubs.acs.org on March 31, 2009

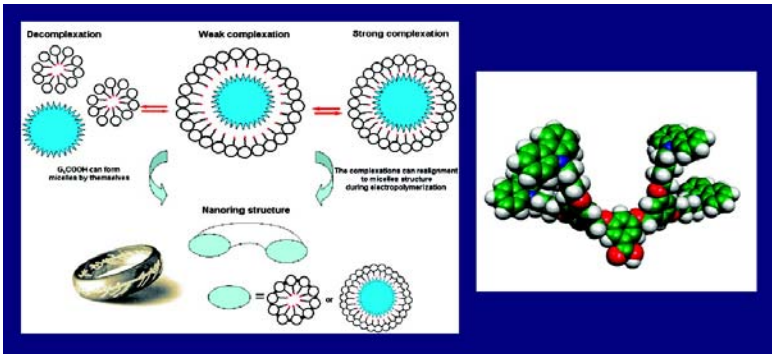

More About This Article

Additional resources and features associated with this article are available within the HTML version:

- Supporting Information
- Access to high resolution figures
- Links to articles and content related to this article
- Copyright permission to reproduce figures and/or text from this article

View the Full Text HTML

ACS Publications
High quality. High impact.

ACS Nano is published by the American Chemical Society. 1155 Sixteenth Street N.W., Washington, DC 20036

Self-Assembly and Electrochemical Oxidation of Polyamidoamine–Carbazole Dendron Surfmer Complexes: Nanoring Formation

Chatthai Kaewtong,[†,‡] Guoqian Jiang,[†] Mary Jane Felipe,[†] Buncha Pulpoka,[‡,*] and Rigoberto Advincula[†,*]

[†]Department of Chemistry and Department of Chemical and Biomolecular Engineering, University of Houston, Houston, Texas 77204-5003, and [‡]Supramolecular Chemistry Research Unit and Organic Synthesis Research Unit, Department of Chemistry, Faculty of Science, Chulalongkorn University, Bangkok 10330, Thailand

ABSTRACT We report a detailed and quantitative study on the supramolecular complexation of amine-functionalized polyamidoamine (PAMAM) dendrimer G_4-NH_2 with carboxylic acid terminal dendrons containing peripheral electroactive carbazole groups of different generations (G_0COOH, G_1COOH, and G_2COOH). While the focus is on a detailed understanding and mechanism of complex formation, subsequent electrochemical oxidation of the dendron surfmers resulted in the formation of *nanoring* structures electrodeposited on the conducting substrate. Complexation was confirmed by NMR, UV–vis, and IR measurements. Critical micelle concentration (CMC), atomic force microscopy (AFM), and X-ray photoelectron spectroscopy (XPS) studies revealed that the ringlike structures were formed during the equilibrium–decomplexation stage and that the electrochemical process did not destroy the complex but rather stabilized it. The different generations of the dendrons provided various structures and complex formation efficacy. This type of template polymerization combined with electrochemically anodic oxidation has not been previously reported.

KEYWORDS: carbazole dendron · PAMAM · complexation · template polymerization · nanoring

Supramolecular nanostructures derived from self-organizing molecules and macromolecules are of high interest for achieving new functions and properties in the fields of material science and chemical biology.[1–6] Dendrimeric self-assembly, especially in the case of polyamidoamine (PAMAM) dendrimers, has attracted increasing attention in recent years because of their unique structures, interesting properties, and ready availability.[7–16] Their potential applications in medicine, catalysis, gene therapy, and nanoreactor systems have been explored in the past decade or so.[17–19] These dendrimers are composed of a central core (ethylenediamine, in this study) with amidoamine branching units that extend outward in a symmetric fashion and consist of *n* generations (layers). Polyamidoamine is a monodispersed, highly branched macromolecule with primary amine functional groups on the surface and amido units at the branch points in the interior including internal tertiary amines. Recently, a number of studies have focused on the interaction and aggregation behavior between PAMAM dendrimers and surfactants in aqueous solution such as SDS,[20–23] poly(ethylene glycol),[24] and dodecanoic acid.[25] However, up to now, there has been no attempt to use PAMAM–surfactant complexes as templates for directed polymerization. Template polymerization is a useful method to obtain multicomponent materials.[26–28] A polymer can be used as a template to associate monomers by noncovalent interactions such as hydrogen bonding, electrostatic forces, dipole forces, and other interactions, followed by polymerization of the monomers on the contours of the template.[29] Thus, a template acts as a structure-directing agent guiding the topology of the polymerization process. In direct templating, a change of dimensions or phase transitions occurs, and the templated material becomes a 1:1 copy of a template. Template polymerization of polyelectrolyte–surfactant monomer (surfmer) complexes is a primary example and has been previously reviewed.[30–34] They were successfully demonstrated in the polymerization of a variety of lipid assemblies with preservation of the mesostructures. However, γ-irradiation has been shown to degrade the monomer in the initiation step of a polymerization reaction within smectic liquid–crystalline layers.[35] Recently, Faul et al.[30,31] have been able to preserve the lamellar phase structure of polyelectrolyte–surfmer surfactant (di(undeccenyl)phosphate and α-ω-diene) complexes through a dithiol polyaddition strategy. The outer shell of a nanosized

*Address correspondence to radvincula@uh.edu, pbuncha@gmail.com.

Received for review February 16, 2008 and accepted July 05, 2008.

Published online July 25, 2008.
10.1021/nn800098j CCC: $40.75

© 2008 American Chemical Society

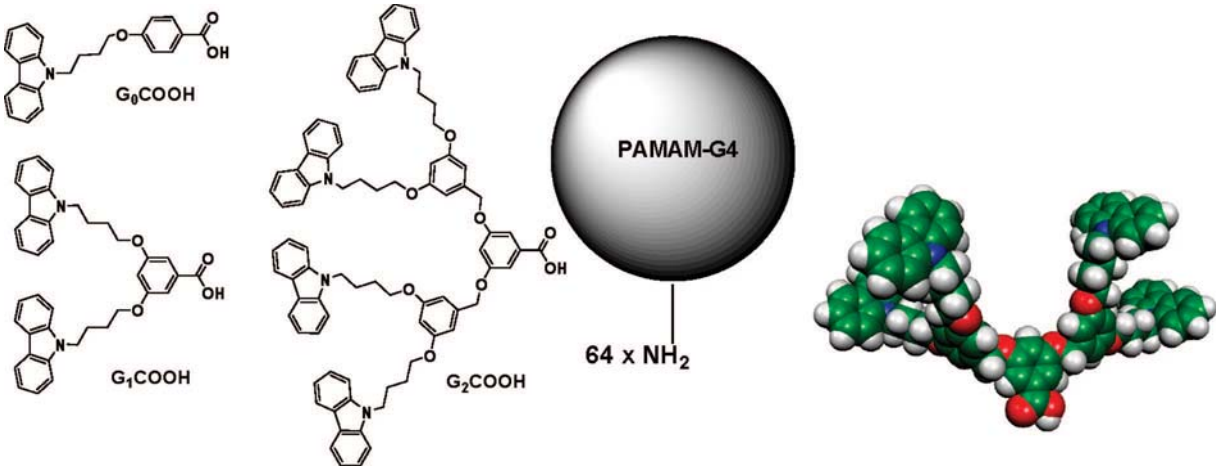

Figure 1. PAMAM dendrimer G_4-NH_2 with carboxylic acid terminal dendrons containing peripheral electroactive carbazole groups of different generations (G_0COOH, G_1COOH, and G_2COOH). The optimized structures of G_2COOH built from the Gaussian 98 B3LYP/STO-3G output file using the "Molekel" software are also shown.

macromolecule can be intracross-linked in a controlled manner through metathesis polymerization techniques. Zimmerman et al. previously reported the "self-assembly" of homoallyl dendrons into a cored dendrimer, and reversibility of the ring-closing metathesis mediated cross-linking of the dendrimers.[36,37]

Electroactive groups such as pyrrole[38,39] and thiophene[40,41] containing surfactants have the potential for producing new hybrid and electro-optical materials. Because of the electroactive moieties, they are not only polymerizable but also potentially electrically conductive when polymerized. Nanowire structures of polypyrrole, polyaniline, and thiophene have been realized which could serve as new conducting fibers.[42–44] On the other hand, carbazole polymers have been of recent interest due to their interesting electrochemical homopolymerization and copolymerization behavior.[45] They exhibit interesting electrochromic properties as well.[46] The ability of polycarbazole to form two distinct oxidation states further leads to multichromic effects.[47–49] Furthermore, polycarbazole is well-known as a hole transport material.[50] Morin and Leclerc reported the synthesis of a series of 2,7-carbazole-based conjugated polymers and their unique electrochemical and optical properties.[51–54] A recent review highlighted the interesting electrochemical and optical properties of oligomeric and polymeric carbazole-based materials as well as their tunable physicochemical properties using different synthetic strategies and substitution patterns.[55]

In this paper, we report a detailed and quantitative study on the supramolecular complexation of amine-functionalized PAMAM dendrimer G_4-NH_2 with carboxylic acid focal point functionalized dendrons containing terminal electroactive carbazole groups of different generations (G_0COOH, G_1COOH, and G_2COOH) (Figure 1). The focus is on a detailed understanding and mechanism of complex formation and subsequent electropolymerization properties with the different generations of the dendron surfmers. In the process, we observed the formation of interesting *nanoring* structures that preceded the electropolymerization process. The rest of the work involved understanding the nature of this nanostructure formation. To the best of our knowledge, there has been no report in which template polymerization was applied with a dendrimer−surfmer complex via electropolymerization.

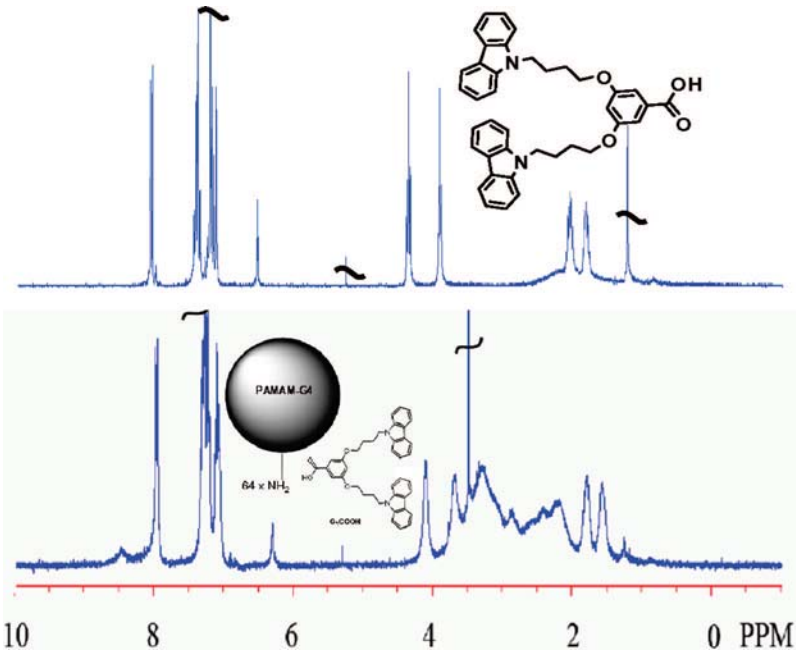

Figure 2. ^{1}H NMR spectra (300 MHz, 298 K) in $CDCl_3$ of 2 mM solutions (based on the concentration of PAMAM) of (a) G_1COOH and (b) complex of PAMAM−G_1COOH.

RESULTS AND DISCUSSION

The amine-terminated, ethylene diamine core, G_4-poly(amidoamine) dendrimer (G_4[EDA] PAMAM-NH_2), has 64 primary amines on the

surface. The surfmer anionic carbazole (CBz) dendrons (G_0COOH, G_1COOH, and G_2COOH) were prepared according to modified procedures recently reported by our group (details in the Supporting Information or SI).[56] The zero-, first-, and second-generation anionic dendronized macromolecules were selected to form ionic supramolecular complexes. The entire set of complexes between the dendron surfactants and PAMAM was carried out with stoichiometric ratios of the carboxylic acid group on the dendrons and the primary amines on the surface. A suspension of CBz dendrons (6.4 μmol) was prepared in MeOH (0.82 mL). It was then stirred at 25 °C, after which the G_4-PAMAM solution (0.1 μmol in 0.18 mL of MeOH) was added dropwise. After 24 h, a clear solution was obtained. The formation of the spherical assemblies of the G_0COOH and G_1COOH with G_4-PAMAM was then monitored by ^{1}H NMR spectroscopy in $CDCl_3$. In the absence of PAMAM, the ^{1}H NMR spectra chemical shifts of G_1COOH were very clear, sharp, and assignable as shown in Figure 2a as well as G_0COOH in Figure S1. When PAMAM was titrated into the G_0COOH and G_1COOH solutions, all signals shifted upfield, and the resonance for the spectra broadened after stirring for 24 h, suggesting the translational movement and compact aggregation of the dendrons to the PAMAM surface.[57–59] The chemical shifts of the PAMAM dendrimer were also detected at $\delta = 2.0-3.5$ ppm. However, despite several attempts, complexation of G_2COOH with PAMAM was not observed, which may be the result of steric effects and lack of solubility in the G_2COOH. The UV−vis spectra before and after the complexation of G_0COOH and G_1COOH with PAMAM are shown in Figure 3a. Absorption peaks are observed at 265, 295, 330, and 345 nm, which are typically assigned to the $\pi-\pi^*$ and $n-\pi^*$ transitions of carbazole.[60–63] In the case of the G_1COOH, it can be dissolved in more polar (MeOH) as well as less polar ($CHCl_3$) solvents. In MeOH, the peaks are ~5 nm blue-shifted when compared with those of $CHCl_3$ solution. On the other hand, G_0COOH could be dissolved very well in $CHCl_3$ but was insoluble in MeOH. This eventually influenced the G_0COOH−PAMAM to have stronger aggregation characteristics as compared to the G_1COOH−PAMAM in MeOH. In all cases, hypsochromic shifts were observed upon addition of PAMAM into the solutions of G_1COOH. As shown in Figure 3b and SI Figure S3, fluorescence studies revealed a decrease in fluorescence emission up to 70% upon addition of PAMAM. The quenching phenomenon is most likely attributed to the conformational change[64–66] due to aggregation of the carbazole groups as they stacked on the periphery of PAMAM. It should be noted that the equilibrium between complexation and decomplexation has an influence on the percentage of quenching. Accordingly, up to 30% of the quenching with G_0COOH−PAMAM is attributed to the formation of complex species, consistent with their aggregation properties.

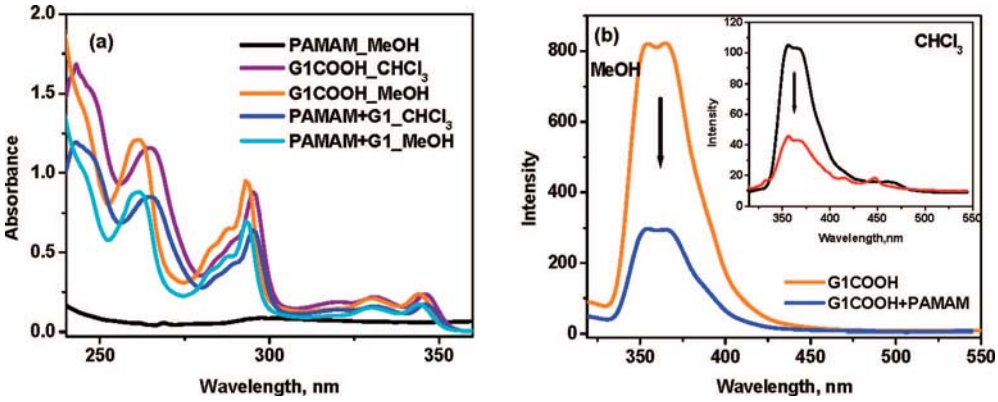

Figure 3. (a) UV−vis absorption spectrum of G_1COOH solutions in MeOH and $CHCl_3$ before and after complexation with PAMAM. (b) Fluorescence emission spectrum of G_1COOH before and after complexation with PAMAM, $\lambda_{ex} = 293$ nm, $\lambda_{em} = 360$ nm.

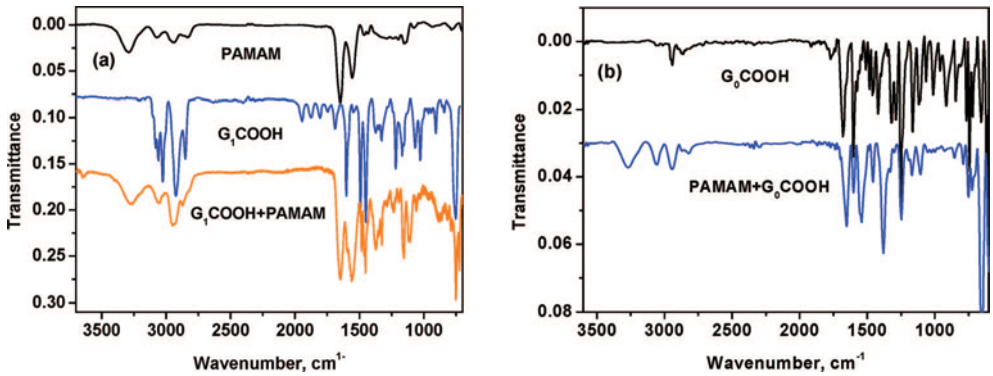

Figure 4. FTIR spectra of (a) PAMAM, G_1COOH, and the G_1COOH−PAMAM complex and (b) G_0COOH and the G_0COOH−PAMAM complex. Resolution is at 4 cm^{-1} for each spectrum.

To further test whether the PAMAM actually formed complexes with G_0COOH and G_1COOH, FT-IR spectra were recorded after 24 h addition of PAMAM solution to G_0COOH and G_1COOH (at 25 °C, clear solutions were obtained). Shown in Figure 4 a are the IR spectra of PAMAM, G_1COOH, and the G_1COOH + PAMAM complex (KBr). The carboxylic acid vibrations for G_1COOH were found to be at 1690 cm^{-1} (C═O stretch, dimer) and at 1373 cm^{-1} (C−O stretch, dimer) and changed to a broad diffuse band between 1500 and 1760 cm^{-1} in the spectrum of the G_1COOH−PAMAM complex result-

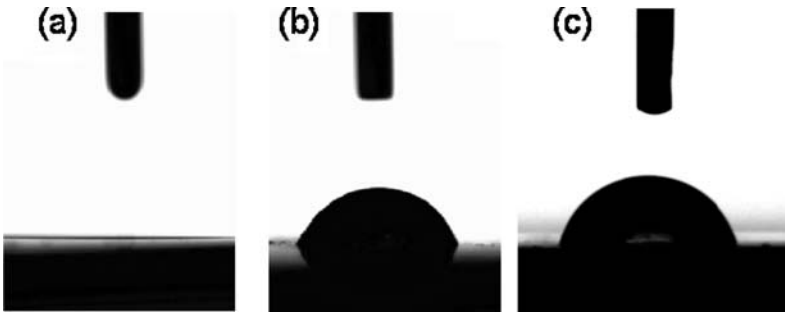

Figure 5. WCA measurement for: (a) PAMAM (0°); (b) complex PAMAM−G_1COOH (55.7°); and (c) complex PAMAM−G_0COOH (80.3°).

ing from the ionic ammonium carboxylate structures. The same results were observed on the studies of PAMAM−G_0COOH, where the carboxylic dimer peaks at 1758 and 1303 cm^{-1} changed to broad diffuse bands of ionic carboxylate structures between 1500 and 1600 cm^{-1}. According to these results, it can be concluded that 1:1 stoichiometric complexes were formed similar to previously reported fluorinated[67] and nonfluorinated[68] polyethyleneimine complexes.

Contact angle measurements were also carried out to investigate the complexation. In this case, the complexation should reduce the hydrophilicity of the PAMAM and the dendrons (Figure 5). The dilute solutions of the PAMAM and the complexes were spin-coated on a precleaned and plasma treated Si-wafer flat substrate. The films prepared from the complexes of G_0COOH and G_1COOH and the PAMAM solutions resulted in a change of the static water contact angle (WCA) (0° to 55.7°, G_1COOH, and 0° to 80.3°, G_0COOH). This confirmed the complexation of PAMAM with dendrons based on a change in the hydrophilic−lipophilic balance (HLB) compared to the completely wetted PAMAM−Si-wafer substrate, with a WCA of 0°. The large increase in WCA is due to the hydrophobicity of the carbazole groups forming the outer shell of the dendrimers. From these results, it can also be inferred that the G_0COOH is strongly associated on the peripheral of the dendrimer and is fully complexed compared to G_1COOH, as confirmed by the larger WCA increase on the former.

The formation of the individual PAMAM−G_1COOH dendrimer−surfmer complexes was directly observed by atomic force microscopy (AFM) as shown in Figure 6 and SI Figure S4. Very dilute solutions of 1 μM of the PAMAM−G_1COOH complexes in MeOH and $CHCl_3$ were spin-casted onto mica substrates. Isolated nanoparticles of the dendrimer complexes were observed on the surface when 10^{-6} M concentration was used. The particle diameter of PAMAM is 4.0 ± 0.5 nm, and PAMAM−G_1COOH complexes in MeOH and $CHCl_3$ are determined to be 7.0 ± 0.5 and 16.5 ± 1.0 nm, respectively. The difference in the complex's size was verified by molecular modeling (Gaussian 98 with B3LYP/STO-3G basic set) (Figure 7). From optimization of the structures, two different conformers were found to have the same minimum energy. The sizable increase with complexation is dependent on the polarity of solvent. It can be noted that conformer **a** will be present in MeOH to avoid the polar solvent and conformer **b** will be present in $CHCl_3$, a more nonpolar solvent. Moreover, by decreasing the generation of dendron to G_0COOH, a smaller increase of the diameter with 4.3 ± 0.5 nm was found, as demonstrated in SI Figure S4. It is clear that G_0COOH has a stronger aggregation after complexation.

Cyclic Voltammetry Studies. The studies on electrochemical oxidation of carbazole have been reported for some time now. Ambrose et al. investigated the mechanism of anodic oxidation of carbazole and its N-substituted derivatives.[69,70] During the anodic oxidation process, coupling of two carbazolium radical cations at 3 and 3′ positions seems to be the predominant pathway, especially in the case of N-substituted derivatives. The highly stable N-substituted 3,3′-dicarbazyl prohibited the formation of more extended conjugation units, e.g., oligo- or polycarbazole. On the other hand, Schreck et al. reported the electrodeposition of a longer conjugation of "polycarbazole" (most likely tetramer) film under protic media.[71,72] More recently, electrochemical analysis also suggested anodic oxidation only led to 3,3′-dicarbazyl formation in the case of 2,7-carbazole-based conjugated polymers.[54] Herein, we aimed to employ cyclic voltammetry to anodically oxidize and cross-link the carbazoles on the PAMAM periphery and understand the effect of CV conditions (monomer concentration, applied potential, etc.) on the eventual optical and morphological properties of the electrode-

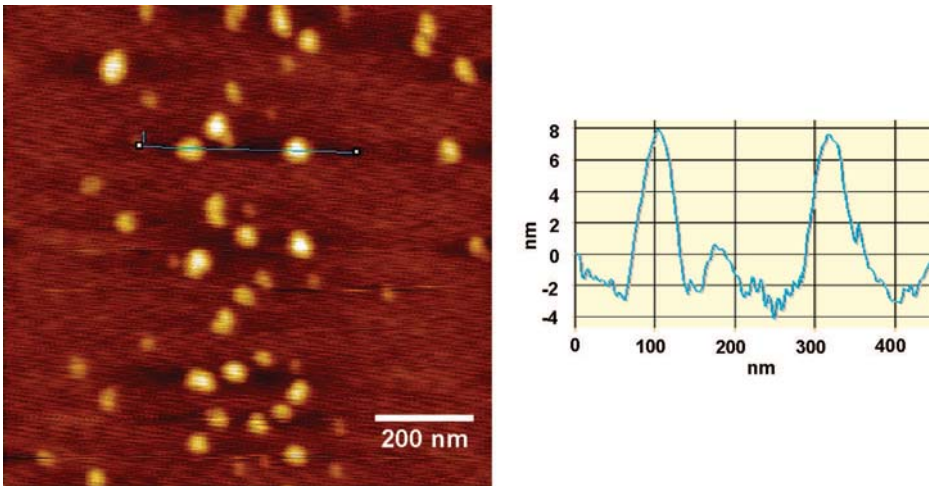

Figure 6. AFM image (1 × 1 μm) of the individual PAMAM−G_1COOH complexes on a mica substrate prepared from MeOH. The average diameter of the complexes was determined to be 7.0 ± 0.5 nm, and here the heights of the chosen particles were estimated to be ~10 nm from the step-depth analysis.

posited films. The precursor complexes (PAMAM−G_0COOH and PAMAM−G_1COOH) were electropolymerized and deposited on ITO substrates. The cyclic voltammetry (CV) curves are shown in Figure 8 and SI Figures S5 and S6. The potentials were cycled from 0 to 1.1, 1.3, and 1.5 V at a scan rate of 50 mV/s against Ag/AgCl reference electrode and platinum counter electrode. At a concentration of 10^{-6} M, no apparent redox peaks were observed on the anodic scan up to a potential of 1.1 V (Figure S5). As we can see from Figure 8a and b, when the potential window increased up to 1.3 and 1.5 V, the first oxidation peak was observed at 1.1 V resulting from the formation of carbazolium radical cations which underwent rapid coupling to 3,3′-dicarbazyls. Starting from the second anodic scan, two new peaks at 0.85 and 1.27 V appeared, corresponding to the radical cation and bication species of the dimer units, respectively. These results were in good agreement with earlier reports.[60,69,70,73] However, at a concentration of 10^{-5} M, the shape of the redox peaks in Figure 8c and d was not as pronounced as those at the lower concentration. This might be due to the nature of greater aggregation of the complexes at the higher concentration. In particular, as shown in Figure 8d, the redox peaks became much broader, indicating a more heterogeneous electron transfer process. This heterogeneous electron transfer is also likely a consequence of thicker films deposited during each CV cycle and can be confirmed by the higher intensity of the absorption peaks (following section). A small difference of the oxidation onsets was recorded in the anodic scans as shown in Figure 8 and Figure S6 and as summarized in Table S1. However, shape and peak positions are obviously unique for different concentrations and potential windows of the dendron complexes. From Table S1, it is obvious that PAMAM−G_1COOH shows a higher $\Delta E(E_{pa} - E_{pc})$ value than that of PAMAM−G_0COOH which indicates a more heterogeneous and slow electron-transfer rate for these complexes.[56]

Spectroelectrochemical Characterization. The electrodeposited films were further characterized by electrochemical UV−vis spectroscopy. The extent of the

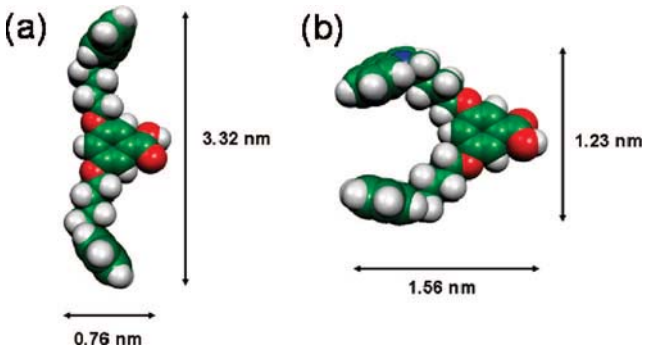

Figure 7. Optimized structures of G_1COOH built from the Gaussian 98 B3LYP/STO-3G output file using the "Molekel" software.

increasing π orbital overlap between neighboring repeating units on conjugated molecules can directly affect the observed energy of the π−π* transition which appears as the absorption maxima in the electronic spectra. The values of the absorption maxima for the different generations are closely linked to their degree of coupling. The extended appearance of the π−π* transition at 420−440 nm, which is attributed to the radical cations (polaronic band or doped state), is shown in Figure 9.[56,60−63,69] The peak between 600 and 1000 nm can be assigned to the π−π* transition of the dications (bipolaronic band or more highly doped state) originating from the formation of the conjugated 3,3′-dicarbazyl species complexing with hexafluorophosphate ions. From the spectra, the peaks

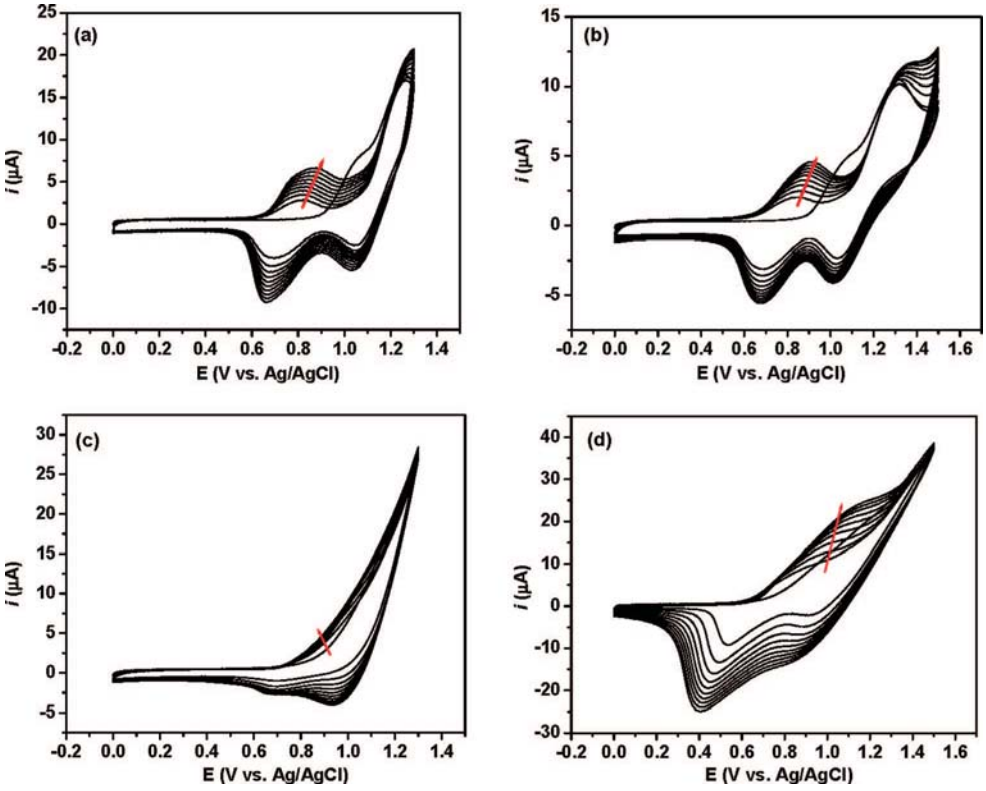

Figure 8. Cyclic voltammograms of the electrochemical polymerization of PAMAM−G_1COOH complexes at a scan rate of 50 mV/s, 10 cycles: (a) 10^{-6} M, potential window from 0 to 1.3 V, (b) 10^{-6} M, potential window from 0 to 1.5 V, (c) 10^{-5} M, potential window from 0 to 1.3 V, (d) 10^{-5} M, potential window from 0 to 1.5 V.

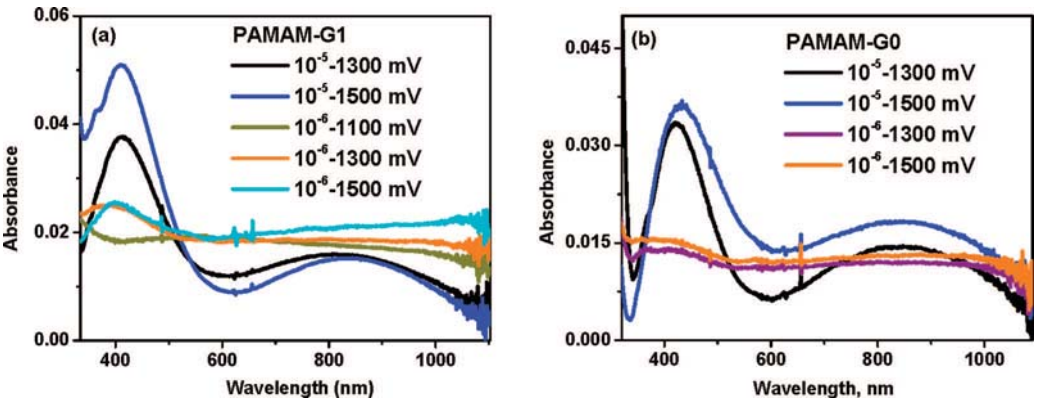

Figure 9. Absorption spectra analysis performed in 0.1 M $TBAPF_6/CHCl_3$ on ITO substrates in the presence of different concentrations and potential windows. (a) PAMAM−G_1COOH, (b) PAMAM−G_0COOH.

at high concentration and highly applied potential show extraordinary increases of the peak intensity at ~430 nm, and the appearance of the broad peak in the 600−1000 nm region confirms the highly conjugated nature of the materials deposited on the ITO substrates.

Morphological Studies. The morphology and molecular orientation of the dendron complexes after electrochemical deposition on ITO substrates have been studied using AFM measurements. In the case of PAMAM−G_1COOH at low concentration (10^{-6} M) and applied potential of 0−1.3 V, the AFM image in Figure 10a showed unique nanostructures (and also in SI Figure S7). These ringlike structures were ~75 nm in diameter and ~13 nm in height. Interestingly, this height is close to the full diameter of a PAMAM−G_1COOH nanoparticle diameter in $CHCl_3$. The diameter of the nanoring structure also closely resembles a donut shape particle that may likely contain a PAMAM core with the G_1COOH shell (Scheme 1). This kind of feature was observed repeatedly with solute evaporation[74] and is presumably related to the overall hydrophobic−hydrophilic balance property.[75,76] To investigate the mechanism that drives the morphological change from the micellar nanosphere (before electro-deposition) to ringlike (donut) nanostructures (after electrodeposition), two experiments were performed to determinate when the nanoring structures are formed as illustrated in Scheme 1.

The micellization phenomenon of G_1COOH was first investigated. If the critical micelle concentration (CMC) is equal to and/or less than the concentration of G_1COOH that was used to make PAMAM−G_1COOH complexes, the nanoring can be generated between the equilibrium of the G_1COOH micellization and the weak complexation equilibrium with the PAMAM. However, if the CMC is higher than the concentration of G_1COOH used, the equilibrium between weak and strong complexation with PAMAM should be preferred. We have studied the solubilization of the dye Nile Red as a function of the concentration of G_1COOH in order to determine the CMC.[77] Shown in Figure S8a is the UV−vis spectra before and after micelle formation, while Figure S8b represented the fluorescence spectra at λ_{ex} = 570 and λ_{em} = 655 nm of different solutions of G_1COOH. The dendron solution was stirred for 2 h in the presence of Nile Red and then filtered to remove unsolubilized dyes. The CMC of this system was found to be 70.0 μM. From the experiment, a 6.4 μM concentration of G_1COOH was used for dendron complexation, and a concentration of 1.0 μM was used for the CV. This means that the nanoring structures could have only formed at the equilibrium between the strong

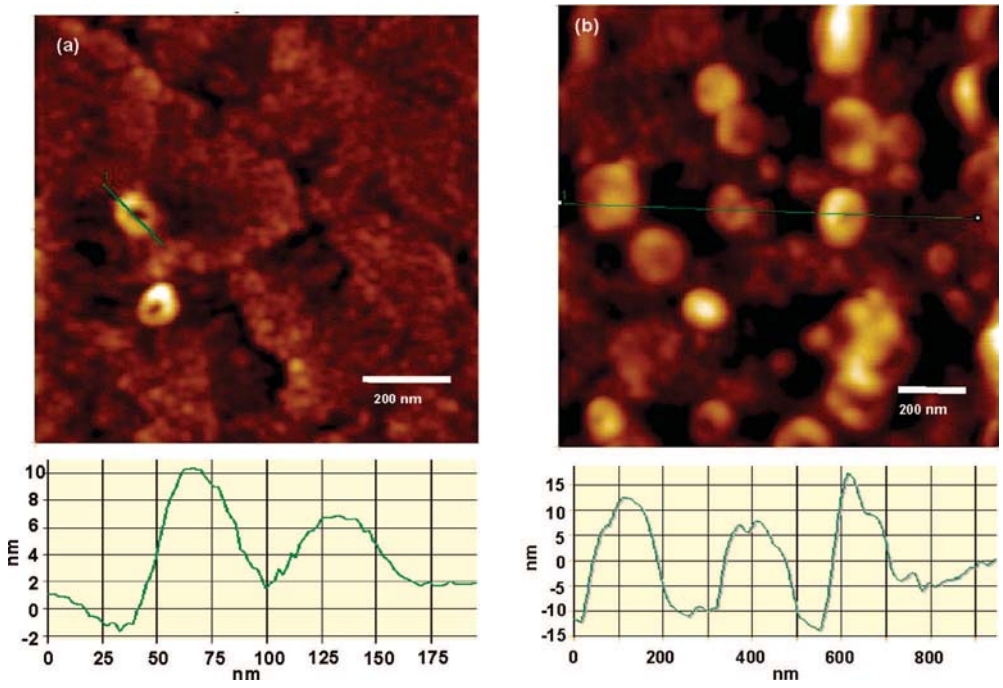

Figure 10. Tapping-mode AFM topography images of PAMAM−G_1COOH complexes after being electropolymerized on ITO at a scan rate of 50 mV/s, 10 cycles: (a) 10^{-6} M, potential window from 0.0 to 1.5 V, (b) 10^{-5} M, potential window from 0.0 to 1.3 V.

complexation and weak complexation stage as presented in Scheme 1 since there are not enough unimers to form free G_1COOH micelles based on these concentrations.

To test whether the nanoring structures could not have developed in the absence of PAMAM, we also studied the electrochemical oxidation of G_1COOH alone. The CV curves in Figure S9 exhibited similar oxidation and reduction peaks of the highly conjugated dicarbazyls. The linear current increase and ΔE change indicated that G_1COOH can also be effectively deposited on ITO with even greater efficiency than the PAMAM−G_1COOH. The in situ spectroelectrochemical studies also showed the typical $\pi-\pi^*$ transitions of the polaronic and bipolaronic bands of conjugated carbazoles. However, *no* ringlike nanostructures were observed on the morphology from the AFM images (Figure S10).

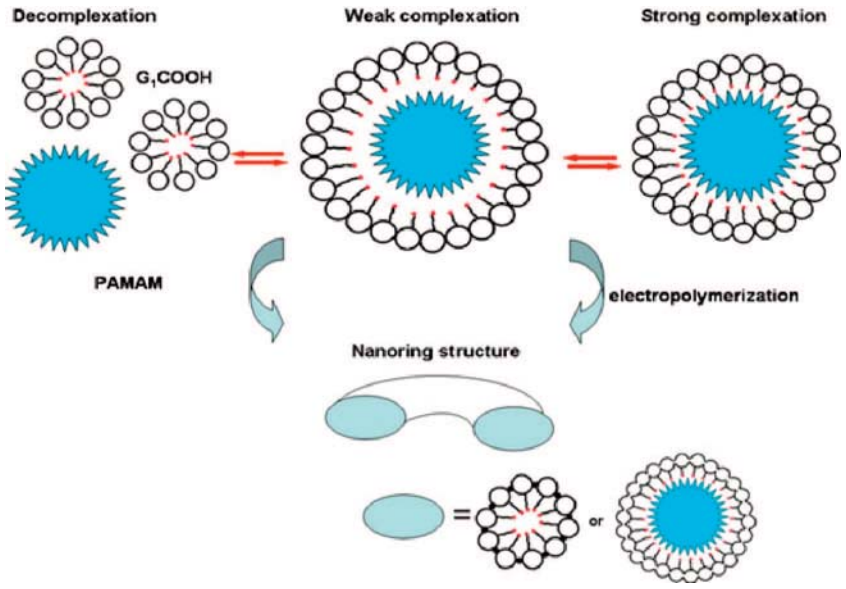

Scheme 1. Description of the formation of the nanoring structures between the equilibrium of decomplexation, weak complexation and strong complexation.

To further understand the components of the deposited film on the ITO, XPS spectroscopy was used to determine the composition of the deposited film based on the C/N ratio. Shown in Figure S11 is the high-resolution XPS spectrum of PAMAM−G_1COOH electrodeposited film on ITO for C and N atoms. In all quantitative analyses, the theoretical value is assumed on the basis of 100% electrografting. For the 10^{-6} M of PAMAM−G_1COOH electrodeposited with an applied potential up to 1.5 V, an experimental value of C/N = 7.95 was obtained which is higher than the theoretical value of PAMAM + G_1COOH at C/N = 7.07. This higher value indicates the incorporation of a slightly larger amount of the surfmer compared to the PAMAM core. Thus, during the electrochemical oxidation of the dendrimer complex, it is possible that the PAMAM was decomplexed into the solution subphase during the nanoring formation near the weak complexation equilibrium. Furthermore, since the surfmers are not likely to form micelles at the 10^{-6} M concentration used, the ring formation resulted in expulsion of the PAMAM and at the same time the electropolymerization of the dendron surfmer units. This explains the higher experimental C/N ratio observed from XPS and is supported by AFM, CMC, and even fluorescence data (carbazole aggregation). The rings then are formed largely due to the formation of a higher ordered core−shell ring (or donut) structure composed of a higher content of G_1COOH shell with PAMAM remaining as an interior template support during the electrochemical CV procedure.

Finally, to test the uniqueness of the dendron complexation phenomenon, we covalently bonded the G_1COOH to PAMAM to form a carbazole amide functionalized dendrimer (PC). The synthesis, purification, and characterization of this derivative are reported in the Supporting Information. The electopolymerization was carried out with the same parameters as with the

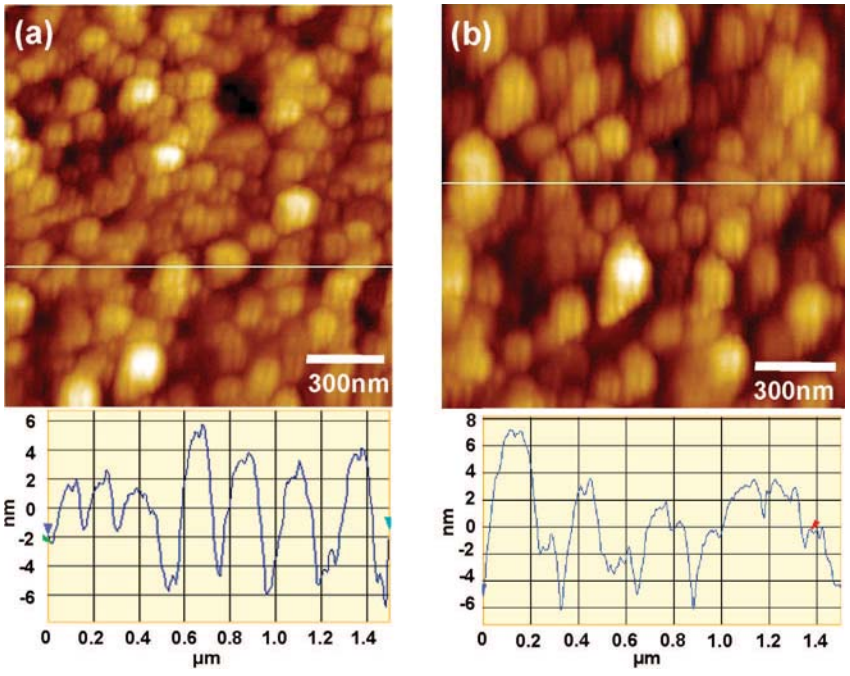

Figure 11. AFM topography images of 2-(3,5-bis(4-(9*H*-carbazol-9-yl)butoxy)phenyl)acetoyl-functionalized PAMAM (PC) after electropolymerization on ITO electrodes at a scan rate of 50 mV/s, 10 cycles: (a) 10^{-6} M, potential window from 0 to 1.3 V, (b) 10^{-5} M, potential window from 0 to1.3 V.

PAMAM−G_1COOH complexes. At the low potential application (1.3 V), a good trend of increasing oxidation potential onset was observed with the increase of cycles, but the CV curves shifted to higher anodic potential (E_{pa}) and the reduction peaks shifted to lower cathodic potential (E_{pc}) compared to the noncovalent PAMAM−dendron complexes as shown in Figure S7. Degradation was observed after applying the higher potential at 1.5 V which may come from the lack of availability of more mobile electroactive monomers. Moreover, the UV−vis spectra revealed the formation of similar polaron and bipolaron peaks as shown in Figure S13. From the morphology (Figure 11) as imaged by AFM, the PC film *did not* show nanoring formation at all but a rough and patchy surface that was macroscopically more nonuniform.

CONCLUSION

We have demonstrated the successful self-assembly and complexation between the dendrimer template (PAMAM G_4-NH_2) and dendron surfmers (G_0COOH, G_1COOH). The increasing steric hindrance of a dendron prevented complexation as in the case of G_2COOH. Hypochromic shifts in the UV−vis spectra and quenching of fluorescence indicated that G_1COOH was trapped around the dendrimer. Ammonium and carboxylate species were observed by FTIR. The isolated sphere size was observed on the mica substrates. The stronger complexation was observed in PAMAM−G_1COOH. The electrochemical oxidation of dendrimer complexes as thin films revealed unusual CV behavior depending upon the generation. PAMAM−G_1COOH showed a higher extent of anodic oxidation, while PAMAM−G_0COOH showed a higher degree of aggregation. More interestingly, nanoring structures were observed as the complex was deposited on ITO indicating a type of supramolecularly-based template electropolymerization of a dendrimer−surfmer complex. The CMC, AFM, and XPS revealed a ringlike or donut structure most likely composed of the PAMAM−core and dendron−carbazole shell. This was formed at the equilibrium of decomplexation and weak complexation. In principle, different generations of dendrons, different dendrimer topologies, and other electroactive surfmer moieties can result in a wider applicability of this method, for electro-optical, drug delivery, sensing, and other nanoscience and materials applications.

EXPERIMENTAL SECTION

Chemicals and Methods. All chemical reagents were purchased from Aldrich Chemical Co. unless otherwise stated. Solvents were acquired from Fisher. Tetrahydrofuran (THF) was distilled over sodium/benzophenone ketyl, and *N*,*N*-dimethylformamide (DMF) was purchased anhydrous or otherwise dried over Linde type 4-Å molecular sieves. Commercially available reagents were used without further purification unless noted otherwise. *N*-(4-Bromobutyl)-9*H*-carbazole was prepared according to literature procedures.[78]

Instrumentation. Nuclear magnetic resonance (NMR) spectra were recorded on a General Electric QE-300 spectrometer operating at 300 MHz for ^{1}H nuclei. UV−vis spectra were recorded using an Agilent 8453 spectrometer. UV−vis measurements of the films were carried out *in situ* on an ITO substrate. This was done using a Teflon flow cell manufactured with a modified ITO window and microscope slide window that was placed in the path of an HP-8453 diode array spectrometer. All FTIR measurements were performed using a Digilab FTS 7000 step scan spectrometer (Digilab, Randolph, MA) equipped with a liquid N_2-cooled MCT detector. KBr pellets were prepared by first mixing the sample solutions with KBr, removing solvents under vacuum, and then pressing the KBr using a 10 ton hydraulic press. The cyclic voltammetry (CV) experiments were carried out on a Princeton Applied Research Parstat 2263 with an ITO substrate as the working electrode coupled with a Pt plate as the counter electrode and a Ag/AgCl wire as the reference electrode. Atomic force microscopy (AFM) imaging was examined in ambient conditions with a PicoSPM II (PicoPlus, Molecular Imaging) in the tapping mode.

Preparation of the Complexes. The amine-terminated, ethylene diamine core, Generation 4 poly(amidoamine) dendrimer (G_4[EDA] PAMAM−NH_2, >99% purity) was purchased from Sigma-Aldrich and used without further purification. It has 64 primary amines on the surface and 180 tertiary amines at branch points within the core. The anionic carbazole (CBz) dendrons (G_0COOH, G_1COOH, and G_2COOH) were prepared according to the modified procedures that have been recently reported by our group, and the synthetic scheme and procedures were shown in the Supporting Information. Complex preparation: zero-, first-, and second-generation anionic dendronized macromolecules were selected to form ionic supramolecular complexes as illustrated in Scheme 1. The entire set of complexations between dendron surfactants and PAMAM was carried out with stoichiometric ratios of the carboxylic acid group on the dendrons and the primary amines on the surface. A suspension of CBz dendrons (6.4 μmol) was prepared in MeOH (0.82 mL). It was then stirred at 25 °C, after which PAMAM G4 solution (0.1 μmol in 0.18 mL of MeOH) was added dropwise. After 24 h, a clear solution was obtained. ^{1}H NMR spectroscopy was then used to monitor the complexation behavior of the CBz dendron and PAMAM every 2 h until complexation was found complete. All samples were kept under nitrogen to avoid any contamination by atmospheric carbon dioxide.

Acknowledgment. The authors acknowledge financial support from NSF-DMR (05-04435), NSF-DMR (06-02896), NSF-DMR (03-15565), Alliance for Nanohealth of Texas, and the Robert A. Welch Foundation (E-1551). B.P. and C.K. acknowledge support from the Thailand Research Fund (TRF) (RMU4880041) and the Royal Golden Jubilee Ph.D Program of TRF (PHD/0137/2546). C.K. also thanks Vithaya Ruangpornvisuti for suggestions and computational calculations on the dendron structures.

Supporting Information Available: Synthesis and characterization details, calculated structure of G_2COOH, UV−vis and fluorescence spectra of G_0COOH before and after complexation, AFM images of PAMAM and the complexes, summary of the CV redox peaks, CV curves of G_1COOH, PAMAM−$G_{0(1)}$ under different conditions and their corresponding AFM images, HR-XPS of the cross-linked polymer, CV curves of PC under different conditions, and spectroelectrochemical spectrum of PC electropolymerization. This material is available free of charge via the Internet at http://pubs.acs.org.

REFERENCES AND NOTES

1. Lehn, J. M. Supramolecular Chemistry and Self-Assembly Special Feature: Toward Complex Matter: Supramolecular

Chemistry and Self-Organization. *Proc. Natl. Acad. Sci. U.S.A.* **2002**, *99*, 4763–4768.
2. Lee, M.; Cho, B.-K.; Zin, W. C. Supramolecular Structures from Rod-Coil Block Copolymers. *Chem. Rev.* **2001**, *101*, 3869–3892.
3. Sarikaya, M.; Tamerler, C.; Jen, A. K.-Y.; Schulten, K.; Baneyx, F. Molecular Biomimetics: Nanotechnology through Biology. *Nat. Mater.* **2003**, *2*, 577–585.
4. Hoeben, F. J. M.; Jonkheijm, P.; Meijer, E. W.; Schenning, A. P. H. J. About Supramolecular Assemblies of π-Conjugated Systems. *Chem. Rev.* **2005**, *105*, 1491–1546.
5. Cornelissen, J. J. L. M.; Rowan, A. E.; Nolte, R. J. M.; Sommerdijk, N. A. J. M. Chiral Architectures from Macromolecular Building Blocks. *Chem. Rev.* **2001**, *101*, 4039–4070.
6. Tomalia, D. A. Birth of A New Macromolecular Architecture: Dendrimers as Quantized Building Blocks for Nanoscale Synthetic Polymer Chemistry. *Prog. Polym. Sci.* **2005**, *30*, 294–324.
7. Fischer, M.; Vögtle, F. Dendrimers: From Design to Application - A Progress Report. *Angew. Chem., Int. Ed.* **1999**, *38*, 884–905.
8. Frechet, J. M. J.; Tomalia, D. A. *Dendrimers and Other Dendritic Polymers*; Wiley Series in Polymer Science; Wiley: New York, 2001.
9. Newkome, G. R.; Moorefield, C. N.; Vögtle, F. *Dendrimers and Dendrons: Concepts, Synthesis, Applications*; Wiley-VCH: Weinheim, 2001.
10. Ossterom, G. E.; Reek, J. N. H.; Kamer, P. C. J.; van Leeuwen, P. W. N. M. Transition Metal Catalysis Using Functionalized Dendrimers. *Angew. Chem., Int. Ed.* **2001**, *40*, 1828–1849.
11. Astruc, D.; Chardac, F. Dendritic Catalysts and Dendrimers in Catalysis. *Chem. Rev.* **2001**, *101*, 2991–3024.
12. Grayson, S. M.; Frechet, J. M. J. Convergent Dendrons and Dendrimers: from Synthesis to Applications. *Chem. Rev.* **2001**, *101*, 3819–3868.
13. Stiriba, S. E.; Frey, H.; Haag, R. Dendritic Polymers in Biomedical Applications: from Potential to Clinical Use in Diagnostics and Therapy. *Angew. Chem., Int. Ed.* **2002**, *41*, 1329–1334.
14. Aulenta, F.; Hayes, W.; Rannard, S. Dendrimers: A New Class of Nanoscopic Containers and Delivery Devices. *Eur. Polym. J.* **2003**, *39*, 1741–1771.
15. Boas, U.; Heegaard, P. M. H. Dendrimers in Drug Research. *Chem. Soc. Rev.* **2004**, *33*, 43–63.
16. Svenson, S.; Tomalia, D. A. Dendrimers in Biomedical Applications-Reflections on the Field. *Adv. Drug Delivery Rev.* **2005**, *57*, 2106–2109.
17. Kim, Y. H.; Webster, O. W. Water Soluble Hyperbranched Polyphenylene: "A Unimolecular Micelle?". *J. Am. Chem. Soc.* **1990**, *112*, 4592–4593.
18. Newkome, G. R.; Moorefield, C. N.; Baker, G. R.; Johnson, A. L.; Behera, R. K. Alkane Cascade Polymers Possessing Micellar Topology: Micellanoic Acid Derivatives. *Angew. Chem., Int. Ed.* **1991**, *30*, 1176–1178.
19. Naylor, A. M.; Goddard, W. A., III; Kiefer, G. E.; Tomalia, D. A. Starburst Dendrimers. 5. Molecular Shape Control. *J. Am. Chem. Soc.* **1998**, *111*, 2339–2341.
20. Watkins, D. M.; Sayed-Sweet, Y.; Klimash, J. W.; Turro, N. J.; Tomalia, D. A. Dendrimers with Hydrophobic Cores and the Formation of Supramolecular Dendrimer-Surfactant Assemblies. *Langmuir* **1997**, *13*, 3136–3141.
21. Wang, C.; Wyn-Jones, E.; Sidhu, J.; Tam, K. C. Supramolecular Complex Induced by the Binding of Sodium Dodecyl Sulfate to PAMAM Dendrimers. *Langmuir* **2007**, *23*, 1635–1639.
22. Mizutani, H.; Torigoe, K.; Esumi, K. Physicochemical Properties of Quaternized Poly(amidoamine) Dendrimers with Alkyl Groups and of Their Mixtures with Sodium Dodecyl Sulfate. *J. Colloid Interface Sci.* **2002**, *248*, 493–498.
23. Sidhu, J.; Bloor, D. M.; Couderc-Azouani, S.; Penfold, J.; Holzwarth, J. F.; Wyn-Jones, E. Interactions of Poly(amidoamine) Dendrimers with the Surfactants SDS, DTAB, and $C_{12}EO_6$: An Equilibrium and Structural Study Using a SDS Selective Electrode, Isothermal Titration Calorimetry, and Small Angle Neutron Scattering. *Langmuir* **2004**, *20*, 9320–9328.
24. Chun, D.; Wudl, F; Nelson, A. Supramacromolecular Assembly Driven by Complementary Molecular Recognition. *Macromolecules* **2007**, *40*, 1782–1785.
25. Chechik, V.; Zhao, M.; Crooks, R. M. Self-Assembled Inverted Micelles Prepared from a Dendrimer Template: Phase Transfer of Encapsulated Guests. *J. Am. Chem. Soc.* **1999**, *121*, 4910–4911.
26. Polowinski, S. Template Polymerisation and Co-Polymerisation. *Prog. Polym. Sci.* **2002**, *27*, 537–577.
27. Szumilewicz, J. Molecular Recognition in Radical Template Polymerization. *Macromol. Symp.* **2000**, *161*, 183–190.
28. Polacco, G.; Cascone, M. G.; Petarca, L.; Maltinti, G.; Cristallini, C.; Barbani, N.; Lazzeri, L. Template Polymerization of Sodium Methacrylate onto Poly(allylamine) Hydrochloride. *Polym. Int.* **1996**, *41*, 443–448.
29. Serizawa, T.; Hamada, K.; Akashi, M. Polymerization within a Molecular-Scale Stereoregular Template. *Nature* **2004**, *429*, 52–55.
30. Ganeva, D.; Antonietti, M.; Faul, C. F. J.; Sanderson, R. D. Polymerization of the Organized Phases of Polyelectrolyte-Surfactant Complexes. *Langmuir* **2003**, *19*, 6561–6565.
31. Ganeva, D.; Faul, C. F. J.; Gotz, C.; Sanderson, R. D. Directed Reactions within Confined Reaction Environments: Polyadditions in Polyelectrolyte-Surfactant Complexes. *Macromolecules* **2003**, *36*, 2862–2866.
32. Mueller, A.; O'Brien, D. Supramolecular Materials *via* Polymerization of Mesophases of Hydrated Amphiphiles. *Chem. Rev.* **2002**, *102*, 727–758.
33. Summers, M.; Eastoe, J. Applications of Polymerizable Surfactants. *Adv. Colloid Interface Sci.* **2003**, *100−102*, 137–152.
34. Lee, Y.-S.; Yang, J.-Z.; Sisson, T. M.; Frankel, D. A.; Gleeson, J. T.; Aksay, E.; Keller, S. L.; Gruner, S. M.; O'Brien, D. Polymerization of Nonlamellar Lipid Assemblies. *J. Am. Chem. Soc.* **1995**, *117*, 5573–5578.
35. Dreja, M.; Lennartz, W. Polymerizable Polyelectrolyte-Surfactant Complexes from Monomeric Ammonium Cations and Polystyrenesulfonate. *Macromolecules* **1999**, *32*, 3528–3530.
36. Zimmerman, S. C.; Zeng, F. W.; Reichert, D. E. C.; Kolotuchin, S. V. Self-assembling Dendrimers. *Science* **1996**, *271*, 1095–1098.
37. Elmer, S. L.; Lemcoff, N. G.; Zimmerman, S. C. Exploring the Reversibility of the Ring-Closing Metathesis Mediated Cross-linking of Dendrimers. *Macromolecules* **2007**, *40*, 8114–8118.
38. Omastova, M.; Trchova, M.; Kovarova, J.; Stejskal, J. Synthesis and Structural Study of Polypyrroles Prepared in the Presence of Surfactants. *Synth. Met.* **2003**, *138*, 447–455.
39. Ikegame, M.; Tajima, K.; Aida, T. Template Synthesis of Polypyrrole Nanofibers Insulated within One-Dimensional Silicate Channels: Hexagonal versus Lamellar for Recombination of Polarons into Bipolarons. *Angew. Chem., Int. Ed.* **2003**, *42*, 2154–2157.
40. Li, G.; Bhosale, S.; Wang, T.; Zhang, Y.; Zhu, H.; Fuhrhop, J.-H. Gram-Scale Synthesis of Submicrometer-Long Polythiophene Wires in Mesoporous Silica Matrices. *Angew. Chem., Int. Ed.* **2003**, *42*, 3818–3821.
41. Spange, S. Insulated Nanowire Bundles through Consecutive Template Synthesis. *Angew. Chem., Int. Ed.* **2003**, *42*, 4430–4432.
42. Cao, Y.; Smith, P.; Heeger, A. J. Counterion Induced Processibility of Conducting Polyaniline and of Conducting Polyblends of Polyaniline in Bulk Polymers. *Synth. Met.* **1992**, *48*, 91–97.
43. Huang, J. X.; Virji, S.; Weiller, B. H.; Kaner, R. B. Polyaniline Nanofibers: Facile Synthesis and Chemical Sensors. *J. Am. Chem. Soc.* **2003**, *125*, 314–315.
44. Acik, M.; Sonmez, G. Nanofabrication of Aligned Conducting Polymers. *Polym. Adv. Technol.* **2006**, *17*, 697–699.

45. Taranekar, P.; Baba, A.; Fulghum, T.; Advincula, R. Conjugated Polymer Network Films from Precursor Polymers: Electrocopolymerization of a Binary Electroactive Monomer Composition. *Macromolecules* **2005**, *38*, 3679–3687.
46. Witker, D.; Reynolds, J. R. Soluble Variable Color Carbazole-Containing Electrochromic Polymers. *Macromolecules* **2005**, *38*, 7636–7644.
47. Gaupp, C. L.; Reynolds, J. R. Multichromic Copolymers Based on 3,6-Bis(2-(3,4-ethylenedioxythiophene))-*N*-alkylcarbazole Derivatives. *Macromolecules* **2003**, *36*, 6305–6315.
48. Sotzing, G. A.; Reddinger, J. L.; Katritzky, A. R.; Soloducho, J.; Musgrave, R.; Reynolds, J. R. Multiply Colored Electrochromic Carbazole-Based Polymers. *Chem. Mater.* **1997**, *9*, 1578–1587.
49. Reddinger, J. L.; Sotzing, G. A.; Reynolds, J. R. Multi-Colored Electrochromic Polymers Derived from Easily Oxidized Bis(2-(3,4-ethylenedioxy)thienyl) Carbazoles. *Chem. Commun.* **1996**, *15*, 1777–1778.
50. Baba, A.; Onishi, K.; Knoll, W.; Advincula, R. C. Investigating Work Function Tunable Hole-Injection/Transport Layers of Electrodeposited Polycarbazole Network Thin Films. *J. Phys. Chem. B* **2004**, *108*, 18949–18955.
51. Morin, J. F.; Leclerc, M. Synthesis of Conjugated Polymers Derived from *N*-Alkyl-2,7-carbazoles. *Macromolecules* **2001**, *34*, 4680–4682.
52. Zottii, G.; Schiavon, G.; Zecchin, S; Morin, J. F; Leclerc, M. Electrochemical, Conductive, and Magnetic Properties of 2,7-Carbazole-Based Conjugated Polymers. *Macromolecules* **2002**, *35*, 2122–2128.
53. Morin, J. F.; Leclerc, M. 2,7-Carbazole-Based Conjugated Polymers for Blue, Green, and Red Light Emission. *Macromolecules* **2002**, *35*, 8413–8417.
54. Morin, J. F.; Drolet, N.; Tao, Y.; Leclerc, M. Synthesis and Characterization of Electroactive and Photoactive 2,7-Carbazolenevinylene-Based Conjugated Oligomers and Polymers. *Chem. Mater.* **2004**, *16*, 4619–4626.
55. Morin, J. F.; Leclerc, M.; Ades, D.; Siove, A. Polycarbazoles: 25 Years of Progress. *Macromol. Rapid Commun.* **2005**, *26*, 761–778.
56. Taranekar, P.; Fulghum, T.; Patton, D.; Ponnapati, R.; Clyde, G.; Advincula, R. Investigating Carbazole Jacketed Precursor Dendrimers: Sonochemical Synthesis, Characterization, and Electrochemical Crosslinking Properties. *J. Am. Chem. Soc.* **2007**, *129*, 12537–12548.
57. Hartmann, P. C.; Dieudonne, P.; Sanderson, R. D. Self-assembly and Influence of the Organic Counterion in the Ternary Systems Dodecylamine/Acrylic Acid/Water and Dodecylamine/Methacrylic Acid/Water. *J. Colloid Interface Sci.* **2005**, *284*, 289–297.
58. Popova, M. V.; Tchernyshev, Y. S.; Michel, D. NMR Investigation of the Short-Chain Ionic Surfactant-Water Systems. *Langmuir* **2004**, *20*, 632–636.
59. Shimizu, S.; Pires, P. A. R.; El Seoud, O. A. ^{1}H and ^{13}C NMR Study on the Aggregation of (2-Acylaminoethyl)trimethylammonium Chloride Surfactants in D_2O. *Langmuir* **2003**, *19*, 9645–9652.
60. Fulghum, T.; Karim, S. M. A.; Baba, A.; Taranekar, P.; Nakai, T.; Masuda, T.; Advincula, R. C. Conjugated Poly(phenylacetylene) Films Cross-Linked with Electropolymerized Polycarbazole Precursors. *Macromolecules* **2006**, *39*, 1467–1473.
61. Taranekar, P.; Fulghum, T.; Baba, A.; Nakai, T.; Patton, D.; Advincula, R. C. Quantitative Electrochemical and Electrochromic Behavior of Terthiophene and Carbazole Containing Conjugated Polymer Network Film Precursors: EC-QCM and EC-SPR. *Langmuir* **2007**, *23*, 908–917.
62. Taranekar, P.; Fan, X.; Advincula, R. Distinct Surface Morphologies of Electropolymerized Polymethylsiloxane Network Polypyrrole and Comonomer Films. *Langmuir* **2002**, *18*, 7943–7952.
63. Inaoka, S.; Advincula, R. Synthesis and Oxidative Cross-Linking of Fluorene-Containing Polymers to Form Conjugated Network Polyfluorenes: Poly(fluoren-9,9-diyl-*alt*-alkan-,-diyl). *Macromolecules* **2002**, *35*, 2426–2428.
64. Hu, D. H.; Yu, J.; Barbara, P. F. Single-Molecule Spectroscopy of the Conjugated Polymer MEH-PPV. *J. Am. Chem. Soc.* **1999**, *121*, 6936–6937.
65. Sluch, M. I.; Godt, A.; Bunz, U. H. F.; Berg, M. A. Excited-State Dynamics of Oligo(p-phenyleneethynylene): Quadratic Coupling and Torsional Motions. *J. Am. Chem. Soc.* **2001**, *123*, 6447–6448.
66. Liu, M.; Kaur, P.; Waldeck, D. H.; Xue, C.; Liu, H. Fluorescence Quenching Mechanism of a Polyphenylene Polyelectrolyte with Other Macromolecules: Cytochrome c and Dendrimers. *Langmuir* **2005**, *21*, 1687–1690.
67. Thunemann, A. F.; Kubowicz, S.; Pietsch, U. Ultrathin Solid Polyelectrolyte-Surfactant Complex Films: Structure and Wetting. *Langmuir* **2000**, *16*, 8562–8567.
68. Thunemann, A. F.; Ruppelt, D.; Ito, S.; Mullen, K. Supramolecular Architecture of a Functionalized Hexabenzocoronene and Its Complex with Polyethyleneimine. *J. Mater. Chem.* **1999**, *9*, 1055–1057.
69. Ambrose, J. F.; Nelson, R. F. Anodic Oxidation Pathways of Carbazoles. 1. Carbazole and N-Substituted Derivatives. *J. Electrochem. Soc.* **1968**, *115*, 1159–1164.
70. Ambrose, J. F.; Carpenter, L. L.; Nelson, R. F. Electrochemical and Spectroscopic Properties of Cation Radicals. 3. Reaction Pathways of Carbazolium Radical Ions. *J. Electrochem. Soc.* **1975**, *122*, 876–894.
71. Mengoli, G.; Musiani, M. M.; Schreck, B. Electrochemical Synthesis and Properties of Polycarbazole Films in Protic Acid Media. *J. Electroanal. Chem.* **1988**, *246*, 73–76.
72. Cattarin, S.; Mengoli, G.; Musiani, M. M.; Schreck, B. Synthesis and Properties of Film Electrodes from N-Substituted Carbazoles in Acid Medium. *J. Electroanal. Chem.* **1988**, *246*, 87–100.
73. Huang, C.; Jiang, G.; Advincula, R. Electrochemical Crosslinking and Patterning of Nanostructured Polyelectrolyte Carbazole Precursor Ultrathin Films. *Macromolecules* **2008**, *41*, 4661.
74. Albertus, P. H.; Schenning, J.; Fransicus, B.; Benneker, G.; Hubertus, P.; Geurts, M.; Liu, X. Y.; Nolte, R. J. M. Porphyrin Wheels. *J. Am. Chem. Soc.* **1996**, *118*, 8549–8552.
75. Lee, E.; Jeong, Y. H.; Kim, J-K.; Lee, M. Controlled Self-Assembly of Asymmetric Dumbbell-Shaped Rod Amphiphiles: Transition from Toroids to Planar Nets. *Macromolecules* **2007**, *40*, 8355–8360.
76. Rakhmatullina, E.; Braun, T.; Chami, M.; Malinova, V.; Meier, W. Self-Organization Behavior of Methacrylate-Based Amphiphilic Di- and Triblock Copolymers. *Langmuir* **2007**, 12371–12379.
77. Suksai, C.; Gómez, S. F.; Chhabra, A.; Liu, J.; Skepper, J. N.; Tuntulani, T.; Otto, S. Controlling the Morphology of Aggregates of an Amphiphilic Synthetic Receptor through Host-Guest Interactions. *Langmuir* **2006**, *22*, 5994–5997.
78. Bo, Z. H.; Zhang, W. K.; Zhang, X.; Zhang, C. M.; Shen, J. C. Synthesis and Properties of Polyester Dendrimers Bearing Carbazole Groups in Their Periphery. *Macromol. Chem. Phys.* **1998**, *199*, 1323–1327.